AEROTHERMODYNAMIC ANALYSIS AND DESIGN OF A ROLLING PISTON ENGINE

A THESIS SUBMITTED TO
THE GRADUATE SCHOOL OF NATURAL AND APPLIED SCIENCES
OF
MIDDLE EAST TECHNICAL UNIVERSITY

BY

GÖKHAN ARAN

IN PARTIAL FULFILLMENT OF THE REQUIREMENTS
FOR
THE DEGREE OF MASTER OF SCIENCE
IN
AEROSPACE ENGINEERING

JUNE 2007

Approval of the Graduate School of Natural and Applied Sciences

_____

Prof. Dr. Canan ÖZGEN
Director

I certify that this thesis satisfies all the requirements as a thesis for the degree of Master of Science.

_____

Prof. Dr. Ismail Hakkı TUNCER
Head of Department

This is to certify that we have read this thesis and that in our opinion it is fully adequate, in scope and quality, as a thesis for the degree of Master of Science.

_____

Prof. Dr. İ. Sinan AKMANDOR
Supervisor

Examining Committee Members

Prof. Dr. Cevdet Çelenligil (METU, AEE) _____

Prof. Dr. İ. Sinan Akmandor (METU, AEE) _____

Assoc. Prof. Dr. Sinan Eyi (METU, AEE) _____

Assist. Prof. Dr. Oğuz Uzol (METU, AEE) _____

Instr. Dr. Tahsin Çetinkaya (METU, ME) _____

I hereby declare that all information in this document has been obtained and presented in accordance with academic rules and ethical conduct. I also declare that, as required by these rules and conduct, I have fully cited and referenced all material and results that are not original to this work.

Name, Last name: Gökhan ARAN

Signature :

ABSTRACT

AEROTHERMODYNAMIC ANALYSIS AND DESIGN OF A ROLLING PISTON ENGINE

Aran, Gökhan

M.Sc., Department of Aerospace Engineering

Supervisor : Prof. Dr. İ.Sinan Akmandor

June 2007, 124 pages

A rolling piston engine, operating according to a novel thermodynamic cycle is designed. Thermodynamic and structural analysis of this novel engine is carried out and thermodynamic and structural variables of the engine were calculated. The losses in the engine, friction and leakage were calculated and their effects on the engine were demonstrated.

Keywords: Thermodynamic analysis of an engine, Structural analysis of an engine, Internal combustion engine, Rotary engine.

ÖZ

DÖNER PİSTONLU MOTOR AEROTERMODİNAMİK ANALİZİ VE TASARIMI

Aran, Gökhan
Y. Lisans, Havacılık ve Uzay Mühendisliği Bölümü
Tez Yöneticisi : Prof. Dr. İ. Sinan Akmandor

Haziran 2007, 124 sayfa

Yeni bir termodinamik çevrim ile çalışan döner pistonlu motor tasarlanmıştır. Motorun termodinamik ve yapısal tasarımı ve analizleri yapılmış, motora ait termodinamik ve yapısal değerler hesaplanmıştır. Motorda oluşacak kayıplar, sürtünme ve kaçaklar hesaplanarak, kayıpların etkisi gösterilmiştir.

Anahtar Kelimeler: Motor termodinamik analizi, Motor yapısal analizi, İçten yanmalı motor, Döngüsel motor.

To My Parents

ACKNOWLEDGMENTS

I would like to express my gratitude to my thesis supervisor Prof. Dr. İbrahim Sinan AKMANDOR for their guidance, advice, criticism, encouragements and insight throughout the research.

I would also like to thank TAI for their great support in using the CAD and FEA Tools during my thesis work.

Special thanks to my family for their endless love and great support through out my studies and my career.

TABLE OF CONTENTS

LIST OF TABLES

LIST OF FIGURES

NOMENCLATURE

a: Radius ratio

A_1: Availability at the beginning of the compression

A_2: Availability at the end of the compression

A_3: Availability at the end of the constant volume combustion

A_4: Availability at the end of the constant pressure combustion

A_5: Availability at the end of the expansion

C_p: Specific Heat Coefficient (Constant p)

C_v: Specific Heat Coefficient (Constant V)

f: Coefficient of Friction

F/A Ratio: Fuel to air ratio (mass)

((F/A)cv/(F/A)): Constant volume combustion Fuel/Air to the total F/A

h: Height of blade

h fuel: Fuel Enthalphy

hc: Compressor height

ht: Turbine height

k: Spring constant

n: Compression ratio

n_2:Expansion ratio

nc: Polytropic compression constant

ne: Polytropic expansion constant

patm: Atmospheric air pressure

$p(\theta)$: Pressure of the compressor/turbine at θ angle

p_0: Pressure before entering the engine

p_1: Pressure at the beginning of the compression

p_2: Pressure at the end of the compression

p_3: Pressure at the end of the constant volume combustion

p_4: Pressure at the end of the constant pressure combustion

p_5: Pressure at the end of the expansion

p_d: Discharge pressure

p_s: Suction pressure

θ : Compressor/Turbine rotor angle

ρ_s : Suction density

R: Universal Gas Coefficient

Rc: Cylinder radius

rc: Compressor rotor radius

Rcc: Compressor cylinder radius

Rct: Turbine cylinder radius

Re: Radius of eccentric

Rr: Roller radius

Rs: Radius of shaft

rt: Turbine rotor radius

Ru : Seal Radius

S_0: Entropy before entering the engine

S_1: Entropy at the beginning of the compression

S_2: Entropy at the end of the compression

S_3: Entropy at the end of the constant volume combustion

S_4: Entropy at the end of the constant pressure combustion

S_5: Entropy at the end of the expansion

t: Blade thickness

Tatm: Atmospheric air temperature

$T(\theta)$: Temperature of the compressor/turbine at θ angle

T_0: Temperature before entering the engine

T_1: Temperature at the beginning of the compression

T_2: Temperature at the end of the compression

T_3: Temperature at the end of the constant volume combustion

T_4: Temperature at the end of the constant pressure combustion

T_5: Temperature at the end of the expansion

tc: Compressor blade thickness

Td: Discharge temperature

Ts: Suction temperature

tt: Turbine blade thickness

$V(\theta)$: Volume of the compressor/turbine at θ angle

xmax: Max. spring compression

δ: Radial clearance between roller and eccentric

δ_c: Min. clearance between roller and cylinder

ε_1: Clearance between roller, blade and plate faces

ε_2: Clearance between eccentric and cylinder plate faces

μ: Viscosity coefficient

LIST OF ACRONYMS

BHP: Brake Horse Power

CAD: Computer Aided Design

EC: External Combustion

ECE: External Combustion Engine

FEA: Finite Element Analysis

IC: Internal Combustion

ICE: Internal Combustion Engine

RPM: Revolution per Minute

SFC: Specific Fuel Consumption

CHAPTER 1

INTRODUCTION

The distinctive feature of our civilization today, one that makes it different from all others, is the wide use of mechanical power. At one time, the primary source of power for the work of peace or war was chiefly man's muscle. Later, animals were trained to help and afterwards the wind and the running stream were harnessed. But, the great step was taken in this direction when man learned the art of energy conversion from one to another. The machine which does this job of energy conversion is called an engine. [1]

An engine is a device which transforms one form of energy into another form. However, while transforming energy from one form to another, the efficiency of conversion plays an important role. Normally, most of the engines convert thermal energy into mechanical work and therefore they are called 'heat engines'. [2]

Heat engine is a device which transforms the chemical energy of a fuel into thermal energy and utilizes this energy to perform useful work.
Heat engines can be broadly classified into two categories:
(i) Internal Combustion Engines (IC Engines)
(ii) External Combustion Engines (EC Engines)

Engines whether Internal Combustion or External Combustion are of two types,
(i) Rotary engines
(ii) Reciprocating engines

A detailed classification of the engines is in the following figure. The reciprocating piston engine based on the Otto and Diesel cycles and, the gas turbine engine based on the Brayton cycle, have largely dominated the market. [3] Despite this fact, for many years, patents on rotary combustion engines [4, 5, 6, 7, and 8] have claimed that rotary engines possess many advantages over reciprocating engines such as having high torque, fewer parts, lower weight and fewer reciprocating imbalance. Although these engines have received little industrial attention, for over 5 decades, rotary compressors have taken an important place in general engineering applications, especially in the capacity range of 10-1000 cc/sec and for delivery pressures in the range of 2-18 bars.

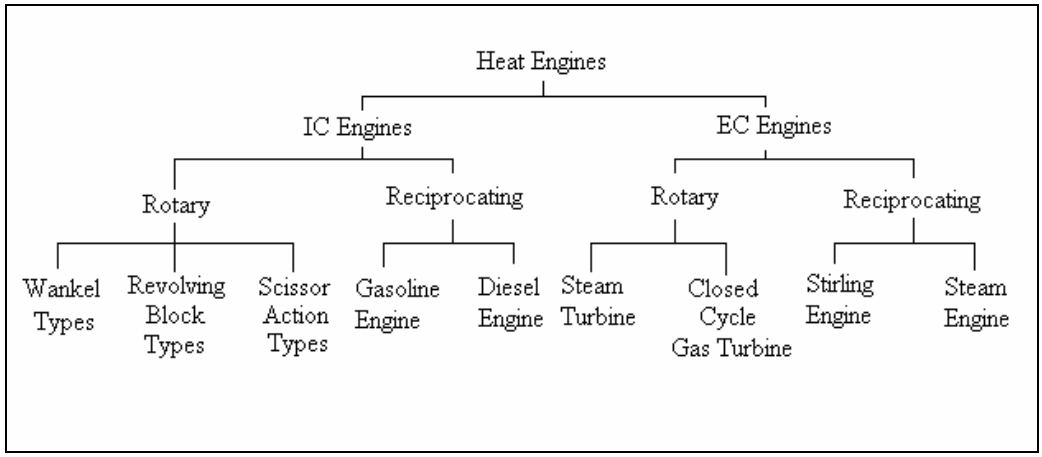

Figure 1.1 Classifications of Heat Engines

In this thesis novel rotary engine was designed and analyzed. The analyzed rotary engine can be classified in rotary IC Engines, in the part of scissor action type part. In the following part rotary engine development, properties of the rotary engines and the novel rotary engine which was described in this thesis were explained.

1.1 Rotary IC Engines

There are three main types of true rotary engines:

1. Wankel types based on eccentric rotors,
2. Scissor action types using vanes or pistons,
3. Revolving block types ('cat and mouse' type[9]).

Engines are closely related to pumps and compressors: the former drives and the latter are driven.

Designs for rotary engines were proposed as early as 1588 by Ramelli, though it took the development of the Otto cycle engine in 1876 and the advent of the automobile in 1896 to set the stage for a proper rotary combustion engine. Furthermore, it took Felix Wankel to catalogue and organizes 862 configuration pairs, of which 278 are impractical. Wankel investigated 149. Prior to 1910, more than 2000 patents for rotary pistons were filed [10].

Other early designs were made by Huygens in 1673 and Kepler. James Watt made a rotary piston steam engine in 1759, as did Ericsson. The American John Cooley made an invention of a sort of reverse Wankel in 1903, which Umpleby applied to internal combustion in 1908, but never developed successfully. Frenchman Sensaud de Lavaud obtained a patent for a four phase rotary piston engine in 1938, two years after Felix Wankel. There were also designs by Pappenheim, Hornblower, Murdoch, Bramah, Flint, Poole, Wright, Marriott, Trotter, Galloway, Parsons, Roots, Wallinder, Skoog, Baylin, Larsen, Ljungström, Behrens, Maillard, and Jernaes. Marsh has made a good summary with diagrams [11].

Today there are lots of different types of rotary engine which people work on them, some of these engines are: The Ball Piston Engine [12], The Rand Cam Engine [13], The Dyna-Cam Engine [14], The Quasiturbine [15], The Rotary of Koushi Akasaka [16].

1.1.1 Advantages of Rotary Engines

- High power to weight ratio,
- Light weight and compact,
- Smooth: no reciprocating motion,
- Easily balanced, less vibrations,
- Extended power stroke,
- Less moving parts: no valves, connecting rods, cams, timing chains. Intake and exhaust timing are accomplished directly by the motion of the rotor.
- Separation of combustion region from intake region is good for hydrogen fuel.
- Lower oxides of nitrogen (NO_x) emissions.

1.1.2 Disadvantages of Rotary Engines

- High surface to volume ratio in combustion chamber, (less thermodynamically efficient)
- Wear and seal problems, (Today with the improving of the material technology these problems are not as critical as in the past.)
- Higher fuel consumption in naive designs. This is relative to the application because the high power of the engine must be considered. Thus Mazda has been successful with the RX-7 sports car, where its fuel economy is comparable to other cars in its class. Only 16 years after the first engine ran, the 1973 oil crisis devastated the RCE before it had sufficiently developed to become more economical. Thus the engine has a more negative reputation regarding fuel consumption than is actually deserved.
- The manufacturing costs can be higher, mostly because the number of these engines produced is not as high as the number of piston engines.

1.2 Novel Rotary Engine

The most important property of the novel rotary engine is the increased the thermal efficiency above the reciprocating engines. This is achieved by implementing a new thermodynamic cycle

The designed novel rotary engine combines the advantages of Otto and Diesel cycles at intake, compression and combustion phases of the thermodynamic cycle, the engine also achieves an expanded power stroke that improves power extraction and efficiency. With a proper thermodynamic and geometrical match of the compressor and turbine working chambers, the expansion process can be improved and lower exhaust pressure and temperature levels can be achieved.

It is well known that for a given compression ratio, the ideal Otto cycle currently provides the most efficient combustion / expansion process since it combines high peak temperature during the isometric (constant volume) heat addition, while still keeping an acceptable mean chamber temperature. However, high peak combustion temperatures can cause auto-ignition of a portion of fuel-air mixture, resulting in engine knocks. Diesel is an improvement of the Otto cycle as it provides higher useful compression ratios and isobaric (constant pressure) heat addition and do not have knock problem as air alone is present during the compression process. The high compression ratios make Diesel engines more fuel efficient but for this same reason, they also become much heavier.

Novel rotary engine is composed of basically three parts, compressor, combustion chamber and the turbine. In the Figure.1.2 the components can be seen. Firstly, air taken into the compressor and compressed up to the desired pressure value into the combustion chamber, to the compressed air in the combustion chamber fuel is injected and is ignited by the spark plug after the combustion in the combustion chamber gasses are taken into the turbine and in the turbine fuel is injected and in the turbine constant pressure combustion takes place after the turbine combustion the products (gasses) of the high temperature and the pressure are expanded through the turbine.

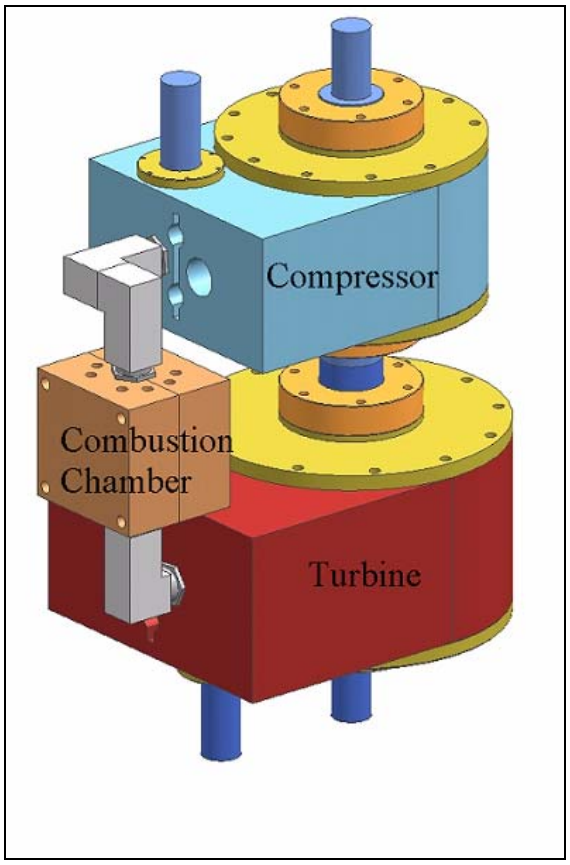

Figure 1.2 Novel Rotary Engine Components

The Working Schematic of the Novel Rotary Engine:

The working schematic explains how engine works. The working cycle is divided into 6 processes, air intake, compression and combustion in the combustion chamber, combustion in the turbine, expansion, and exhaust. Every process is explained by the help of the figures.

Air Intake:

Air is taken to the compressor by the one revolution of the compressor rotor.

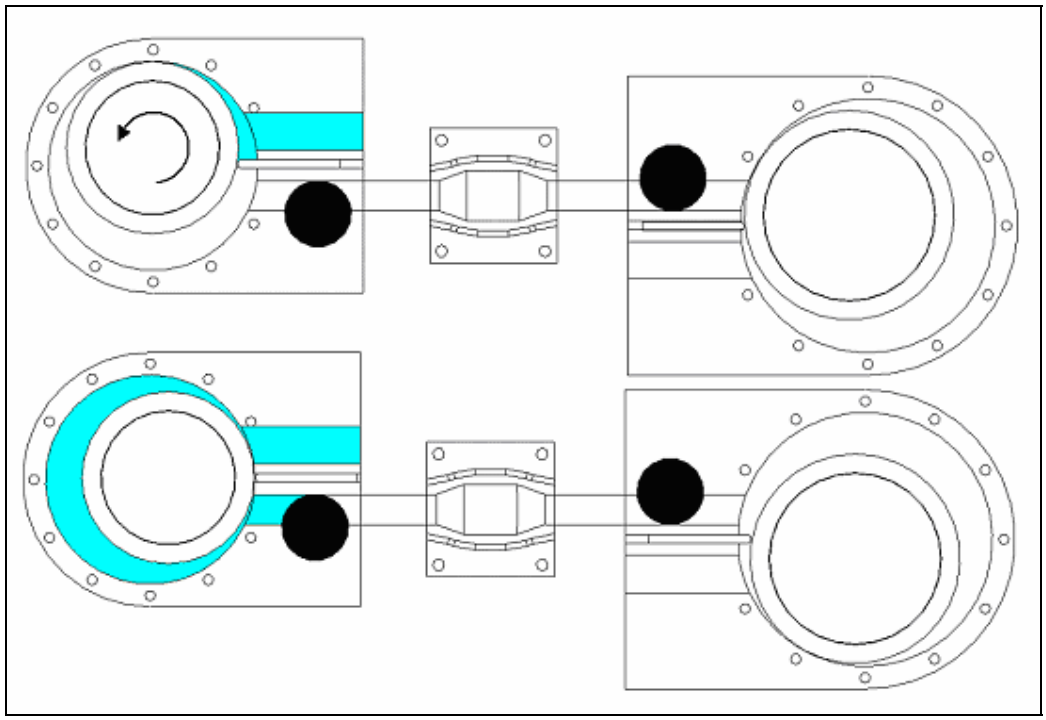

Figure 1.3 Air Intake

Compression:

Air is compressed after it is taken to the compressor, when the rotor reaches the 180^{o} position, compressor valve opens and the air is compressed to the combustion chamber through the 180 degree when the new turn starts, rotor reaches 360^{o} compressor valve closes.

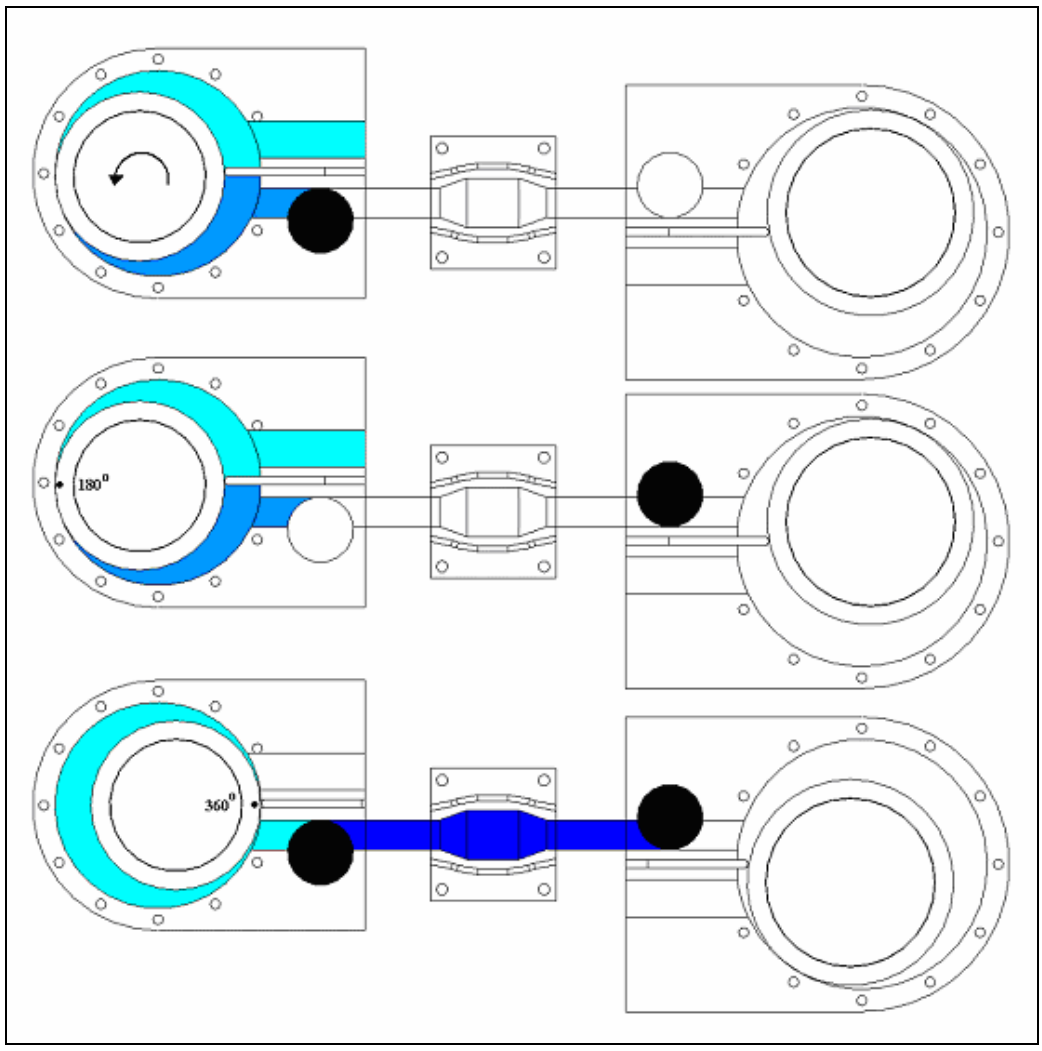

Figure 1.4 Compression

Combustion in the Combustion Chamber:

After air is compressed, fuel is injected to the combustion chamber and it is ignited by the spark plug and the combustion duration is 90^{o} turbine/compressor rotor.

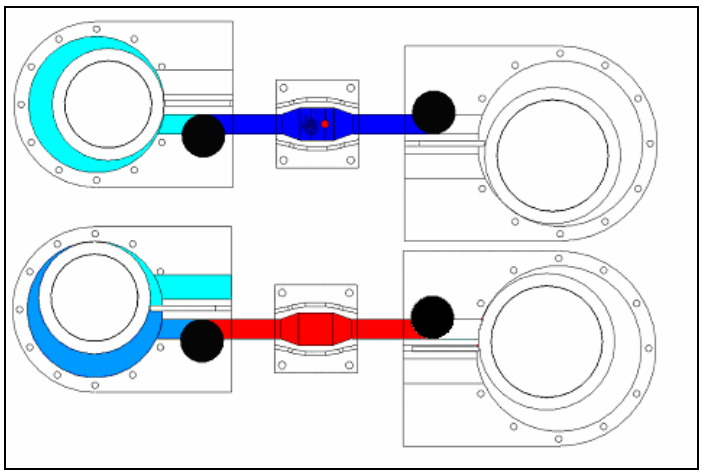

Figure 1.5 Combustion in the Chamber Combustion

Combustion in the Chamber Combustion:

Combustion in the turbine begins at 30^{o} and ends at 45^{o} which was explained in detail in the thermodynamics part.

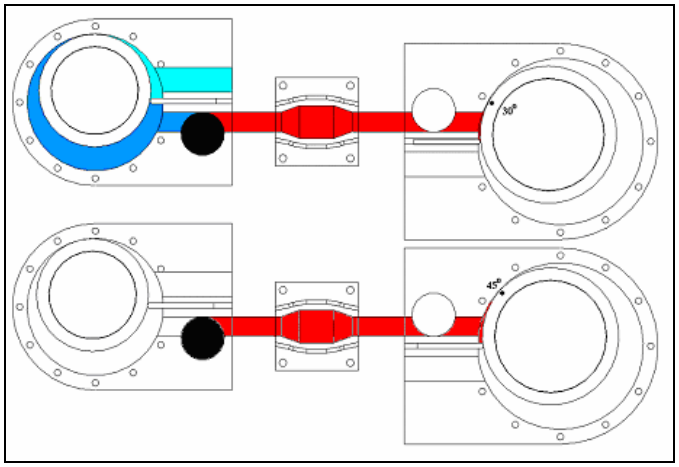

Figure 1.6 Combustion in the Turbine

Expansion:

Expansion begins just after the combustion in the turbine and when the turbine rotor is at 120^{o}, the turbine inlet valve closes, and gasses are expanded through the turbine until the rotor reaches the end of the turn.

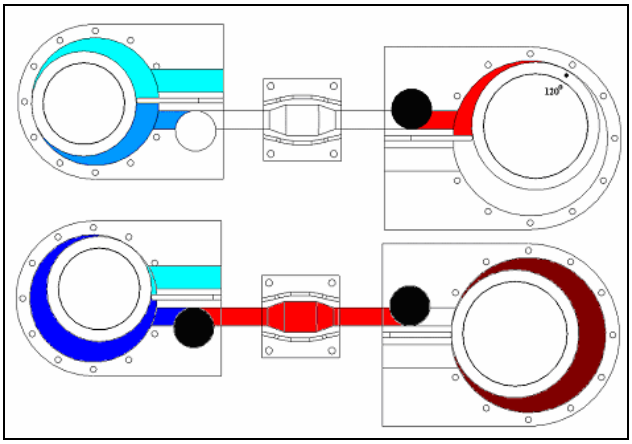

Figure 1.7 Expansion

Exhaust:

Exhaust process is throwing the expanded gasses away from the turbine.

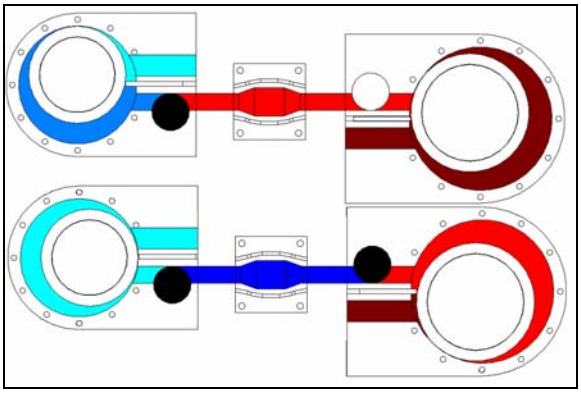

Figure 1.8 Exhaust

1.2.1 Applications

The rolling piston engine can be used in various applications such as automobile engine, generator power source, marine and general aviation applications.

The new engine is light weight, smooth and compact and it is designed for the general aviation applications.

Engines in aviation applications must be:

- lightweight, as a heavy engine increases the empty weight of the aircraft & reduces it's payload.
- small and easily streamlined; large engines with substantial surface area, when installed, create too much drag, wasting fuel and reducing power output.
- powerful, to overcome the weight and drag of the aircraft.
- reliable, as losing power in an airplane is a substantially greater problem than an automobile engine seizing. Aircraft engines operate at temperature, pressure, and speed extremes, and therefore need to operate reliably and safely under all these conditions.
- repairable, to keep the cost of replacement down. Minor repairs are relatively inexpensive.

Aircraft engines run at high power settings for extended periods of time. In general, the engine runs at maximum power for a few minutes during taking off, then power is slightly reduced for climb, and then spends the majority of its time at a cruise setting—typically 65% to 75% of full power. And the rolling piston engine efficiency is higher than any engines so with less fuel it can handle all the operation modes.

The design of aircraft engines tends to favor reliability over performance. The engine, as well as the aircraft, needs to be lifted into the air, meaning it has to

overcome lots of weight. The thrust to weight ratio is one of the most important characteristics for an aircraft engine. The rolling piston engine is about one half the weight and size of a traditional four stroke cycle piston engine of equal power output, and much lower in complexity. In an aircraft application, the power to weight ratio is very important, making the rolling piston engine a good choice. Another difference in aviation engine is that the aircraft spend the vast majority of their time traveling at high speed. This allows aircraft engines to be air cooled, as opposed to requiring a radiator. In the absence of a radiator aircraft engines can boast lower weight and less complexity. The rolling piston engine is air cooled engine and it has less weight than water cooled engines.

In the power range of 0 - 400 HP, the rolling piston engine has many advantages over the piston engines and the gas turbines. When the power needs are over 400 HP gas turbines are more effective.

The rolling piston engine can be used in target drone, UAV and aircraft which has 0 -400 HP power requirements.

1.3 Outline of the Thesis

In chapter two, the novel engine thermodynamic analysis was done. Operating cycle of the novel rotary engine is being introduced. The P-V and T-S diagrams, basic equations and the efficiency calculations are given. Also in chapter two, the thermodynamic design code written to dimension the engine is explained and the dimension calculations of the novel engine are given.

The third chapter consists of the structural and mechanical design of the novel rotary engine with the dimensions taken from the thermodynamic design code. The structural analysis of the critical components and the material selection are explained and the results are presented.

The fourth chapter includes the engine losses. In this part kinematics analysis of the engine moving components are done. After the kinematics analysis the results are used to calculate the geometrical relations and the friction losses. At the end of the chapter leakage loss is calculated.

In chapter five, all the work done in this thesis was summarized, the future work for this study is given and the application of this thesis in the industry was explained.

CHAPTER 2

THERMODYNAMIC DESIGN OF THE NOVEL ROTARY ENGINE

2.1 INTRODUCTION

It is well known that for a given compression ratio, the ideal Otto cycle currently provides the most efficient combustion / expansion process as it combines high peak temperature during the isochoric (constant volume) heat addition, while still keeping an acceptable mean chamber temperature. However, high peak combustion temperatures can cause auto-ignition of a portion of fuel-air mixture, resulting in engine knocks. Diesel is an improvement of the Otto cycle as it provides higher useful compression ratios and isobaric (constant pressure) heat addition and do not have knock problem as air alone is present during the compression process. The high compression ratio makes Diesel engines more fuel-efficient but for this same reason, they also become much heavier. Compared to the Otto cycle, Diesel cycle also delivers less power for the same displacement. For the compression and combustion phases of the cycle, the ideal would be to follow a limited combustion pressure cycle that would first use a combined isochoric heat addition followed by isobaric and/or isothermal heat additions. As mentioned in a prior patent, such hybrid engine process has been developed (Texaco TCCS, Ford PROCO, Ricardo, MAN-FM and KHD-AD) but they have been proven impractical. This is probably because the piston engine was forced unsuccessfully to follow the hybrid Otto-Diesel thermodynamic cycle.

It is important to understand that, not only the thermodynamics but also the kinematics and the fluid mechanics are involved when adapting a thermodynamic cycle to an engine.

The engine designed in this thesis naturally follows the new limited peak thermodynamic cycle (Figure 2.1 and 2.2).

This novel cycle [17], combines the advantages of Otto and Diesel cycles at intake, compression and combustion phases by limiting the peak combustion temperature. The present cycle also has an expanded power stroke. With a proper thermodynamic and geometrical match of the compressor and turbine working chambers volumes, ambient exhaust pressure levels can be achieved. [18]

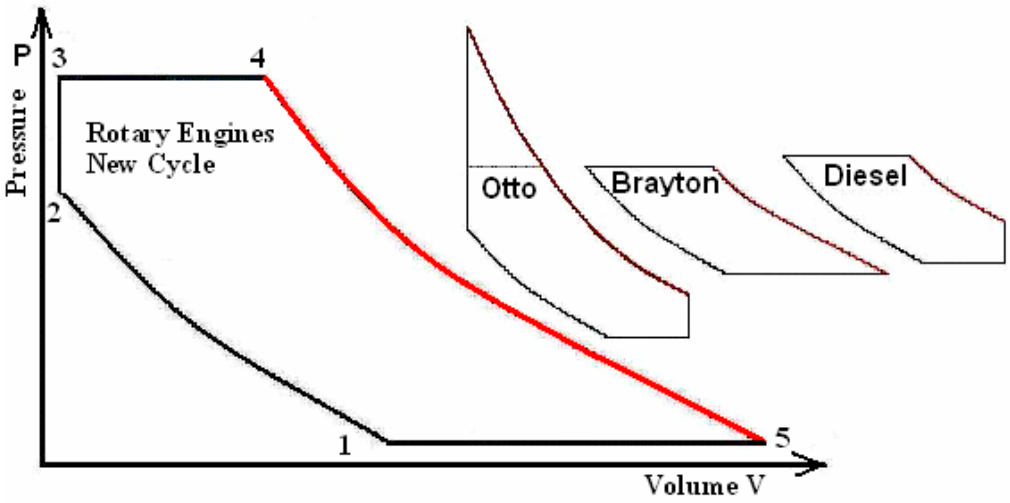

Figure 2.1 Novel Thermodynamic Cycle (p – V)

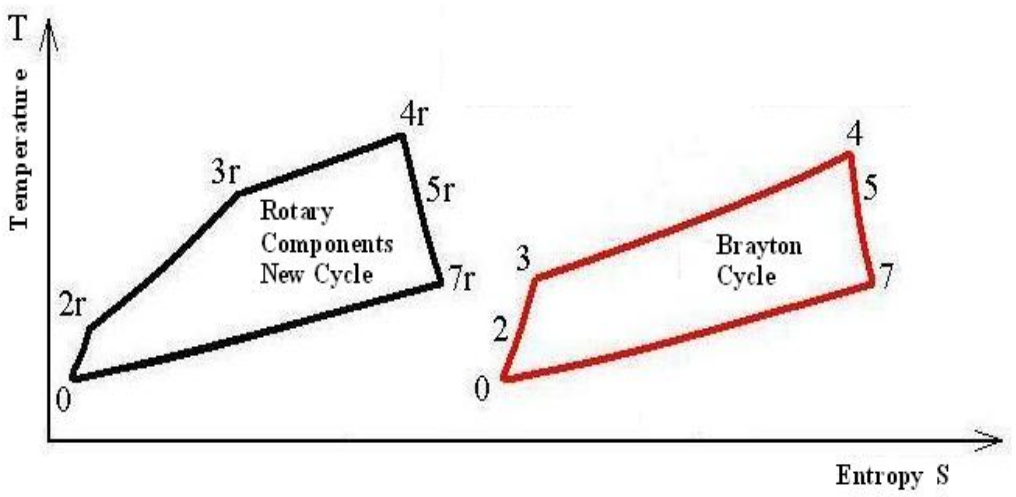

Figure 2.2 Novel Thermodynamic Cycle (T – S)

By limiting the peak combustion pressures, the present design of the novel engine also provides an expanded power stroke that improves power extraction. It is possible to derive the new cycle ideal thermal efficiency by writing the proper temperature, pressure and specific volume relations within the thermal efficiency definition (Equation 2.1 and 2.2) given below.

$$\eta_{th} = \frac{Qin - Qout}{Qin} = 1 - \frac{Qout}{Qin} \qquad \text{Eq.2.1}$$

$$\eta_{th} = \frac{mC_p(T_5 - T_1)}{mC_v(T_3 - T_2) + mC_p(T_4 - T_3)} \qquad \text{Eq.2.2}$$

$$\eta_{th} = \frac{k(T_5 - T_1)}{(T_3 - T_2) + k(T_4 - T_3)} \qquad \text{Eq.2.3}$$

Writing all of the temperatures in terms of T_1 to simplify the efficiency equation,

$$\eta_{th} = 1 - \frac{kT_1\left(r_{cr}\lambda\left(n/n_2\right)^{k-1} - 1\right)}{T_1\left(\lambda n^{k-1} - n^{k-1}\right) + kT_1\left(r_{cr}\lambda n^{k-1} - \lambda n^{k-1}\right)} \qquad \text{Eq.2.4}$$

Where,

$$r_{cr} = \frac{V_4}{V_3} \qquad \lambda = \frac{P_3}{P_2} \qquad n = \frac{V_1}{V_2} \qquad \text{Eq.2.5}$$

Comparing with the Otto cycle thermal efficiency given below (Eq.2.6), it is seen that the new thermodynamic cycle thermal efficiency has a much higher degree of freedom as Equation 2.4 is defined in terms of 3 variables all defined above, compared to only one variable $n = V_1 / V_2$ for the Otto cycle. As temperature upper limit restricts the increase of Otto cycle volume ratio n, the Otto thermal efficiency reaches a modest peak value. As for the diesel cycle thermal efficiency given below (Eq.2.7), it is even lower because the term A is bigger than 1.

$$\eta_{th\,Otto} = 1 - \frac{1}{r^{k-1}} \qquad \text{Eq.2.6}$$

$$\eta_{th\,Diesel} = 1 - \frac{1}{r^{k-1}} A \qquad \text{Eq.2.7}$$

As the bracketed term in Equation 2.11 is always less than 1, the new thermodynamic cycle thermal efficiency is guaranteed to be always bigger than those pertaining to Otto and Diesel cycles.

2.2 THERMODYNAMIC DESIGN CODE

This thermodynamic design code is written to calculate the necessary geometry of the novel rotary engine for the desired performance values and to determine the thermodynamic properties during compression, combustion and expansion phases which will be used in the structural analysis of the engine parts.

Firstly, performance parameters (power output, rpm) of the novel rotary engine that will be designed are decided upon as target values. After describing the performance of the engine, the critical parameters of the engine such as maximum temperature during combustion, fuel to air ratio, compression ratio are specified. By processing the basic inputs (atmospheric properties, thermodynamic constants and desired engine properties) and the geometric inputs (basic dimensions of the engine), the code calculates the properties for the compression phase, constant volume and constant pressure combustion phases and the expansion and exhaust phases, and matches the compressor and turbine geometry. After finalizing the engine geometry, the code makes the necessary thermodynamic calculations to determine the power output, and thermal efficiency. If the required power output is not at the desired level, then the compressor geometry is revised and the compressor – turbine matching is re-calculated. After finalizing the engine geometry, the thermal efficiency and the thermal properties during compression, combustion and expansion phases which will be used in the structural analysis of the engine parts are calculated.

The flowchart of the thermodynamic code is given in Figure 2.3.

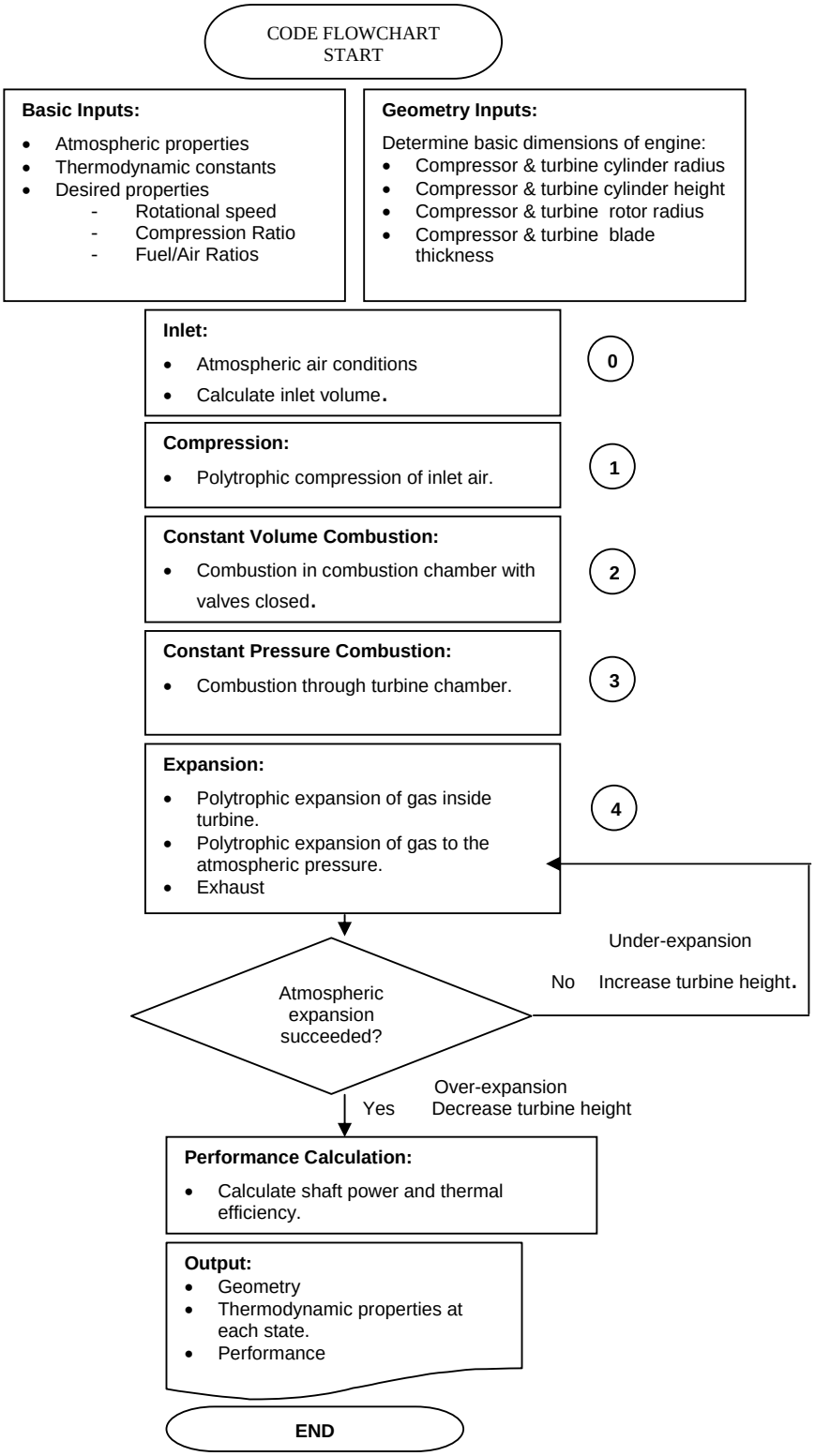

Figure 2.3 Flowchart of the Thermodynamic Code

2.2.1 INPUTS

In the thermodynamic design code the following parameters are inputs of the code and the code calculated the necessary thermodynamics parameter as described in the calculation part.

Table 2.1 Thermodynamic Design Code Inputs

Rcc	Compressor cylinder radius
hc	Compressor height
tc	Compressor blade thickness
rc	Compressor rotor radius
Rct	Turbine cylinder radius
ht	Turbine height
tt	Turbine blade thickness
rt	Turbine rotor radius
Patm	Atmospheric air pressure
Tatm	Atmospheric air temperature
Cp	Specific heat constant (constant pressure)
Cv	Specific heat constant (constant volume)
nc	Polytropic compression constant
ne	Polytropic expansion constant
F/A Ratio	Fuel/Air ratio (mass)
((F/A)cv/(F/A))	Constant volume combustion Fuel/Air ratio to the total F/A ratio
h fuel	Fuel Enthalpy
n	Compression ratio

2.2.2 CALCULATIONS

In the code both 1st Law and 2nd Law thermodynamics analysis are performed.

The calculations of the code are divided into two groups.

In the first part energy based 1st Law analysis are described, in the 2nd part entropy based 2nd Law analysis are described.

In the following paragraphs thermodynamic calculations for all processes will be determined.

2.2.2.1 1st LAW ANALYSIS

2.2.2.1.1 Air Intake

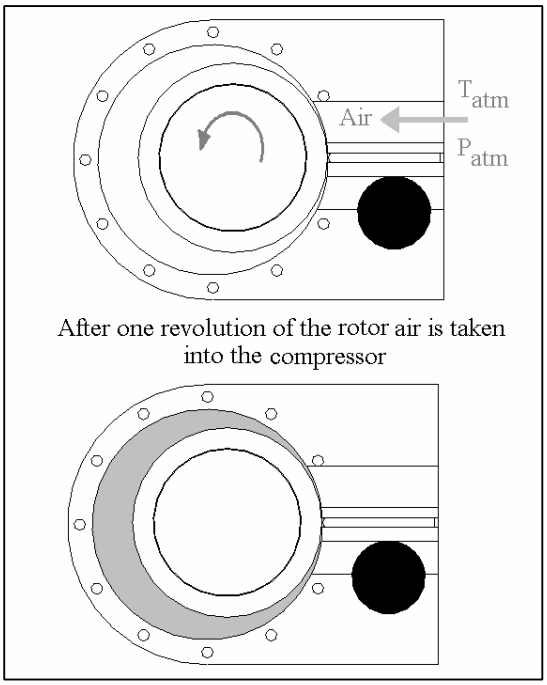

Figure 2.4 Air Intake Process

Air is taken to the compressor through the inlet port of the compressor, by the rotation of the rotor air at the pressure P_{atm} and at the T_{atm} is sucked to the compressor. And when the rotor rotates 360^o, the maximum compressor volume is reached and the air intake process is accomplished.

Air before entering the engine:

$p_0=p_{atm}$

$T_0=T_{atm}$

Air Intake Process:

$$\theta = 0,2\pi$$

$$V(\theta) = \frac{1}{2} hRcc^2 f(\theta)$$

$$f(\theta) = \begin{bmatrix} (1-a^2)\theta - \frac{1}{2}(1-a)^2 \sin 2\theta - a^2 \sin^{-1}((\frac{1}{a}-1)\sin\theta) \\ -a(1-a)\sin\theta\sqrt{1-(\frac{1}{a}-1)^2 \sin^2\theta} \end{bmatrix}$$

Eq.2.8

The method which describes how volume rotor angle relationship is established and it is described in the chapter 3.

$$p(\theta) = p_{atm} \quad \text{Eq.2.9}$$

$$T(\theta) = T_{atm} \quad \text{Eq.2.10}$$

when $\theta = 2\pi$ air intake process is over,

$$V_1 = V(2\pi) \quad \text{Eq.2.11}$$

$$T_1 = T_{atm} \quad \text{Eq.2.12}$$

$$p_1 = p_{atm} \quad \text{Eq.2.13}$$

2.2.2.1.2 Compression

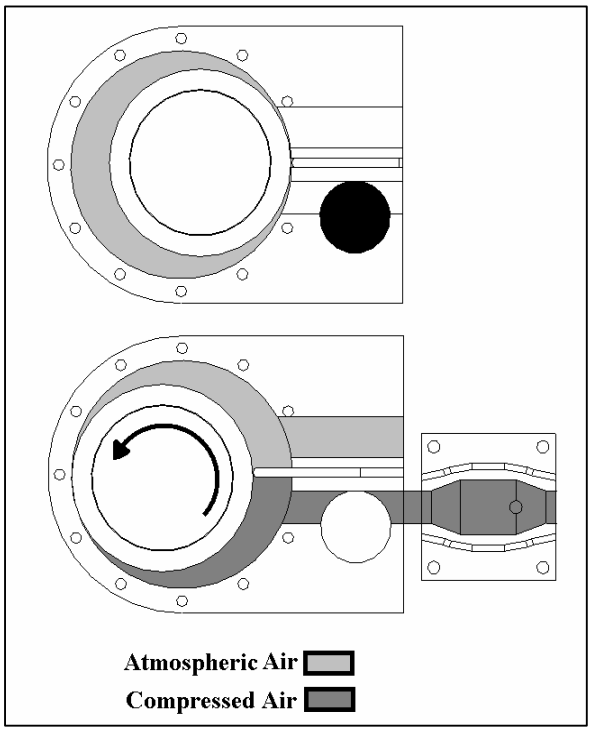

After the air is taken to the compressor, atmospheric air is compressed by the rotation of the rotor and when the rotor comes to the 180^o position compressor valve opens and the air is compressed to the combustion chamber. (Valve angles and engine timing is described in the following parts.)

And the volume of the combustion chamber is defined by the compression ratio.

Figure 2.5 Compression Process

Compression Process:

$$n = \frac{V(2\pi)}{V_b} \qquad \text{Eq.2.14}$$

n = 4.5 and compressor volume $V(2\pi)$ is 450 cc so, V_b, combustion chamber volume is 100 cc.

$$\theta = 0,2\pi \qquad \text{Eq.2.15}$$

$$V(\theta) = V_1 - \frac{1}{2} hRcc^2 f(\theta) - \frac{1}{2} tchc\delta_e$$

$$f(\theta) = \left[\begin{array}{l} (1-a^2)\theta - \frac{1}{2}(1-a)^2 \sin 2\theta - a^2 \sin^{-1}((\frac{1}{a}-1)\sin\theta) - \\ a(1-a)\sin\theta\sqrt{1-(\frac{1}{a}-1)^2 \sin^2\theta} \end{array} \right] \qquad \text{Eq.2.16\&17}$$

$$p(\theta) = p_s \left[\frac{V(2\pi)}{V(\theta)} \right]^{nc} \qquad \text{Eq.2.18}$$

$$T(\theta) = T_s \left[\frac{T(2\pi)}{T(\theta)} \right]^{nc-1} \qquad \text{Eq.2.19}$$

where nc is 1.3 which is the advised value for rolling piston type compressor and also for SI engines.[19]

$$V_2 = V_b \qquad \text{Eq.2.20}$$

$$T_2 = T(2\pi) \qquad \text{Eq.2.21}$$

$$p_2 = p(2\pi) \qquad \text{Eq.2.22}$$

To determine the work done for compression and the heat transfer,

$${}_1Q_2 + U_1 = U_2 + {}_1W_2 \qquad \text{Eq.2.23}$$

$${}_1Q_2 = \left[\frac{R}{k-1} - \frac{R}{n_c - 1} \right] \left[T_2 - T_1 \right] \qquad \text{Eq.2.24}$$

$${}_1W_2 = \frac{1}{n_c - 1} \left[p_1 v_1 - p_2 v_2 \right] = \frac{R}{n_c - 1} \left[T_1 - T_2 \right] \qquad \text{Eq.2.25}$$

2.2.2.1.3 Combustion

In the engine there are two combustion processes. At first compressed air is mixed with fuel and combusted in the combustion chamber at constant volume and then in turbine fuel is injected and constant pressure turbine combustion takes place.

- **Constant Volume Combustion (Combustion Chamber Combustion)**

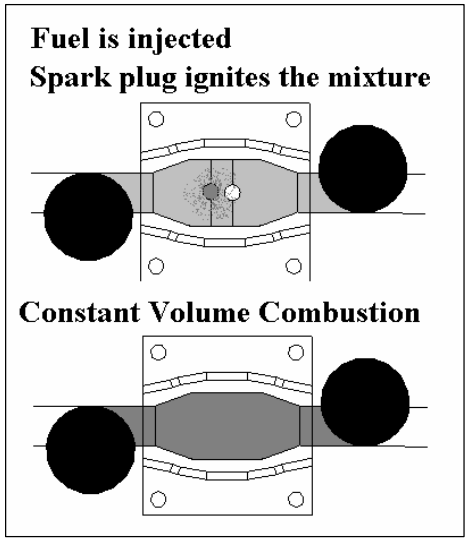

Air is compressed to the combustion chamber and fuel is injected directly into the combustion chamber and then spark plug ignites the fuel as it mixes with air. This type of engines are referred as stratified-charge engines from the need to produce in the mixing process between the fuel jet and air in the engine a ”stratified” fuel-air mixture, with an easily ignitable composition at the spark plug at the time of ignition.[19]

Figure 2.6 Constant Volume Combustion

And the combustion duration is 90 o degree compressor/turbine rotor. (compressor and turbine are fixed together, they have same angular speed)

Constant Volume Combustion

Fuel: Gasoline $C_{8.26}H_{15.5}$
F/A ratio: 0.02
$((F/A)_{cv})/(F/A)_{total}$: 0.7 Eq.2.26

Before calculating the actual combustion reaction stoichiometric reaction is derived to calculate equivalence ratio. (Φ **)**

Stoichiometric Reaction:

General formula for combustion:

$$C_N H_M + (N + \frac{M}{4})(0_2 + 3.773N_2) \longrightarrow NCO_2 + \frac{M}{2} H_2O + (N + \frac{M}{4})3.773N_2$$

Eq.2.27

for gasoline:

N=8.26 Eq.2.28

M=15.5 Eq.2.29

$$C_{8.26}H_{15.5} + 12.135(0_2 + 3.773N_2) \longrightarrow 8.26CO_2 + 7.75H_2O + 45.785N_2$$

$$m_{fuel} = (8.26 \times 12 + 15.5 \times 1) kg / kmol \quad \text{Eq.2.30}$$

$$m_{fuel} = (114.62) kg / kmol$$

$$m_{air} = 12.135(32 + 3.773 \times 28.16) kg / kmol \quad \text{Eq.2.31}$$

$$m_{air} = (1677.635) kg / kmol$$

$$(F / A)_{stoichoimetric} = \frac{114.62}{1677.635} \quad \text{Eq.2.32}$$

$$(F / A)_{stoichoimetric} = 0.068$$

Equivalence Ratio:

$$(F / A)_{cv} = \frac{(F / A)_{cv}}{(F / A)_{total}} (F / A)_{total} \quad \text{Eq.2.33}$$

$$(F / A)_{cv} = 0.014$$

$$\Phi = \frac{(F / A)_{cv}}{(F / A)_{stoichiometric}} = \frac{0.014}{0.068} \quad \text{Eq.2.34}$$

$\Phi = 0.2$ (This is the general case for ultra lean mixtures [19])

Actual Reaction:

Generic form:

$$C_N H_M + \frac{1}{\Phi}(N + \frac{M}{4})(0_2 + 3.773N_2) \longrightarrow NCO_2 + \frac{M}{2}H_2O + (N + \frac{M}{4})3.773N_2$$

Eq.2.35

$$C_{8.26}H_{15.5} + \frac{1}{0.2}12.135(0_2 + 3.773N_2) \longrightarrow 8.26CO_2 + 7.75H_2O + 45.785N_2$$

$$C_{8.26}H_{15.5} + 60.675(0_2 + 3.773N_2) \longrightarrow 8.26CO_2 + 7.75H_2O + 45.785N_2$$

After writing the chemical reaction the energy balance between the reactants and the products is established to calculate the temperature of the products.

$$\left(\Delta U_{\underset{T_R' \longrightarrow T_R}{R}}\right) - \xi Q_L = \left(\Delta U_{\underset{T_R' \longrightarrow T_P}{P}}\right)$$

Eq.2.36

T_R': Reference temperature (0 K)

T_R: Reactants temperature (T_2)

T_P: Products temperature

$\left({}_R Q_P\right)$: Heat release of the combustion

$\left(Q_L\right)$: Heat loss during the combustion

$\left(\Delta U_{\underset{T_R' \longrightarrow T_R}{R}}\right)$: Reactants internal energy change

$\left(\Delta U_{\underset{T_R' \longrightarrow T_P}{P}}\right)$: Products internal energy change

ξ : The heat transfer efficiency (0.8 [19])

The internal energy of the components in reactant and product side of the chemical equation is calculated as;

$$\left(\Delta U\right) = \sum n_i \left(\Delta u_i\right)$$

Eq.2.37

n_i: mole number of the components

Δu_i : Internal energy change of the species

$$(\Delta u_i) = \int_{T_R^{\circ}}^{T} C_{vi}(T).dT \qquad \text{Eq.2.38}$$

For each species C_v is calculated as,

$$C_v = A + BT \qquad \text{Eq.2.39}$$

$$(\Delta u_i) = AT + \frac{1}{2}BT^2$$

C_v values for the components are taken from [19] and they are seen on the following table.

Table 2.2 Coefficients of Species Thermodynamic Properties

Coefficients of Species Thermodynamic Properties		
Species	A	B
CO_2	17.43	1.90×10^{-2}
H_2O	22.81	9.81×10^{-3}
O_2	18.73	5.70x10-$^{-3}$
N_2	20.32	3.99×10^{-3}
$C_{8.26}H_{15.5}$	-108.4	0.5

During the combustion there is a heat loss from the hot gases in the combustion chamber to the combustion chamber walls. This heat loss is calculated as convection from the gasses to the combustion chamber.

$$Q_L = h_c A_{cc} (Tp - T_{cc}) \qquad \text{Eq.2.40}$$

T_p: Combustion products temperature (gas temperature after the combustion)
T_{cc}: Combustion chamber temperature before combustion

Convection coefficient is calculated and in the thermal analysis this coefficient is used.

$$h_c = ka\frac{\mathrm{Re}^b}{2Rcc} \qquad \text{Eq.2.41}$$

a and b are the empiric coefficients which are taken as;

a = 0.49 Eq.2.42

b = 0.7 Eq.2.43

(These values are taken from [19])

In the formula above k is the thermal conductivity of the air.

And the variation of k is seen on the following graph.

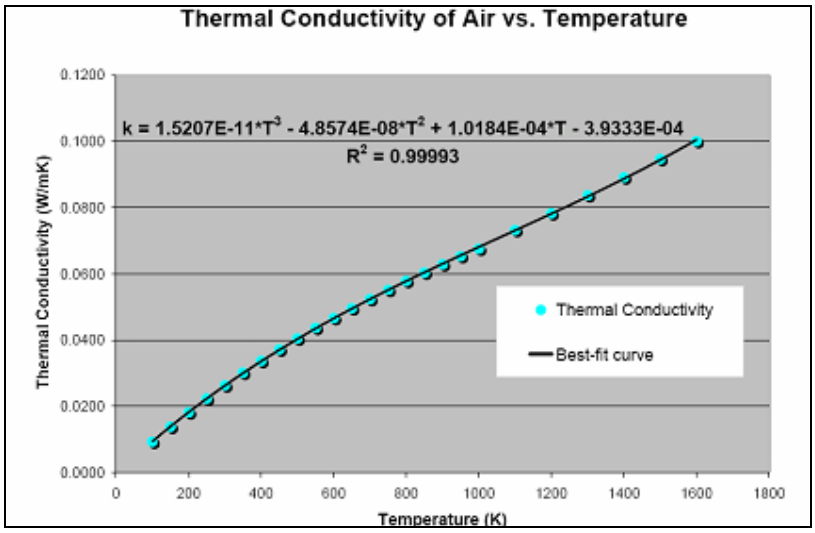

Figure 2.7 Thermal Conductivity of Air vs. Temperature

At the end by using the energy balance equation for the combustion is found by iterative solution, first T_p is estimated and then all internal energies and heat loss are calculated then T_p is checked by the help of the energy balance equation when LHS of the equation is equal to the RHS of the equation T_p is found.

For Constant Volume Combustion:

$\theta = 2\pi, \frac{5\pi}{2}$ (360 to 450 rotor rotation degree)

$T(\theta) = T_P$ Eq.2.44

$p(\theta) = \frac{RTp}{v}$ Eq.2.45

and R Specific Gas Constant

$R = \frac{R_0}{M_{mix}}$ Eq.2.46

M_{mix}, molecular weight,

$M_{mix} = \frac{\sum M_i n_i}{\sum n_i}$ Eq.2.47

Finally,

$T_3 = T_P$ Eq.2.48

$p_3 = p\left(\frac{5\pi}{2}\right)$ Eq.2.49

$V_3 = V_2$ Eq.2.50

- **Constant Pressure Combustion (Turbine Combustion)**

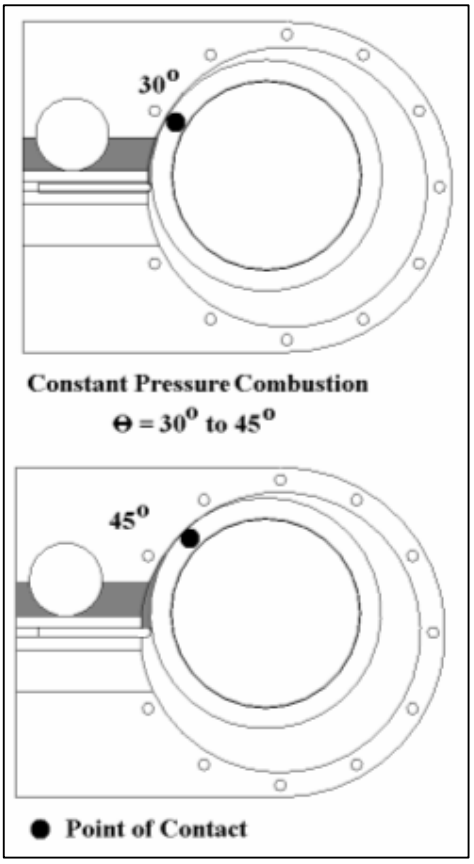

After the combustion, combusted gases are taken to the turbine because the mixture is ultra lean and extra combustion in the turbine is possible, by doing so one can get extra energy without much increase in the temperature. When the gasses are in the turbine fuel is injected to the turbine as in the combustion chamber and spark ignites the mixture. The chemical reaction of the combustion is similar to the constant volume combustion instead of the energy balance equation because in here there is a work term in the equation because of the volume change, but the internal energies and the other thermal property calculations are similar , so only differences are explained.

Figure 2.8 Constant Pressure Combustion

Equivalence Ratio:

$$(F/A)_{cp} = \left(1 - \frac{(F/A)_{cv}}{(F/A)_{total}}\right)(F/A)_{total} \qquad \text{Eq.2.51}$$

$$(F/A)_{cp} = 0.006$$

$$\Phi = 0.08 \qquad \text{Eq.2.52}$$

Actual Reaction:

$$C_{8.26}H_{15.5} + 242.7(0_2 + 3.773N_2) \longrightarrow 8.26CO_2 + 7.75H_2O + 45.785N_2$$

And the energy balance,

$$\left(\Delta U_R\right)_{T_R' \longrightarrow T_R} - \zeta_t Qt_L = \left(\Delta U_P\right)_{T_R' \longrightarrow Tp} + {}_RW_P \qquad \text{Eq.2.53}$$

Qt_L : Heat loss

ζ_t : Heat transfer efficiency

$${}_RW_P = p_4V_4 - p_3V_3 \qquad \text{Eq.2.54}$$

$$V_3 = V_2 \qquad \text{Eq.2.55}$$

$$\lambda = \frac{P_3}{P_2} \qquad \text{Eq.2.56}$$

$${}_RW_P = P_4V_4 - \lambda P_2V_2 \qquad \text{Eq.2.57}$$

$$p_4V_4 = n_PR_0T_P \qquad \text{Eq.2.58}$$

$$p_2V_2 = n_RR_0T_R \qquad \text{Eq.2.59}$$

So, similar to the combustion in the combustion chamber T_P for the constant pressure combustion is found.

In turbine combustion duration of the combustion is made certain by the fuel volume V_4 is found after the calculations as 1.9 10^{-5} m^3 which correspond to the volume when the rotor of the turbine is at 45 degree (Figure2.5).

Constant Pressure Combustion:

When the gases are first taken into the turbine, turbine rotor is at 30 ^{0} to the turbine cylinder to avoid any negative direction rotation of the engine just after the static

neutral equilibrium point. At lower part, constant pressure combustion is described in terms of turbine rotor angles

$\theta = \frac{\pi}{6}, \frac{\pi}{2}$ (30^o to 45^o turbine rotor angle)

$$T(\theta) = T_P \quad \text{Eq.2.60}$$

$$p(\theta) = \frac{RTp}{v} \quad \text{Eq.2.61}$$

Finally,

$$T_4 = T_P, \quad \text{Eq.2.62}$$

$$p_4 = p_3 \quad \text{Eq.2.63}$$

$$V_4 = V\left(\frac{\pi}{2}\right) \quad \text{Eq.2.64}$$

2.2.2.1.4 Expansion

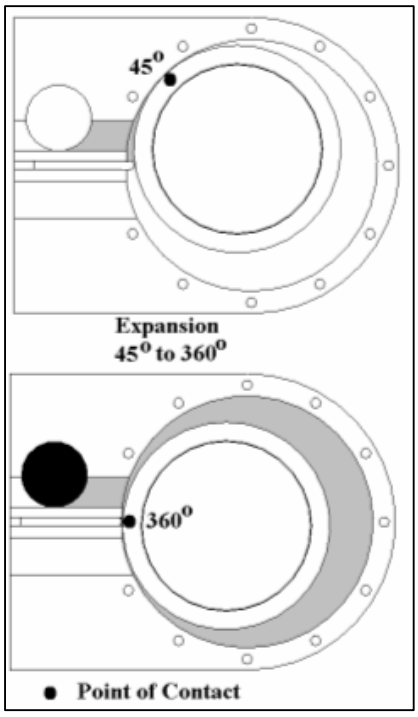

When the constant pressure combustion is over, combusted gasses begin to expand trough the rotation of the rotor when the volume of the turbine increases. The expansion process begins at the 45^o and continuous to the 360^o degree.

Figure 2.9 Expansion Process

Expansion Process:

$$\theta = \frac{\pi}{2}, 2\pi$$

$$V(\theta) = \frac{1}{2} hRct^2 f(\theta) - \frac{1}{2} tht\delta_e$$

$$f(\theta) = \begin{bmatrix} (1-a^2)\theta - \frac{1}{2}(1-a)^2 \sin 2\theta - a^2 \sin^{-1}((\frac{1}{a}-1)\sin\theta) - \\ a(1-a)\sin\theta\sqrt{1-(\frac{1}{a}-1)^2 \sin^2\theta} \end{bmatrix} \quad \text{Eq.2.65}$$

$$p(\theta) = p_4\left[\frac{V_4}{V(\theta)}\right]^{ne} \quad \text{Eq.2.66}$$

$$T(\theta) = T_4\left[\frac{T_4}{T(\theta)}\right]^{ne-1} \quad \text{Eq.2.67}$$

where ne is 1.25 which is the lower value for SI engines.[19]

$$V_5 = V(2\pi) \quad \text{Eq.2.68}$$

$$T_5 = T(2\pi) \quad \text{Eq.2.69}$$

$$p_5 = p(2\pi) \quad \text{Eq.2.70}$$

And also in the turbine atmospheric expansion is achieved so,

$$p_5 = p_{atm} \quad \text{Eq.2.71}$$

To calculate the work and heat transfer,

$${}_4Q_5 + U_4 = U_5 + {}_4W_5 \quad \text{Eq.2.72}$$

$${}_4Q_5 = \left(\frac{R}{n_e - 1} - C_v\right)(T_4 - T_5)$$

$${}_4W_5 = \frac{R}{ne-1}(T_4 - T_5) = \frac{1}{ne-1}(p_4 v_4 - p_5 v_5) \quad \text{Eq.2.73}$$

2.2.2.1.5 Exhaust

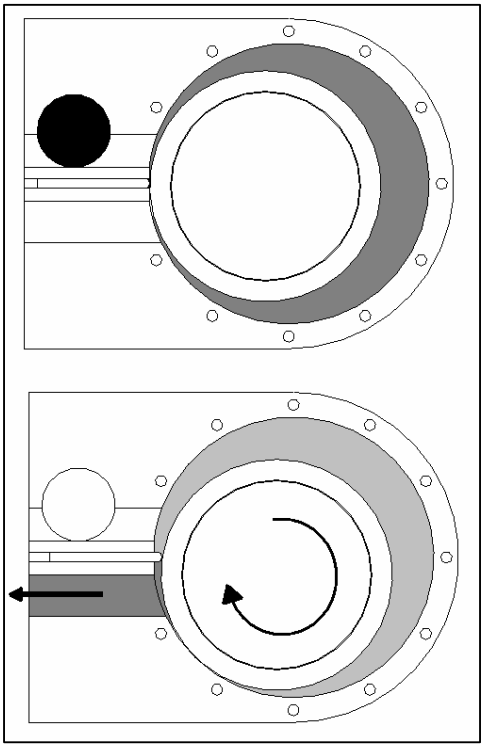

In the exhaust process expanded gasses to the atmospheric pressure are taken out of the engine. In one revolution of the turbine rotor, all gasses are taken out and process ends.

Exhaust Process:

$\theta = 0,2\pi$ (Turbine rotor angle)

$p(\theta) = p_{atm}$ Eq.2.74

$T(\theta) = T_{atm}$ Eq.2.75

When $\theta = 2\pi$ exhaust process is over,

$V_6 = V(2\pi)$ Eq.2.76

$T_6 = T_{atm}$ Eq.2.77

$p_6 = p_{atm}$ Eq.2.78

Figure 2.10 Exhaust Process

2.2.2.2 1st Law Analysis Results

Engine Dimensions:

Table 2.3 Engine Dimensions

Compressor		
Rcc	(m)	0,07
hc	(m)	0,09
tc	(m)	0,006
rc	(m)	0,0575

Turbine		
Rct	(m)	0,095
ht	(m)	0,11
tt	(m)	0,006
rt	(m)	0,07

Processes:

1-2: Polytrophic Compression
2-3: Constant Volume Combustion
3-4: Constant Pressure Combustion
4-5: Polytrophic Expansion

Table 2.4 Results of the 1st Law Analysis

Temperatures		
T_1	298,15	K
T_2	497,17	K
T_3	1414,8	K
T_4	1695,7	K
T_5	919,29	K

Volumes		
V_1	450,62	cc
V_2	100,14	cc
V_3	100,14	cc
V_4	131,77	cc
V_5	1425,	cc

Pressures		
P_1	101320	Pa
P_2	929050	Pa
P_3	2643900	Pa
P_4	2643900	Pa
P_5	101320	Pa

Entropies		
s_1	6863,05	J/kg
s_2	6740,42	J/kg K
s_3	7490,30	J/kg K
s_4	7672,11	J/kg K
s_5	7936,00	J/kg K

Compression		
W_{1-2}	-190,4	kJ/kg
Q_{1-2}	-47,70	kJ/kg

Combustion		
Q_{2-3}	658	J/kg
Q_{3-4}	282	kJ/kg
W_{3-4}	1,24	kJ/kg

Expansion		
Q_{4-5}	308,92	kJ/kg
W_{4-5}	822,83	kJ/kg

n_f	0,67	
	42,75	HP
Power	57,33	kW

In the table above n_f is the fuel conversion efficiency of the engine which is described as net work output of the engine over fuel energy. (W_{net}/Q_f)

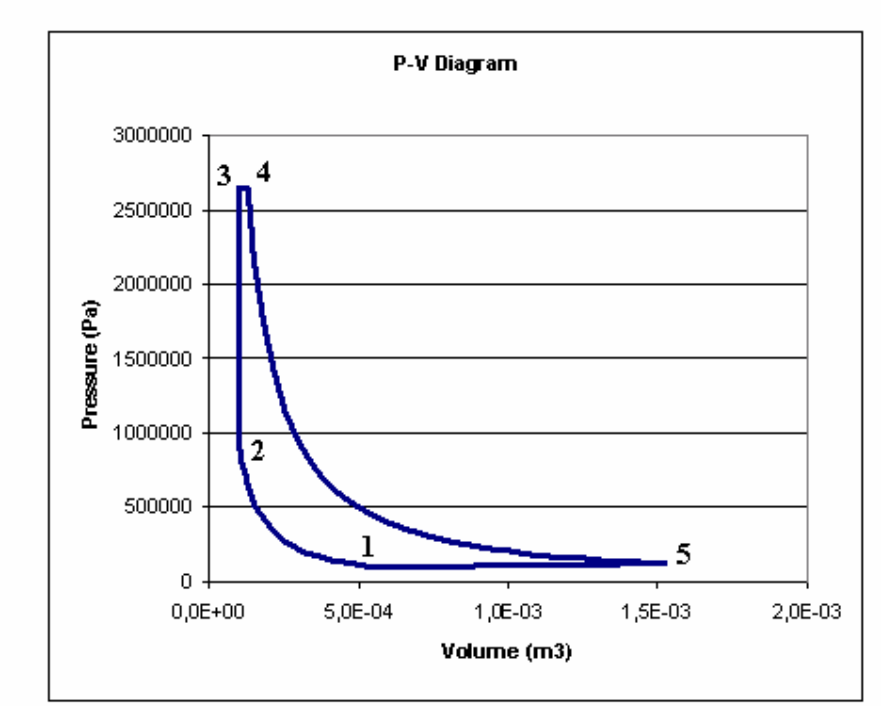

Figure 2.11 p-V Diagram

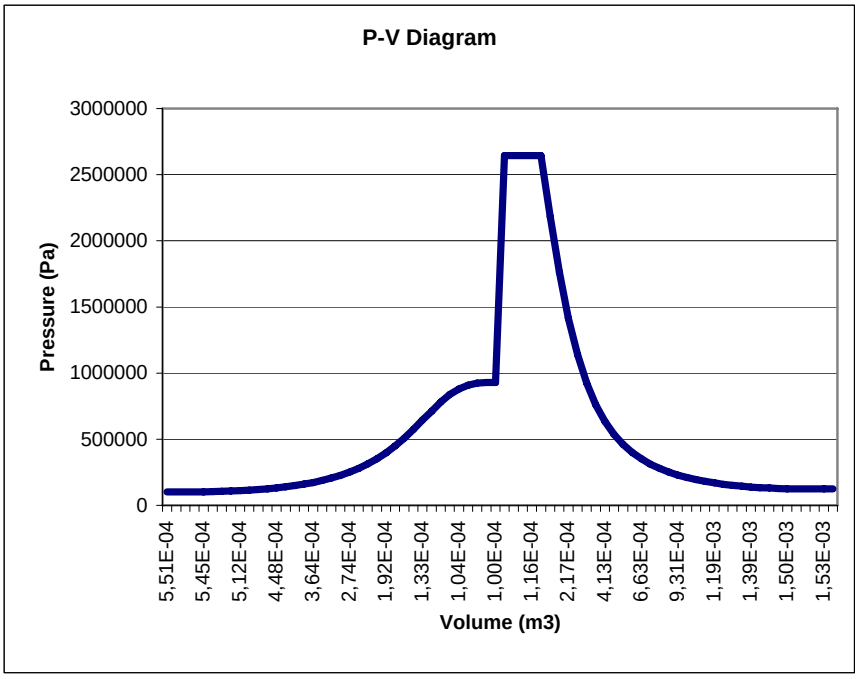

Figure 2.12 Open p-V Diagram

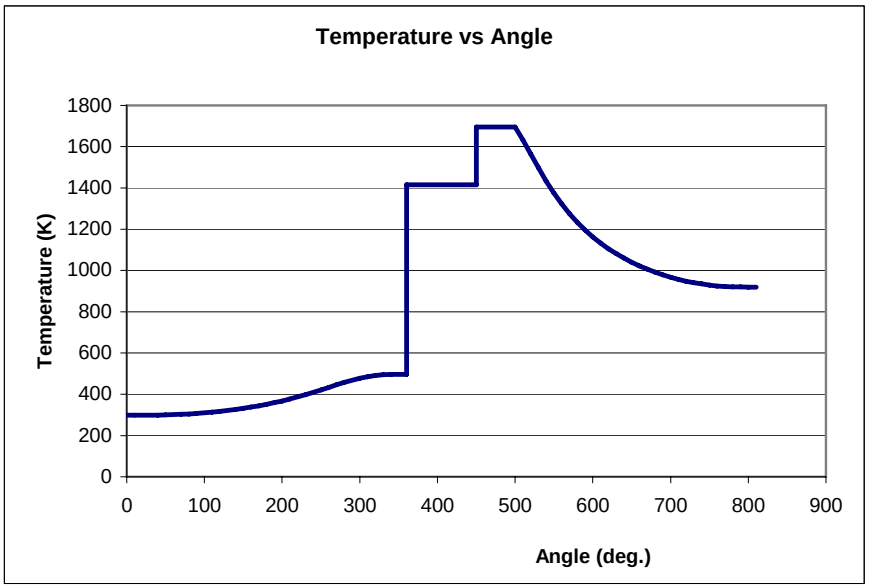

Figure 2.13 Temperatures to Engine Angle Diagram

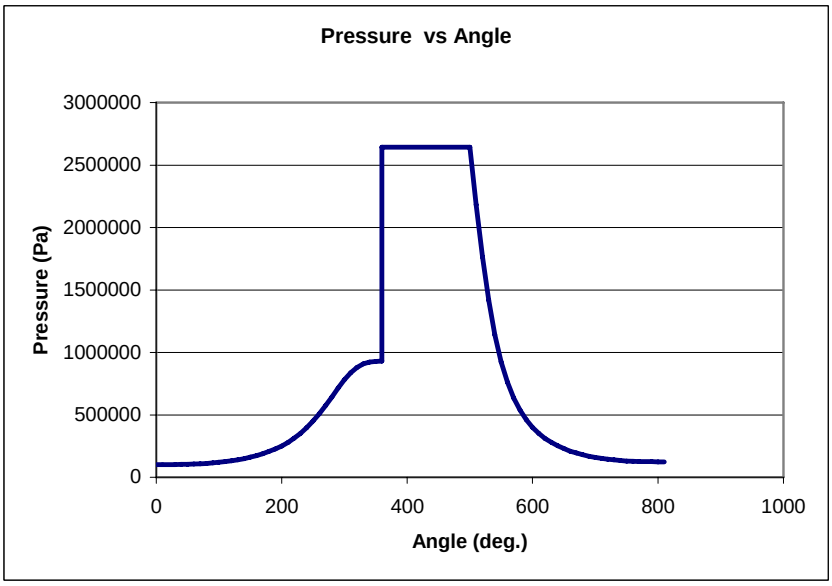

Figure 2.14 Pressures to Engine Angle Diagram

2.2.2.3 2nd Law Analysis

2.2.2.3.1 Entropy Change

The cycle is assumed as ideal to calculate the entropy change trough the cycle.

Compression:

Compression process is assumed as polytrophic, entropy change is calculated as,

$$s_2 - s_1 = c_v \ln\left(\frac{T_2}{T_1}\right) + R\ln\left(\frac{v_2}{v_1}\right) \quad \text{Eq.2.79}$$

Constant Volume Combustion:

$$s_3 - s_2 = c_v \ln\left(\frac{T_3}{T_2}\right) \quad \text{Eq.2.80}$$

Constant Pressure Combustion:

$$s_4 - s_3 = c_p \ln\left(\frac{T_4}{T_3}\right) \quad \text{Eq.2.81}$$

Expansion:

Expansion process is assumed as isentropic process, entropy change is calculated as,

$$s_5 - s_4 = c_v \ln\left(\frac{T_5}{T_4}\right) + R\ln\left(\frac{v_5}{v_4}\right) \quad \text{Eq.2.82}$$

2.2.2.3.2 Availability Analysis

The amount of useful work that can be extracted from the gasses in the engine at each operating point is one of the most important engine performance calculations. The problem is determining the maximum possible work output when a system is taken from one state to another. The first and second laws of thermodynamics are together defines this maximum work as availability [20] or exergy [21].

Availability for each process in the cycle analysis shows the availability transfer and losses in the availability. [22]

The change in availability between states i and j is given by

$$A_j - A_i = m(a_j - a_i) = m[(u_j - u_i) + p_0(v_j - v_i) - T_0(s_j - s_i)] \qquad \text{Eq.2.83}$$

The appropriate normalizing quantity for availability analysis is the thermomechanical availability of the fuel supplied to the engine ($m_f dg$). However, it is more convenient to use Q_f which is $m_f Q_{LHV}$ as the normalizing quantity since it can be related to the temperature rise during combustion. Thermomechanical availability of the fuel and the heat given by the fuel differ only a few percent for common hydrocarbon fuels.

And in the analysis dead state is :
P_0=1 atm
T_0=298.15 K

Compression:
Compression process is assumed as polytropic.

$$A_1 + {}_1W_2 = A_2 + {}_1Q_2\left(1 - \frac{T_0}{T}\right) \qquad \text{Eq.2.84}$$

$$A_2 - A_1 = {}_1W_2 - {}_1Q_2\left(1 - \frac{T_0}{T}\right)$$

$$m[(u_2 - u_1) + p_0(v_2 - v_1) - T_0(s_2 - s_1)] = {}_1W_2 - {}_1Q_2\left(1 - \frac{T_0}{T}\right)$$

Constant Volume Combustion:

In the combustion it is assumed that there is no heat transfer, adiabatic combustion.

$$A_2 = A_3 + {}_2A_{u3} \qquad \text{Eq.2.85}$$

Volumes and internal energies remain constant.

In the Eq.2.78 ${}_2A_{u3}$ is the used availability during the combustion process (2 to 3) which is then used for the constant pressure combustion.

Constant Pressure Combustion:

Constant Pressure Combustion is assumed as adiabatic combustion.

$$A_3 = A_4 + {}_3W_4 + {}_3A_{u4} \qquad \text{Eq.2.86}$$

$$m[(u_4 - u_3) + p_0(v_4 - v_3) - T_0(s_4 - s_3)] = {}_3W_4 + {}_3A_{u4}$$

$$h_3 = h_4 \qquad \text{Eq.2.87}$$

$$u_3 + p_3v_3 = u_4 + p_4v_4$$

$$u_4 - u_3 = p_3v_3 - p_4v_4$$

Expansion:

Expansion process is assumed as polytropic.

$$A_5 + {}_4W_5 = A_5 + {}_4Q_5\left(1 - \frac{T_0}{T}\right) \qquad \text{Eq.2.88}$$

$$m[(u_5 - u_4) + p_0(v_5 - v_4) - T_0(s_5 - s_4)] = {}_4W_5 - {}_4Q_5\left(1 - \frac{T_0}{T}\right)$$

2.2.2.4 2nd Law Analysis Results

Availability change during states is seen on the following table.

Table 2.5 Availability Changes

a_2-a_1	178740	J/kg
a_3-a_2	-223580	J/kg
a_4-a_3	-55398	J/kg
a_5-a_4	-633680	J/kg

Normalized availability changes with the fuel energy are on the following table.

Table 2.6 Normalized Availability Changes

$(a_2-a_1)/Q_f$	0.19014
$(a_3-a_2)/Q_f$	-0.23785
$(a_4-a_3)/Q_f$	-0.05893
$(a_5-a_4)/Q_f$	-0.67412

In the analysis heat transfer and work transfer are not ignored so to understand the engine characteristic, work output and fuel energy usage normalized work quantities are necessary. In the following table work/fuel energy can be seen.

Table 2.7 Normalized Works through the Processes

$_1W_2/Q_f$	-0.20255
$_3W_4/Q_f$	0.00132
$_4W_5/Q_f$	0.87535

In the upper table:

$_1W_2/Q_f$: Fuel energy used for the compression

$_3W_4/Q_f$: Work output in terms of fuel energy during constant pressure combustion

$_4W_5/Q_f$: Work output in terms of fuel energy during expansion

The sum of normalized work quantities give the thermal efficiency of the engine which is found on the 1st Law Analysis.

$\eta_f = 0.67$

The thermal efficiency found here is the same value as found before.

A fundamental measure of the effectiveness of any practical engine is the ratio of the actual work delivered compared with the maximum work. This ratio is called as the availability conversion efficiency.

$$\eta_a = \frac{W_{net}}{\Delta Wu_{\max}} \qquad \text{Eq.2.89}$$

$\Delta Wu_{\max}$ is the maximum useful work transfer to the environment.

$\Delta Wu_{\max}$ can be calculated as a control volume approach around the engine. If we apply 1st Law for this control volume,

$$\Delta Q - \Delta Wu_{\max} = \Delta H \qquad \text{Eq.2.90}$$

And from the 2nd Law,

$$\frac{\Delta Q}{T} \le \Delta S \qquad \text{Eq.2.91}$$

So,

$$\Delta Wu_{\max} \le -\left(\Delta H - T\Delta S\right) \qquad \text{Eq.2.92}$$

$$\Delta Wu_{\max} \le -\left(\Delta G\right) \qquad \text{Eq.2.93}$$

If we return to the Eq.2.88,

$$\eta_a = \frac{W_{net}}{\Delta Wu_{\max}} = -\frac{W_{net}}{\Delta G}$$

$$\eta_a = \frac{W_{net}}{\Delta H}\frac{\Delta H}{\Delta G} = \eta f \frac{\Delta H}{\Delta G}$$

For gasoline $\frac{\Delta H}{\Delta G}$ =-5219.9/-5074.6 =1.0286

$\eta_a = 0.65$

Availability conversion efficiency shows the amount of the availability destroyed in combustion, plus the inability of the ideal cycle to use the availability remaining at the end of the cycle.

CHAPTER 3

STRUCTURAL ANALYSIS of the ENGINE

3.1 Compressor & Turbine

3.1.1 Compressor & Turbine Parts

The rolling piston compressor and turbine are designed by using the geometric data taken from the thermodynamic design code. The design is achieved in CAD environment.

The rolling piston compressor and turbine are composed of a cylinder, upper and lower plates, upper and lower bearing housings, an eccentric, blade, blade spring, roller, a discharge valve and its bearing housing, two timing pulleys and one timing belt and two ports (Figure 3.1.1 and 3.1.2).

As the blade divides the compressor and turbine housing into two parts, for one complete revolution, compressor discharges one unit of compressed air and turbine gets one unit of combusted gases. The compressor valve is so designed that it discharges compressed air to the discharge port at designed angles of roller and turbine intake valve gets combusted gasses into the turbine at designed angles of roller.

The discharge valve and inlet valve are coupled with the rotary compressor rotor with the help of two timing pulleys and one timing belt and revolves at the same rpm with the rotor. The position of the discharge valve relative to the compressor rotor is adjusted with the timing pulleys such that it discharges the compressed air to discharge port at correct times same timing is also done for the turbine intake valve.

An oil pump is used to lubricate the compressor inner surface and the three bearings. (Two main eccentric bearings and one discharge valve bearing)

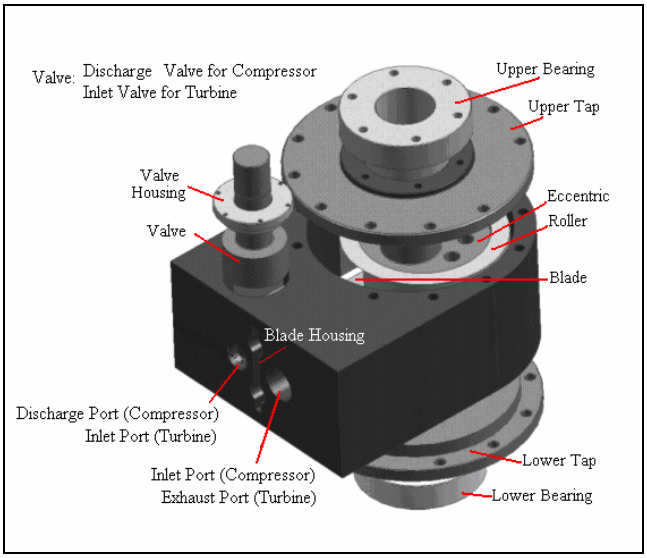

Figure 3.1 Compressor & Turbine Parts

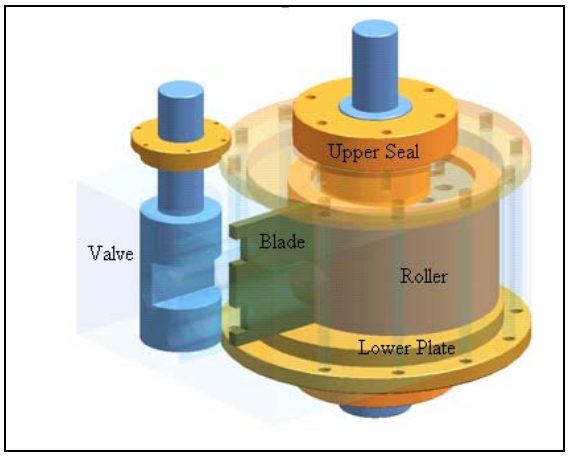

Figure 3.2 Compressor& Turbine Inner Parts

3.1.1.1. Compressor & Turbine Cylinders

Compressor and turbine cylinders are the main body of the compressor and turbine. Eccentric and roller (rotor) is mounted eccentrically in the cylinders.

One discharge port and one inlet port are placed on the compressor cylinder. In the turbine cylinder inlet and exhaust ports are placed.
On the discharge port discharge valve is placed to control the compressed air discharging time.

Blade has housing on the cylinder and in the blade housing there is a spring to keep blade in touch with the roller. And this spring can be adjusted by using the bolts behind the spring, by tightening the bolts blade can be closer to the roller.

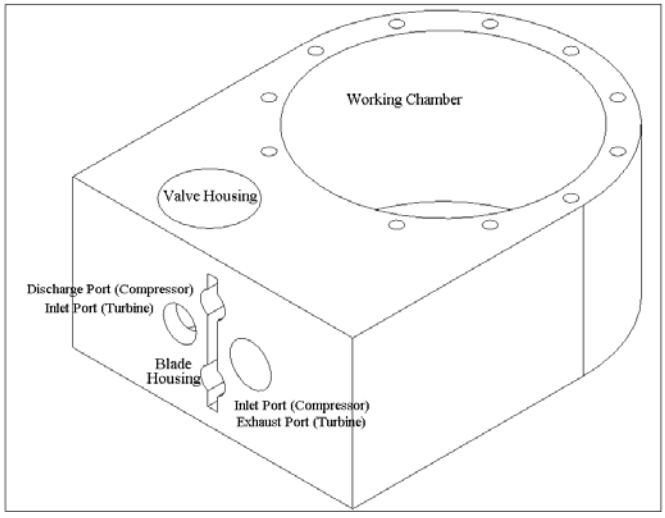

Figure 3.3 Compressor & Turbine Cylinder

3.1.1.2. Compressor & Turbine Plates

Compressor & turbine upper plates and lower plates are similar so the explanation for the plates is done here.

On the plates there exists bearing surfaces for the rotor. And also eccentric and roller rolls under/over the plates, this makes plate critical parts. And plates are mounted to the cylinder by the bolts.

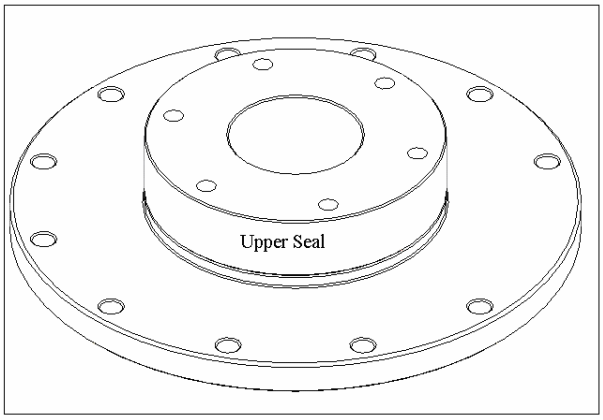

Figure 3.4 Compressor & Turbine Upper Plates

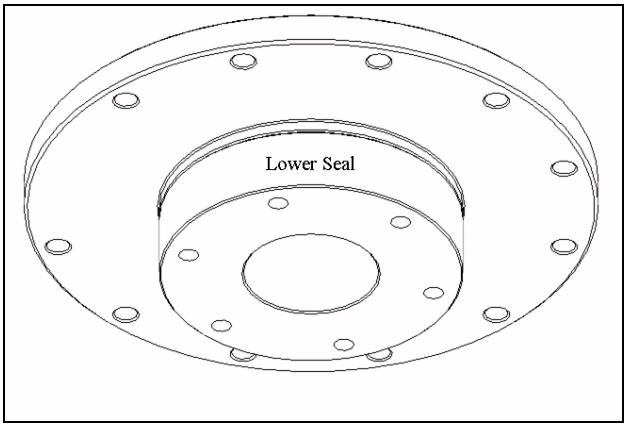

Figure 3.5 Compressor & Turbine Lower Plates

3.1.1.3. Compressor & Turbine Eccentrics

Eccentric is placed in the cylinder and it has two bearings on the plates.

Eccentric is not directly connected to the air there is roller between eccentric and the air. Eccentric has oil channels for heat rejection and lubrication purposes.

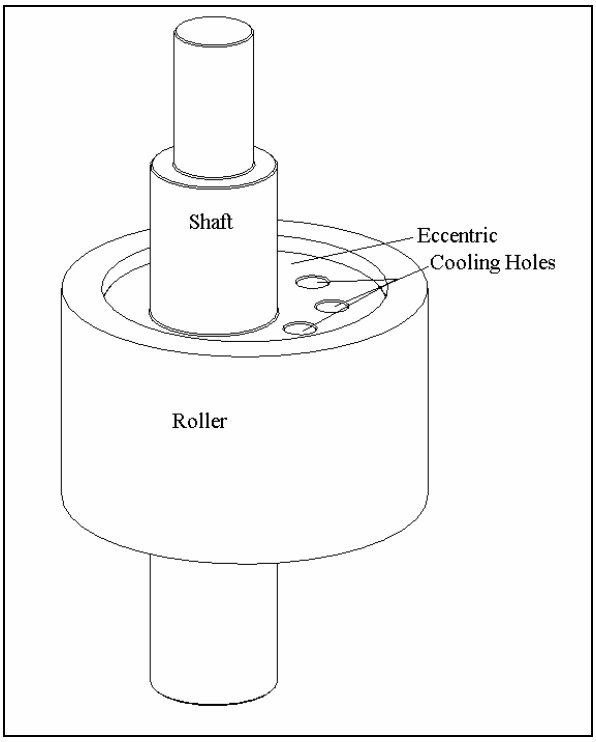

Figure 3.6 Compressor & Turbine Rotor

3.1.1.4. Compressor & Turbine Rollers

Roller is placed on the eccentric.

Roller is in the contact with the blade and also it rotates through the cylinder without touching.

Among the parts of the compressor & turbine it is the most critical rotary part, because any fault of the roller causes pressure loss in the compressor.

By just replacing the roller the compressor mean time between failures is increased.

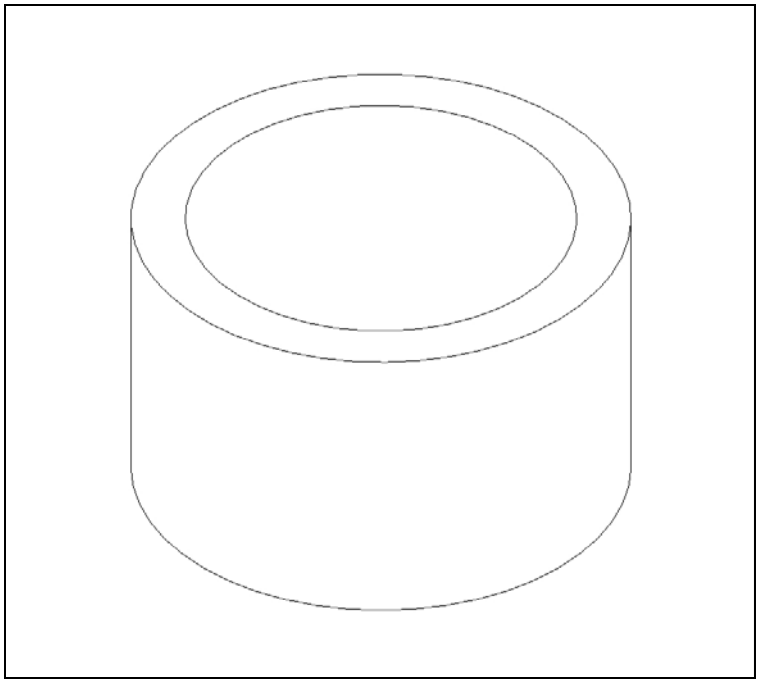

Figure 3.7 Compressor & Turbine Roller

3.1.1.5. Compressor & Turbine Blades

Compressor and turbine blades are sliders that work through the housing in the cylinders.

A spring is placed behind it to support the spring.
Spring is used to push the blade to the roller and also to guarantee the blade to be in touch with the roller all the time.

When the roller pushes it to the housing in the cylinder spring is compressed and by the rotation of the roller blade spring discharges its energy to the blade so blade can always be in contact with the roller.

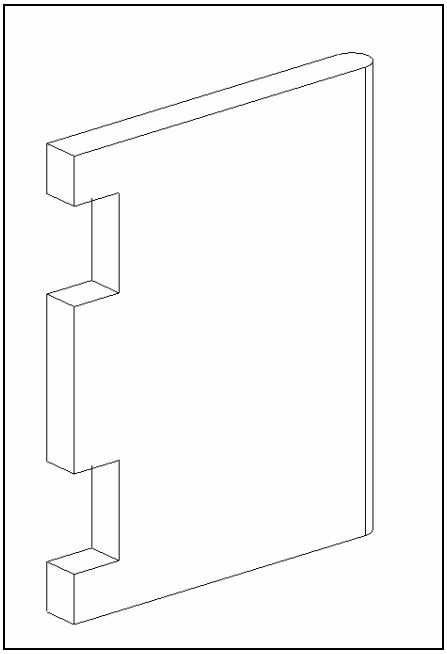

Figure 3.8 Compressor & Turbine Blade

3.1.1.6. Compressor Discharge Valve & Turbine Inlet Valves

Discharge valve is placed with in its housing inside the cylinder of the compressor and the turbine inlet valve is placed with in its housing inside the cylinder of the turbine.

Valves are directly coupled with the rotor by the help of timing pulleys and timing belt and rotate at the same rpm with the rotor.

Discharge and inlet timing is adjusted by the timing pulleys and belt.

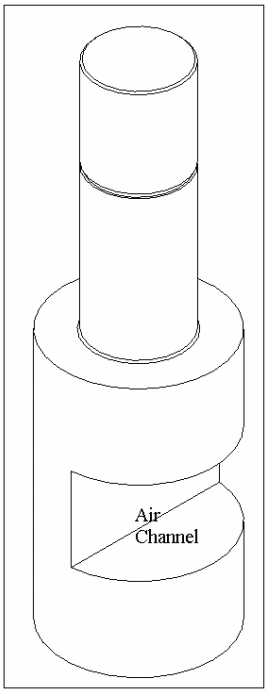

Figure 3.9 Compressor Discharge Valve & Turbine Inlet Valve

3.1.2. Material Selection

H13 Hot Work Tool Steel is selected as the material of the compressor & turbine.

The selection criteria of the material are given below;

- Excellent wear resistance and hot toughness.
- High thermal shock resistance.
- Good thermal conductivity and tolerate some water cooling in service.
- High temperature tensile strength.
- Good machinability.

3.1.3. Thermal and Structural Analysis of Compressor & Turbine

Structural analyses of the rotating eccentric (rolling piston) compressor & turbine of the novel engine are done in NX NASTRAN Environment (Finite Element Program). The aim of this work is to select the material of the compressor parts. To do the structural analysis, firstly the critical parts are defined as follows;

- Stress distribution on the housing and the plates of the compressor & turbine due to pressure and temperature exerted by the compressed air onto the inner surfaces.
- Stress distribution on the rotor due to pressure and temperature exerted by the air, together with the centrifugal force caused by rotation.
- Stress distribution on the blade due to pressure and temperature exerted by the air, together.
- Stress distribution on the valve due to pressure and temperature exerted by the air, together with the centrifugal force caused by rotation.

To make the structural analysis of the compressor & turbine, the necessary temperature and pressure data is taken from the thermodynamic design code where the temperature and pressure data is given with respect to compressor & turbine rotor angle as explained in the previous chapter.

In the analyses following method is used:

Boundary Conditions

Defined on the figures

Loads

Convection on divided surfaces

Pressure load on divided surfaces

Assumptions

Temperature and pressure values calculated by the thermodynamic code are approximated on the divided inner surfaces.

Compressor: Convection Heat Transfer Coefficient for compressed air is approximated as 40 W/m^2 .K Convection Heat Transfer Coefficient for cooling air is approximated as 100 W/m^2 .K

Turbine: Convection Heat Transfer Coefficient for combusted air is approximated as 50 W/m^2.K. Convection Heat Transfer Coefficient for cooling air is approximated as 100 W/m^2 .K

The calculation of the heat transfer coefficients are explained in the thermodynamics part.

Firstly, thermal analyses of the parts are done to determine the temperatures on each node due to convection between the air and the inner surfaces and between the cooling air and the outer surfaces of the parts.

Secondly, structural analyses of the parts are done to determine the stress distribution and the deformation on the parts. The temperatures calculated in the thermal analysis are applied to the nodes as thermal load and the air pressure is applied to the inner surfaces of the parts as pressure load.

The results of the analysis showed that the stress values on the parts are in the elastic region and most of the cases are much below the yield tensile strength of the material and can be safely used.

3.1.3.1 Thermal and Structural Analysis of the Compressor

3.1.3.1.1 Thermal and Structural Analysis of the Compressor Cylinder

Loads on the compressor cylinder are seen on the figure 3.10.

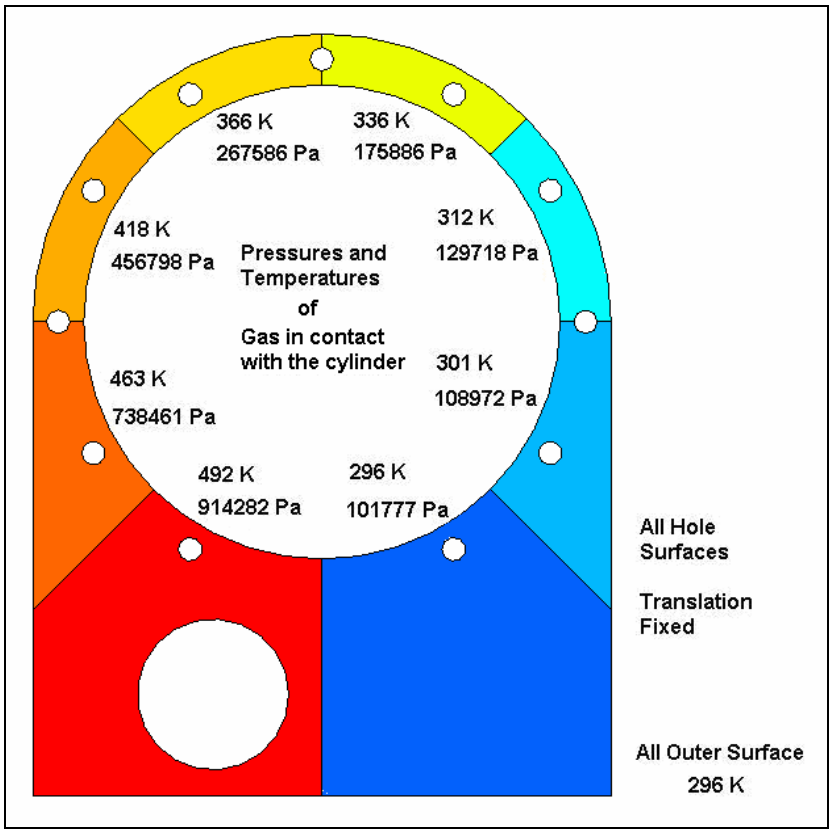

Figure 3.10 Structural Analysis Model of the Compressor Cylinder

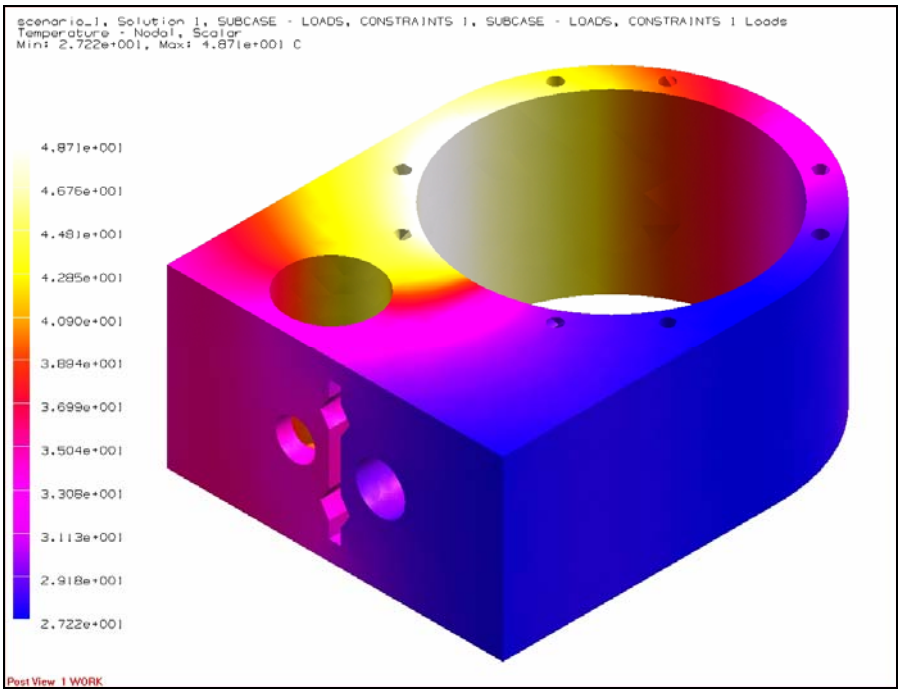

Figure 3.11 Temperature Distributions on Compressor Cylinder

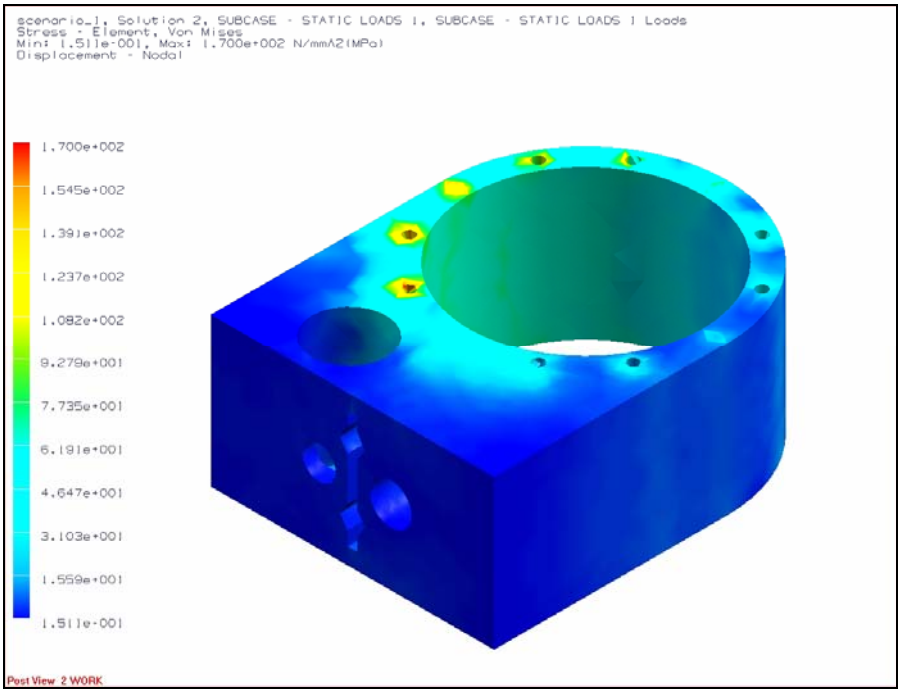

Figure 3.12 Stress Distributions on the Compressor Cylinder

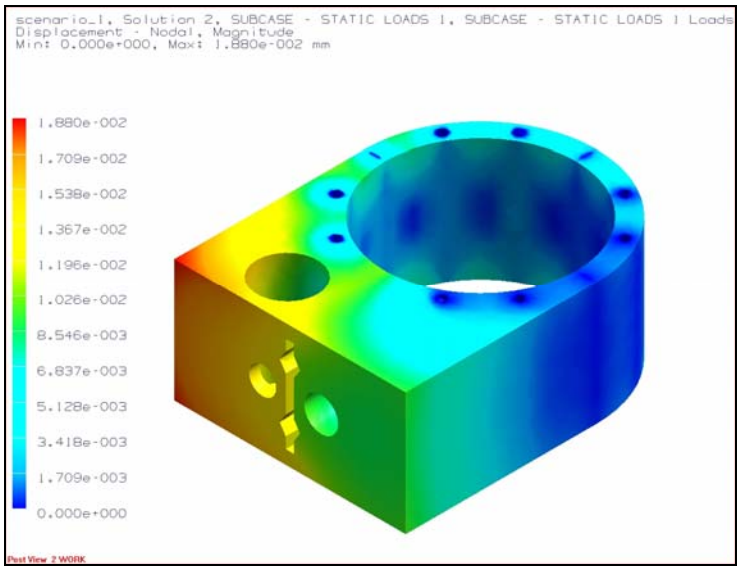

Figure 3.13 Deformations on the Compressor Cylinder

3.1.3.1.2 Thermal and Structural Analysis of the Compressor Plates

Loads on the compressor plates are seen on the figure 3.14.

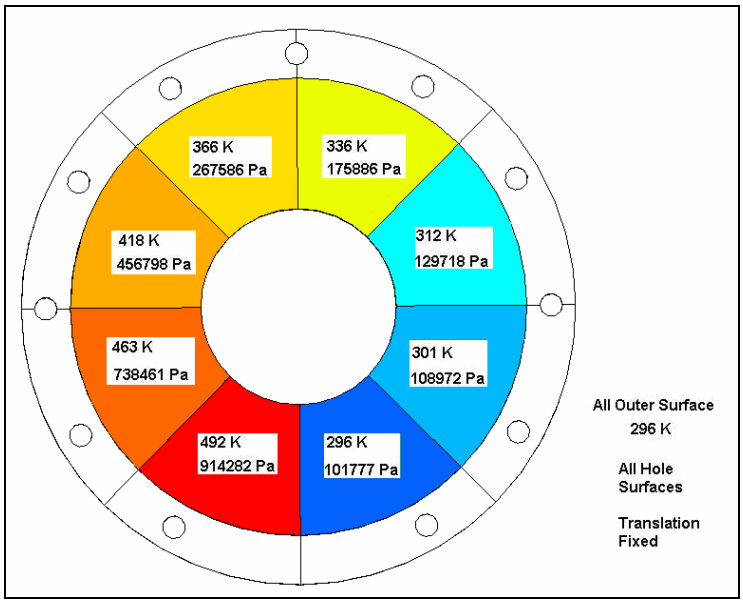

Figure 3.14 Structural Analysis Models of the Compressor Plates

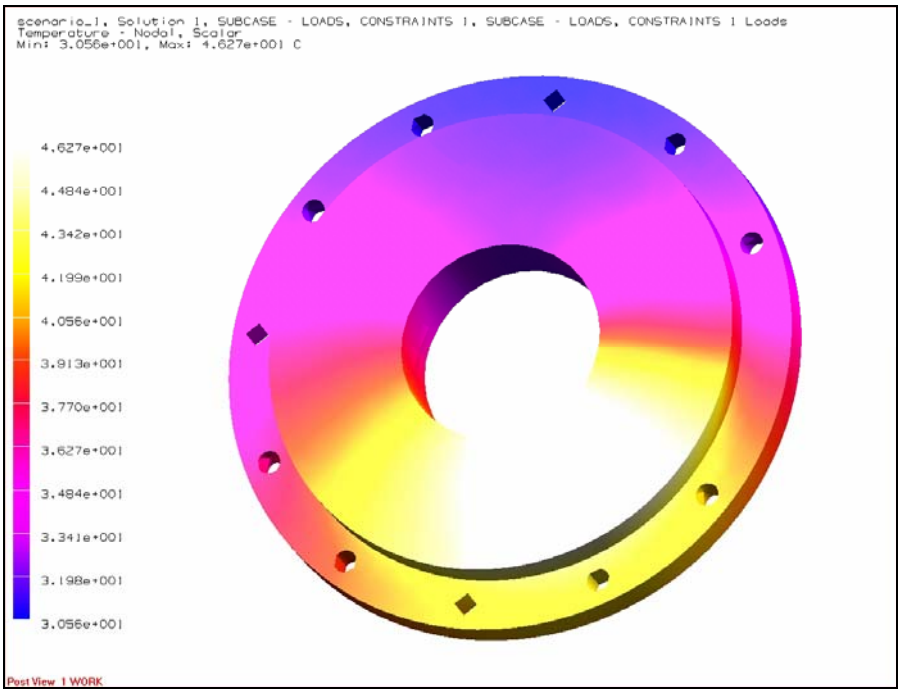

Figure 3.15 Temperature Distributions on Compressor Plates

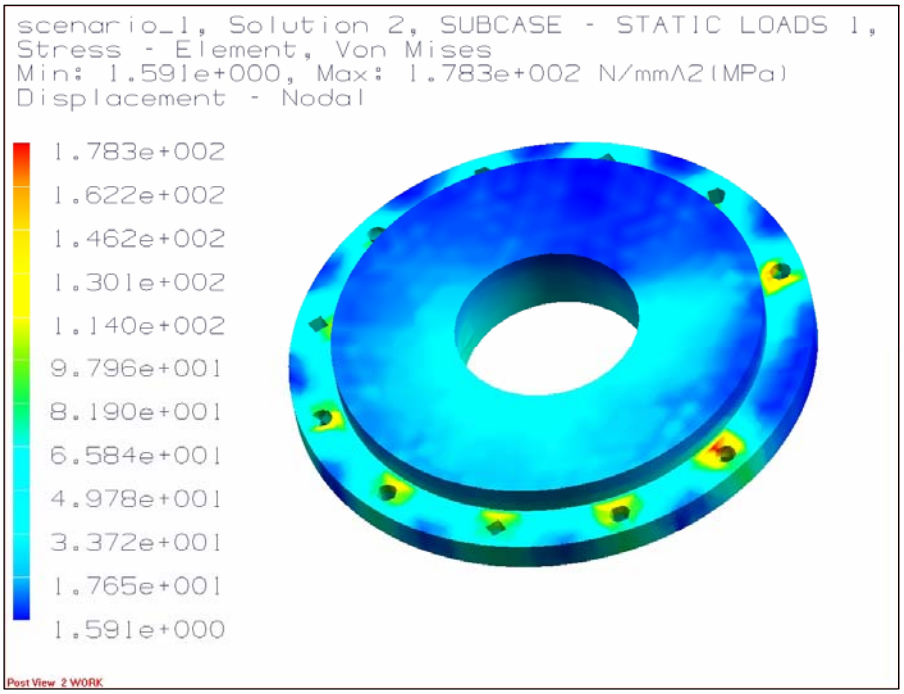

Figure 3.16 Stress Distributions on the Compressor Plates

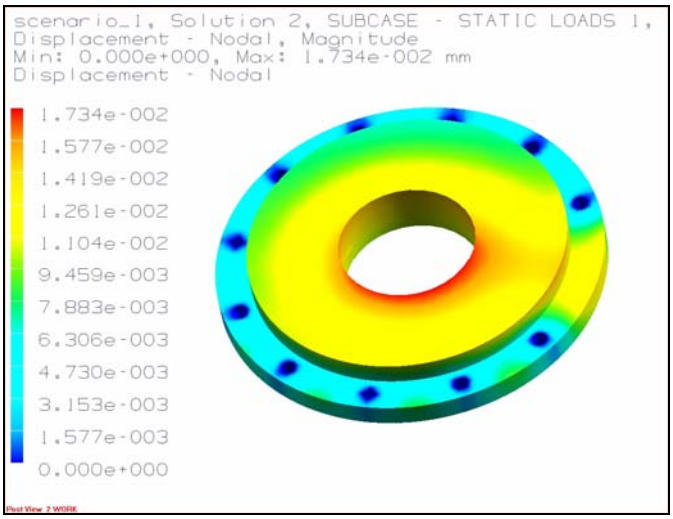

Figure 3.17 Deformations on the Compressor Plates

3.1.3.1.3 Thermal and Structural Analysis of the Compressor Rotor

Compressor rotor has pressure and temperature loads as the other components but it also has angular velocity of 6000 RPM.

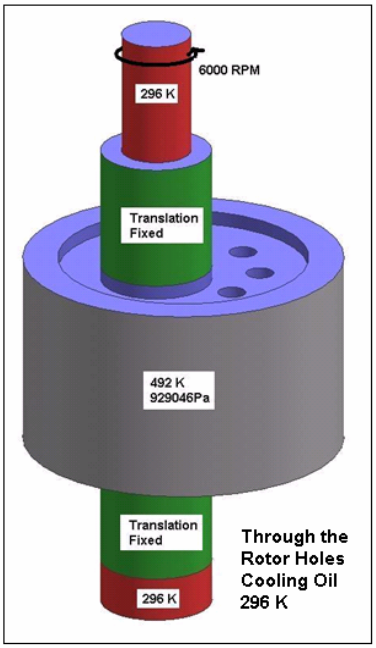

Figure 3.18 Structural Analysis Model of the Compressor Rotor

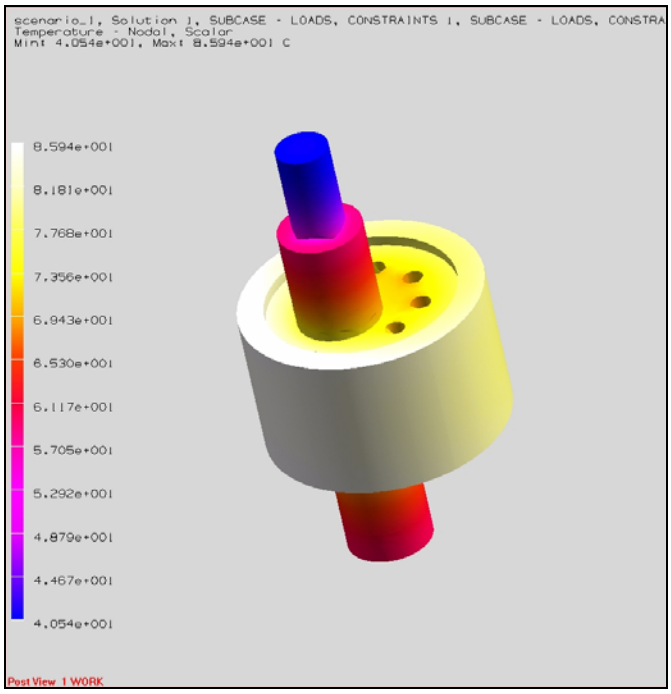

Figure 3.19 Temperature Distributions on Compressor Rotor

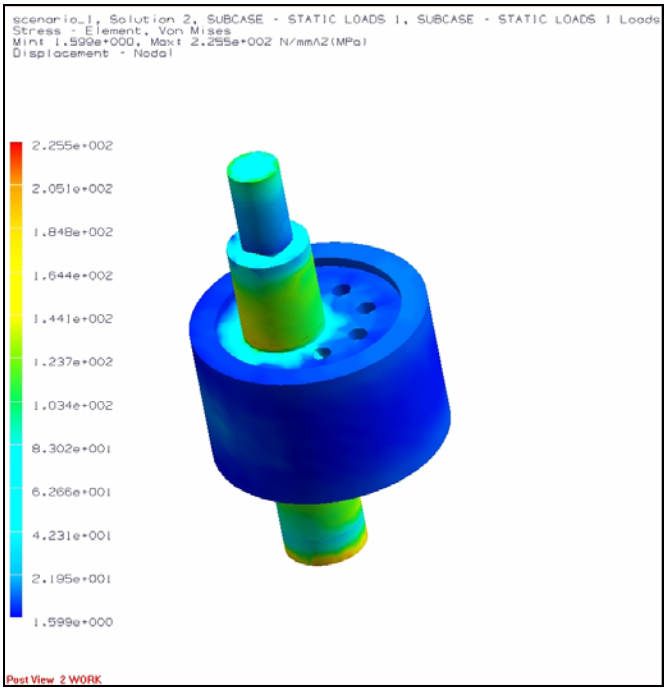

Figure 3.20 Stress Distributions on the Compressor Rotor

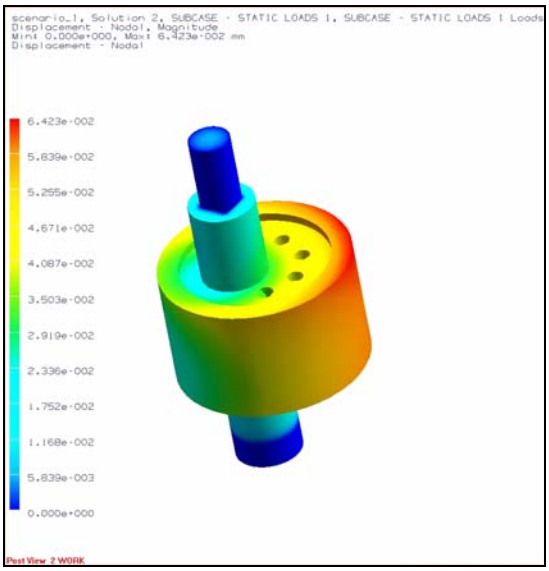

Figure 3.21 Deformations on the Compressor Rotor

3.1.3.1.4 Thermal and Structural Analysis of the Compressor Blade

Loads on the compressor blade are seen on the figure 3.22.

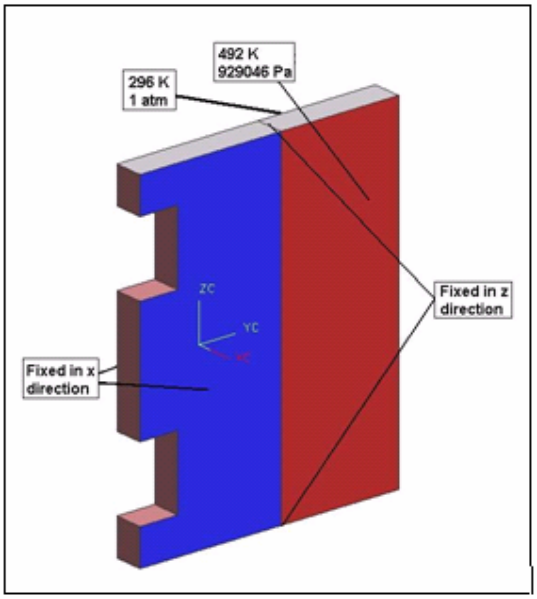

Figure 3.22 Structural Analysis Model of the Compressor Blade

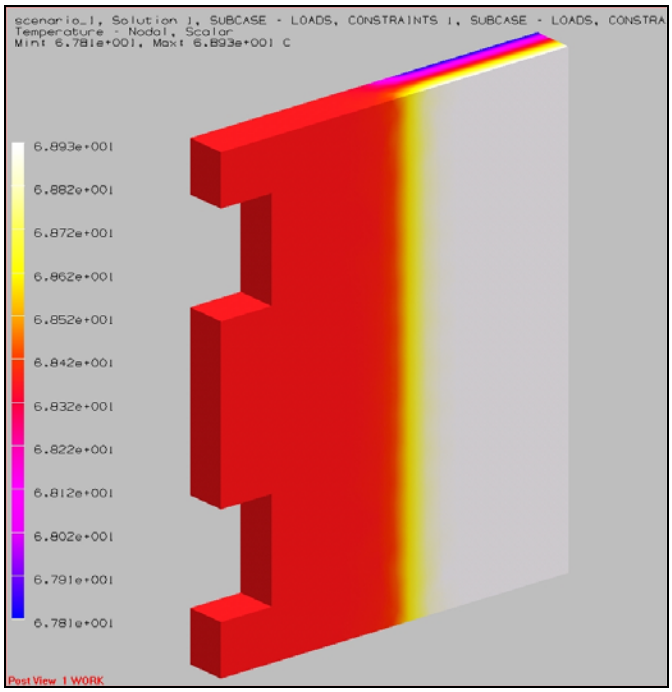

Figure 3.23 Temperature Distributions on Compressor Blade

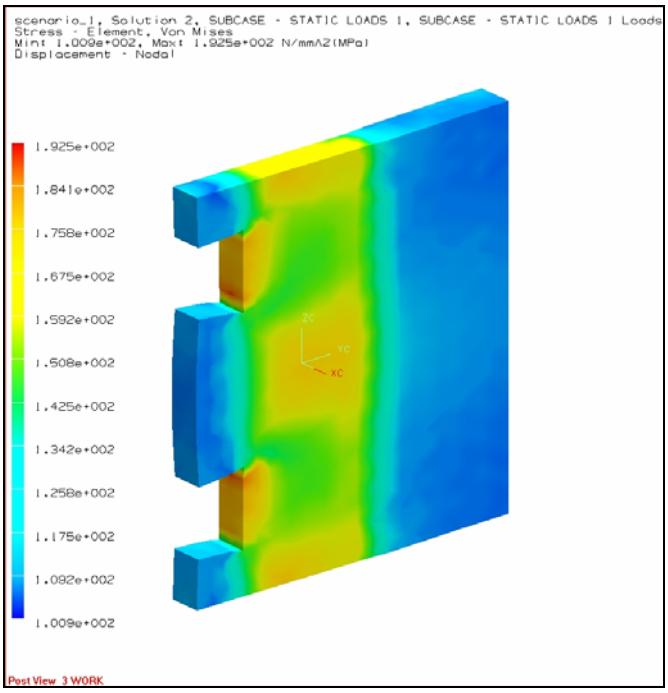

Figure 3.24 Stress Distributions on the Compressor Blade

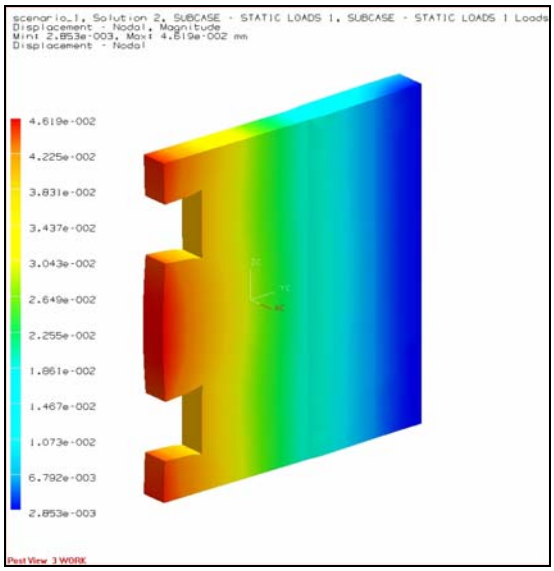

Figure 3.25 Deformations on the Compressor Blade

3.1.3.1.5 Thermal and Structural Analysis of the Compressor Discharge Valve

Compressor discharge valve has temperature, pressure loads as the other components and also it has 6000 RPM angular speed like the rotor.

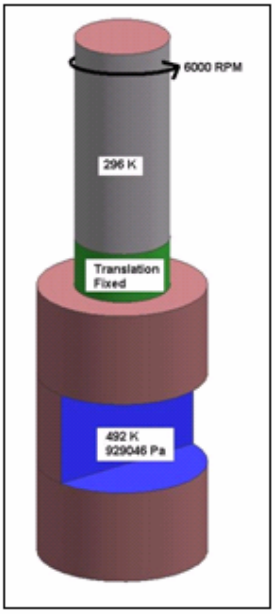

Figure 3.26 Structural Analysis Model of the Compressor Discharge Valve

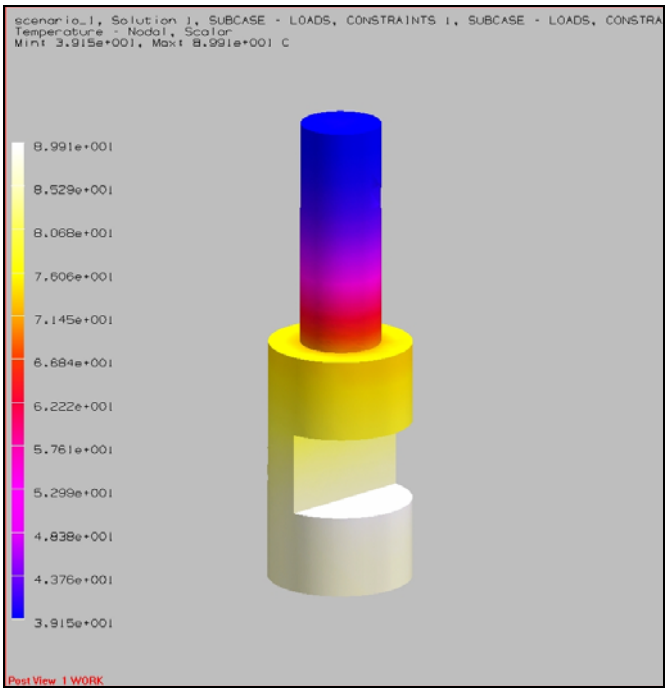

Figure 3.27 Temperature Distributions on the Compressor Discharge Valve

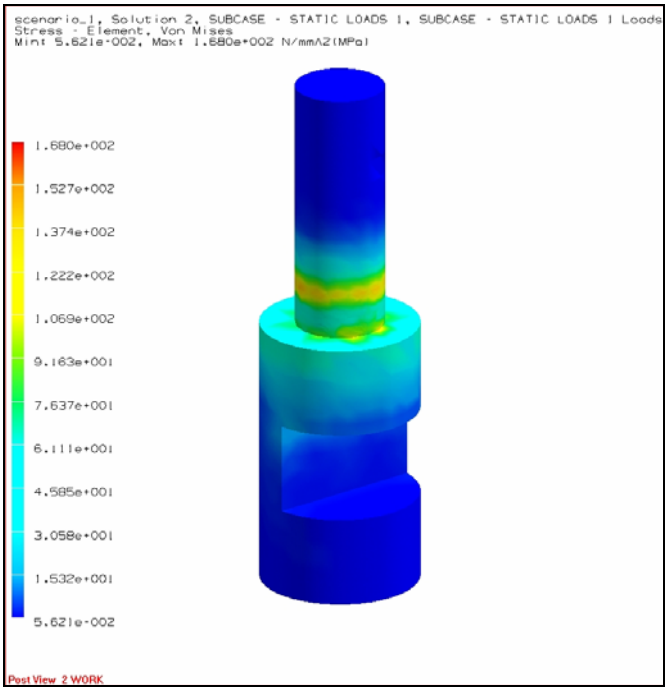

Figure 3.28 Stress Distributions on the Compressor Discharge Valve

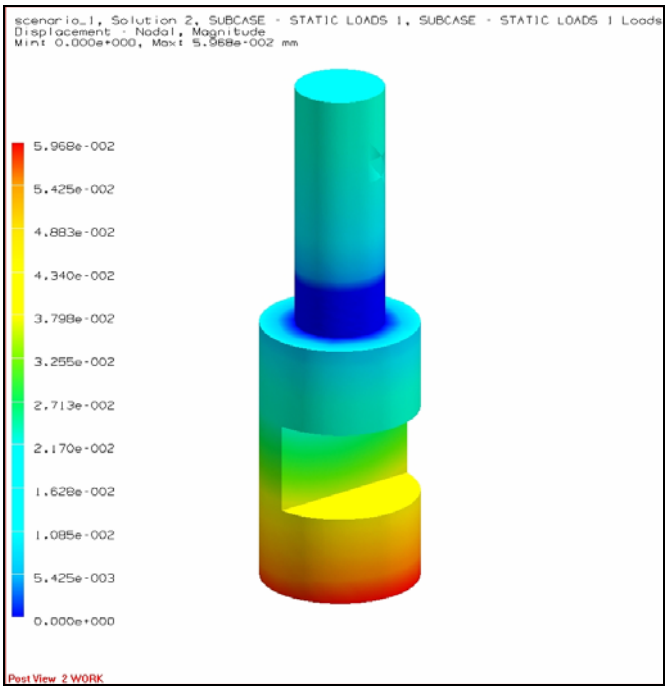

Figure 3.29 Deformations on the Compressor Discharge Valve

3.1.3.1.6 Thermal and Structural Analysis Results of the Compressor Parts

The results of the analysis for the compressor are seen on the Table 3.1

Table 3.1 Thermal and Structural Analysis Results of the Compressor Parts

COMPRESSOR					
	Cylinder	**Plates**	**Rotor**	**Blade**	**Discharge Valve**
Max. Temperature (^{o}C)	48.70	46.3	85.9	68.9	89.9
Max. Stress (Mpa)	170	178	225	192	168
Max. Deformation (mm)	1.88e-02	1.73e-02	6.42e-02	4.62e-02	5.97e-02

3.1.3.2 Thermal and Structural Analysis of Turbine

3.1.3.2.1 Thermal and Structural Analysis of the Turbine Cylinder

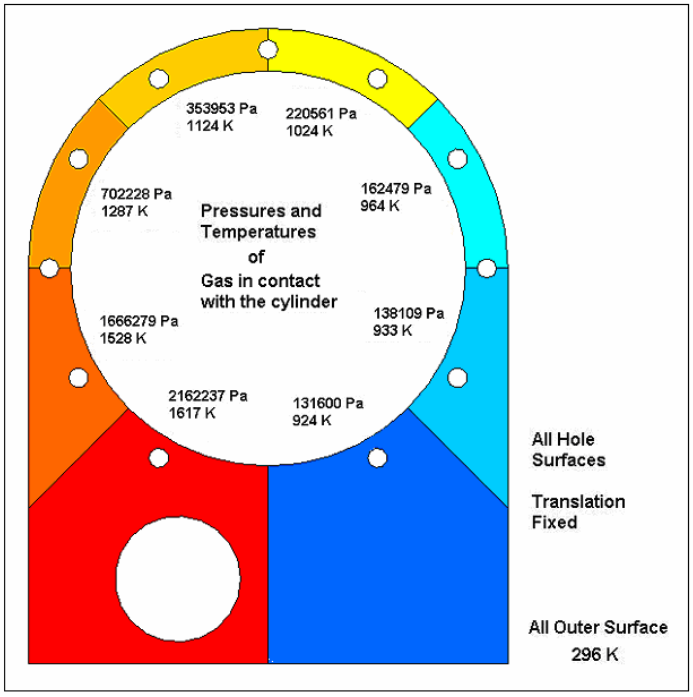

Figure 3.30 Structural Analysis Model of the Turbine Cylinder

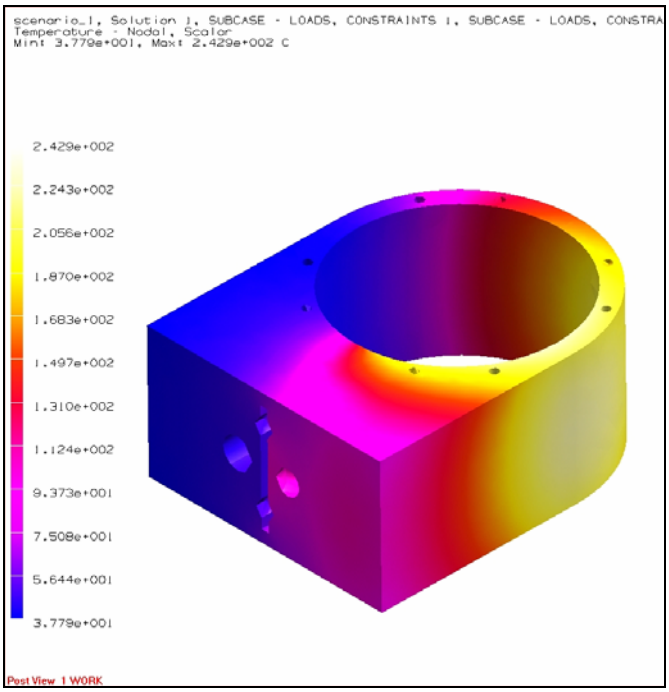

Figure 3.31 Temperature Distributions on Turbine Cylinder

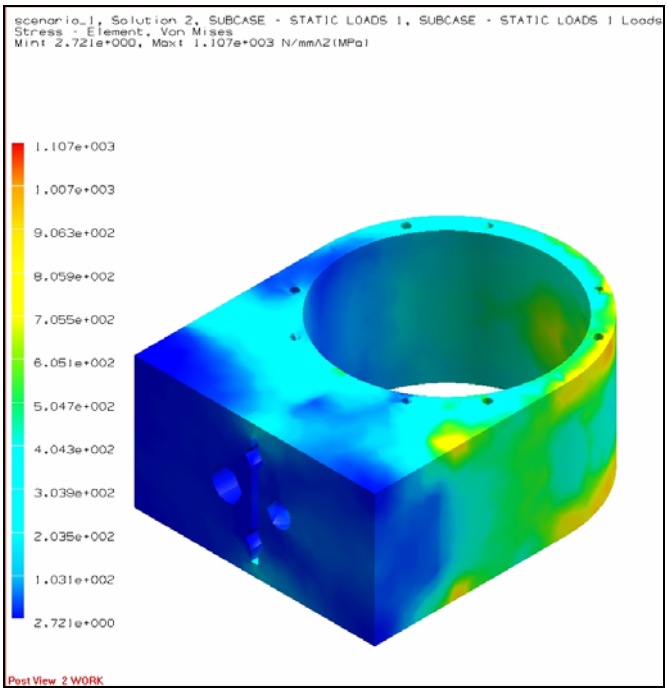

Figure 3.32 Stress Distributions on the Turbine Cylinder

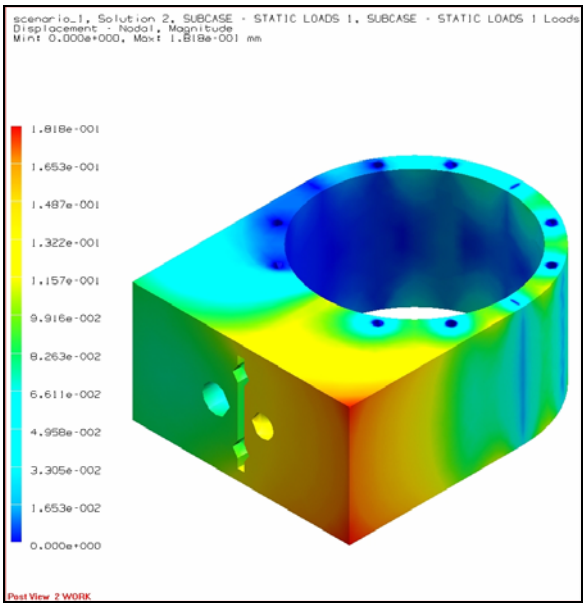

Figure 3.33 Deformation on the Turbine Cylinder

3.1.3.2.2 Thermal and Structural Analysis of the Turbine Plates

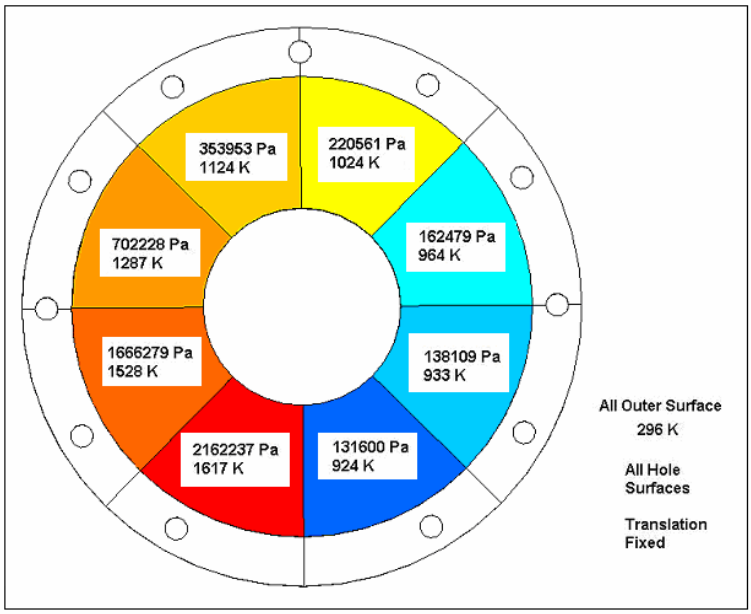

Figure 3.34 Structural Analysis Models of the Turbine Plates

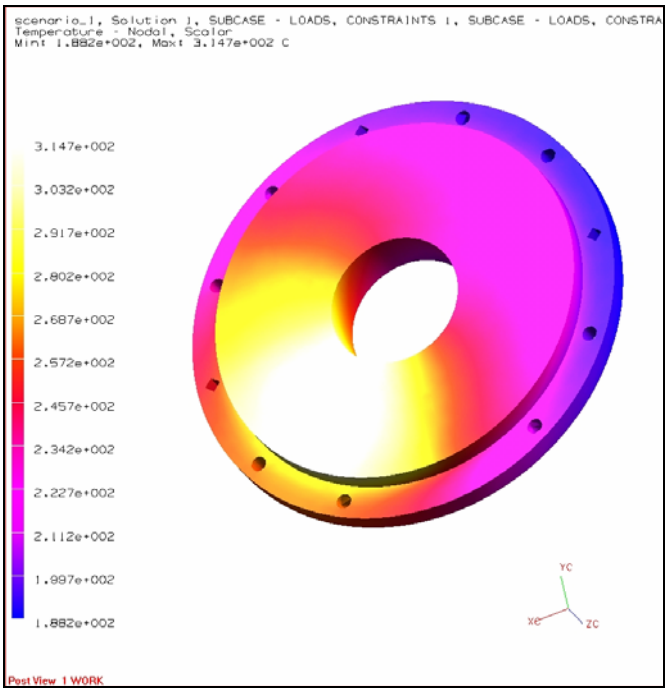

Figure 3.35 Temperature Distributions on Turbine Plates

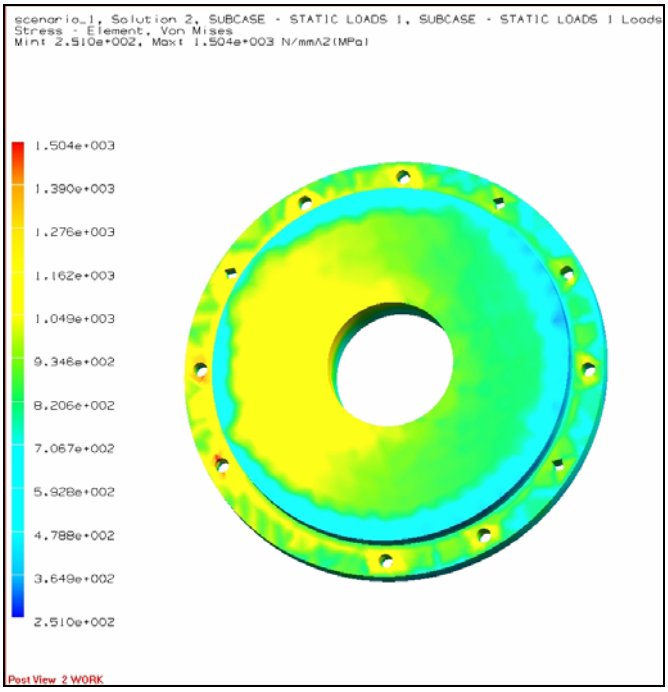

Figure 3.36 Stress Distributions on the Turbine Plates

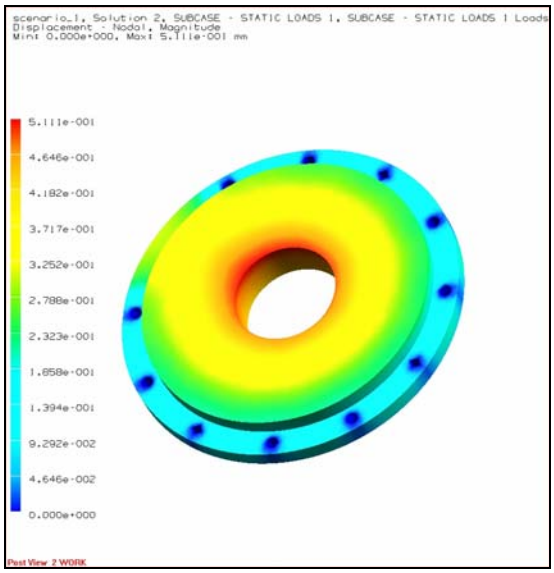

Figure 3.37 Deformations on the Turbine Plates

3.1.3.2.3 Thermal and Structural Analysis of the Turbine Rotor

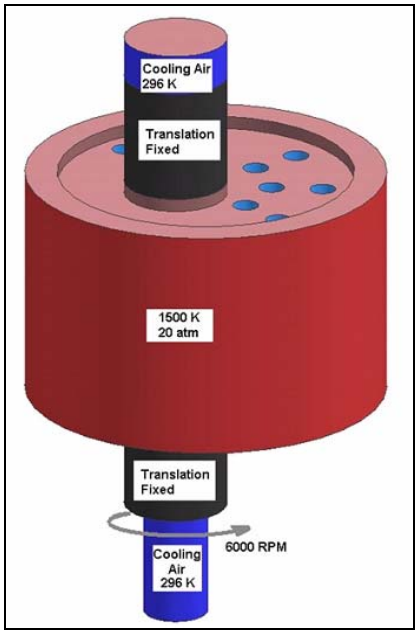

Figure 3.38 Structural Analysis Model of the Turbine Rotor

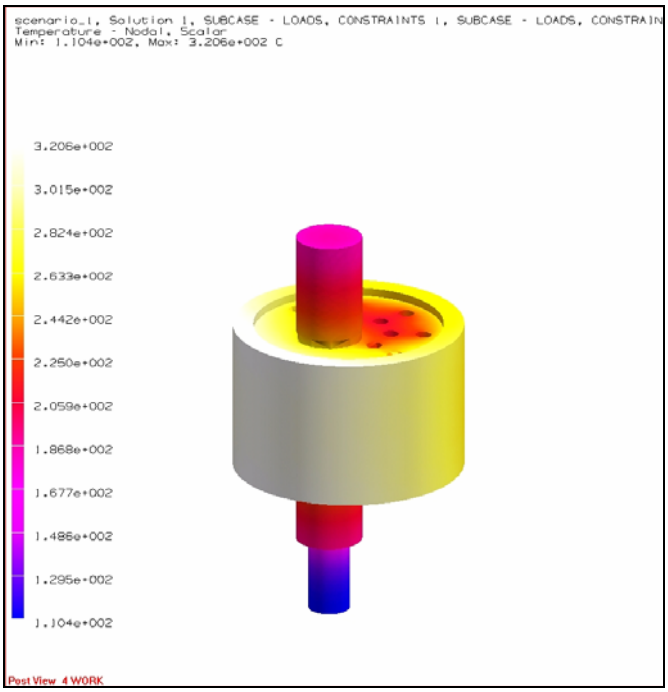

Figure 3.39 Temperature Distributions on Turbine Rotor

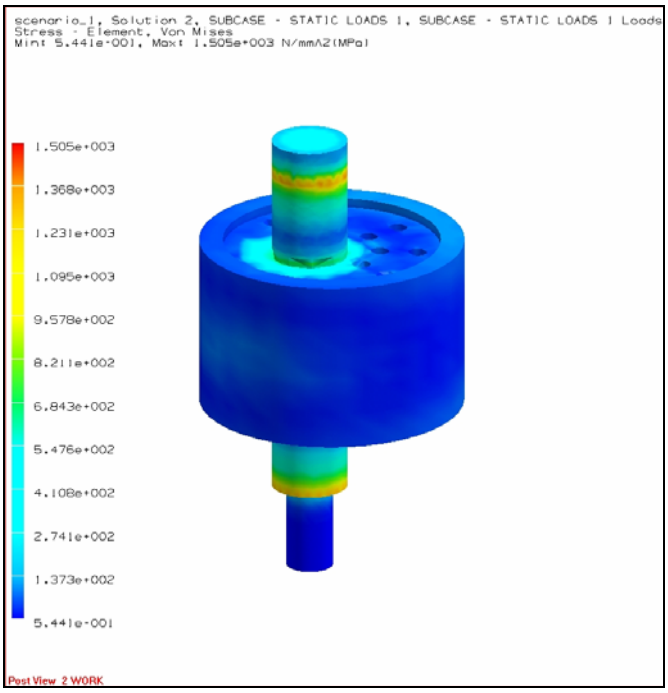

Figure 3.40 Stress Distributions on the Turbine Rotor

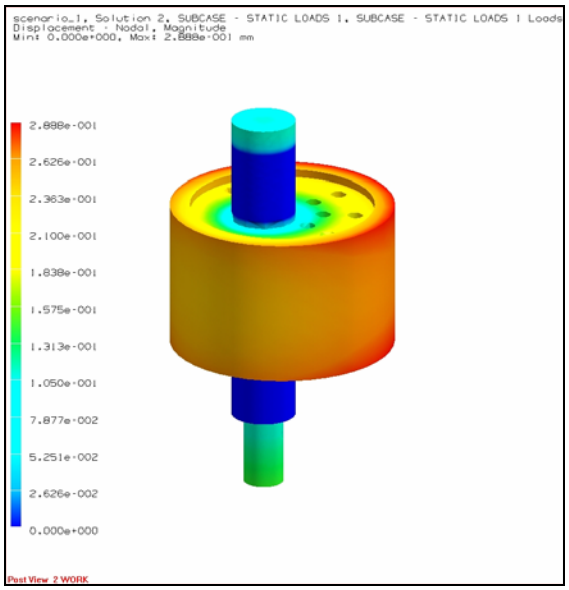

Figure 3.41 Deformations on the Turbine Rotor

3.1.3.2.4 Thermal and Structural Analysis of the Turbine Blade

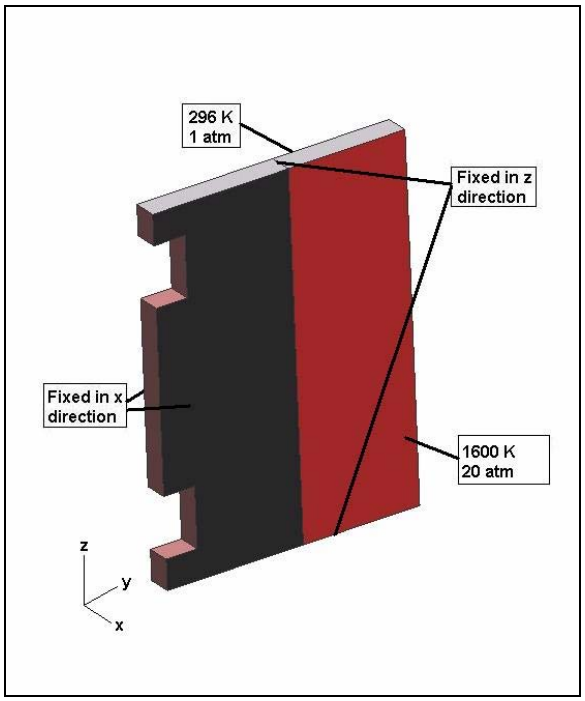

Figure 3.42 Structural Analysis Model of the Turbine Blade

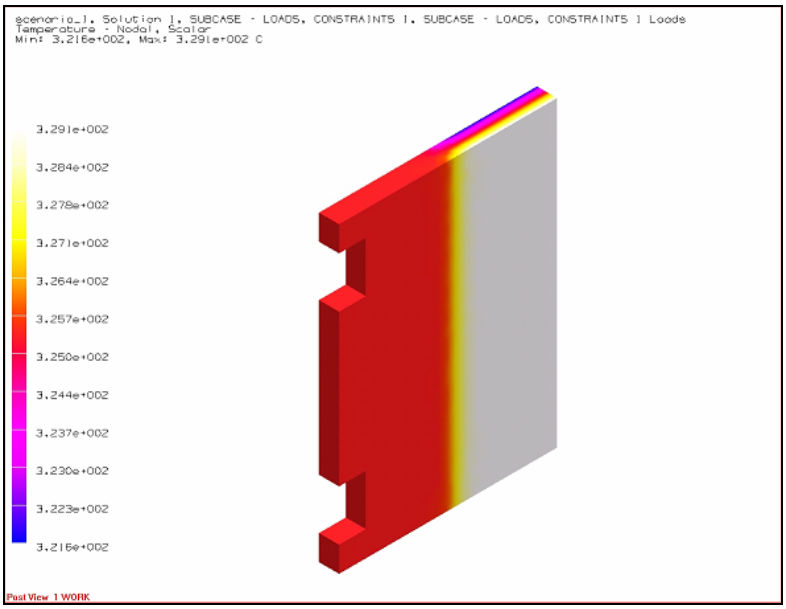

Figure 3.43 Temperature Distributions on Turbine Blade

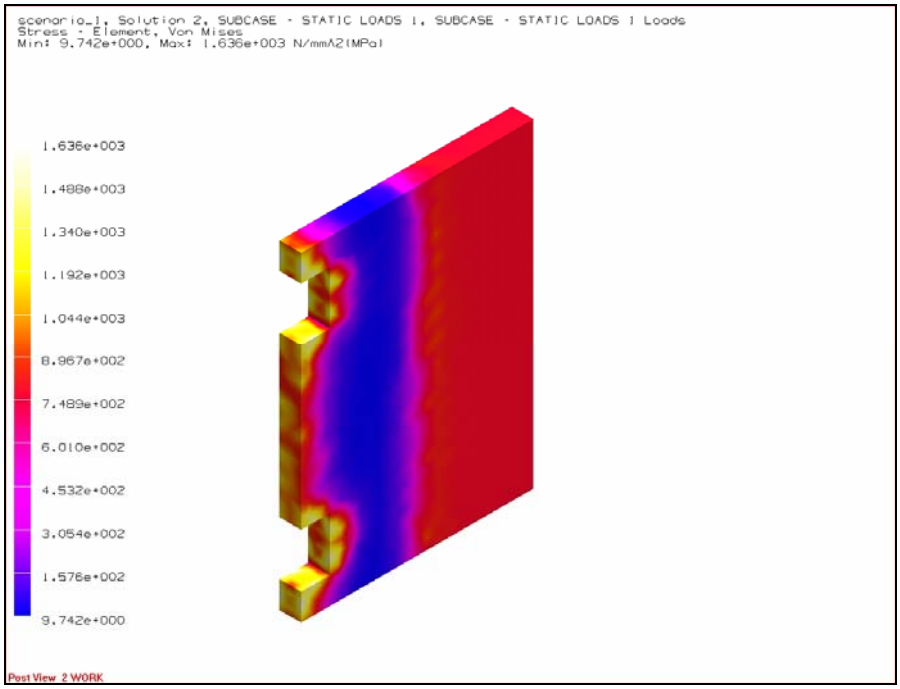

Figure 3.44 Stress Distributions on the Turbine Blade

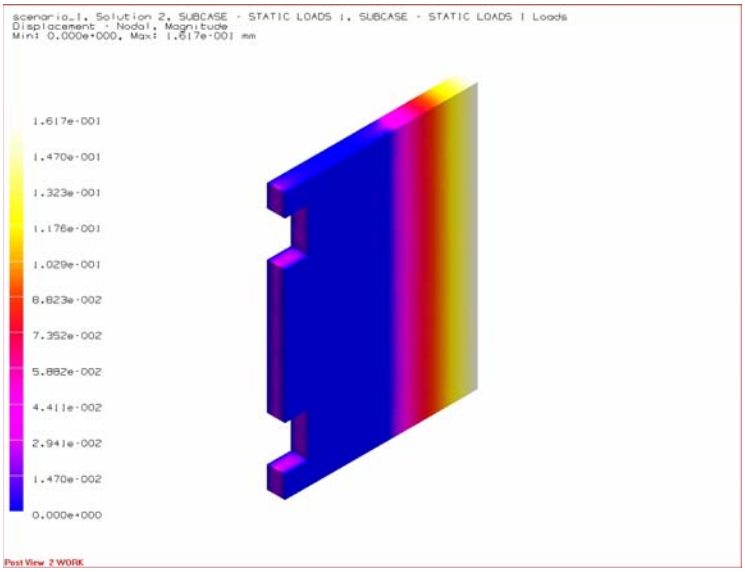

Figure 3.45 Deformations on the Turbine Blade

3.1.3.2.5 Thermal and Structural Analysis of the Turbine Inlet Valve

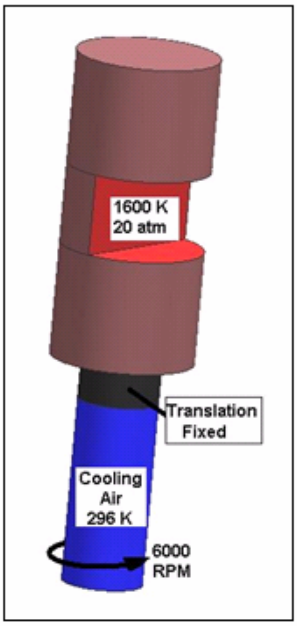

Figure 3.46 Structural Analysis Model of the the Turbine Inlet Valve

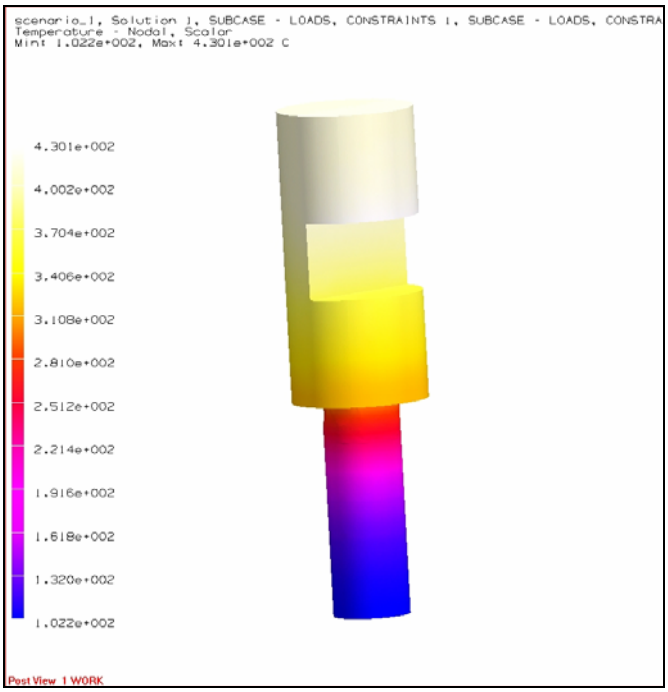

Figure 3.47 Temperature Distributions on the Turbine Inlet Valve

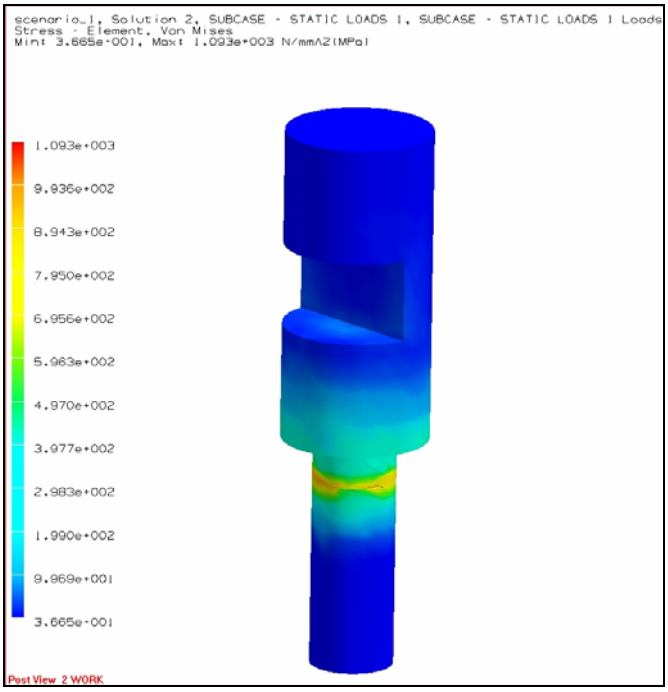

Figure 3.48 Stress Distributions on the Turbine Inlet Valve

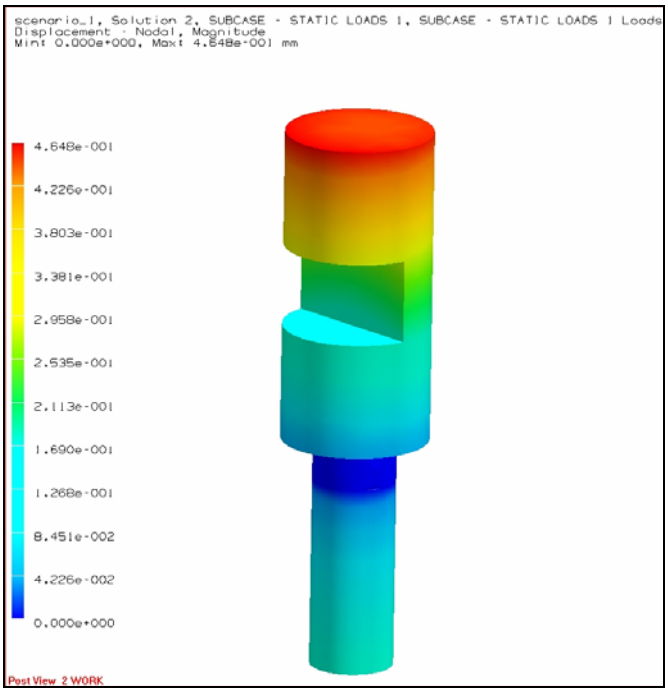

Figure 3.49 Deformations on the Turbine Inlet Valve

3.1.3.2.6 Thermal and Structural Analysis Results of the Turbine Parts

The results of the analysis for the turbine are seen on the Table 3.2

Table 3.2 Thermal and Structural Analysis Results of the Turbine Parts

TURBINE					
	Cylinder	**Plates**	**Rotor**	**Blade**	**Discharge Valve**
Max. Temperature (^{o}C)	243	314.7	320.6	329.1	430.1
Max. Stress (Mpa)	1107	1504	1505	1636	1093
Max. Deformation (mm)	1.82 e-01	5.11e-01	2.88e-01	1.62e-01	4.65e-01

3.1.4 Discussions of the Thermal and Structural Analysis

The structural analyses of the turbine & compressor parts are done using H13 material (see the Appendix for the material properties).

The temperatures of the gasses are defined by the thermodynamic design code. Temperature distributions of the parts are calculated by using FEA program NX Nastran. Convection between the gasses and the parts, convection between the cooling air and the parts and conduction through the parts are calculated by using the program. Empirical formulas are used to calculate the convection coefficients.

In the structure analysis of the compressor & turbine cylinders the stress values are much below the yield strength value of the material. The high stress concentrations are found where the gasses temperature is high and the bolt holes. The stress on the bolt holes are much higher because of the displacement restrictions caused by the bolts.

The structure analysis results of the compressor & turbine plates are similar to the cylinders because they are affected by the same gasses. The critical result obtained from this analysis is the deflection on the inner surface of the turbine plate. In manufacturing of the engine tolerances should be arranged to satisfy the turbine plate inner surface deflection.

Compressor & turbine rotors are under the heavy loads. Temperature, pressure and centrifugal loads are applied to the rotors. The main reason causing high stress on the rotors is the temperature. Analysis shows that effective turbine cooling by the oil is necessary to work properly.

In the analysis more loads than actual ones are applied to the compressor & turbine blades. Actual pressure and temperatures are changing with the position of the rotor and extension of the blade. In actual case, when the blades extensions are maximum the temperature and pressures of the gasses are lower than the maximum pressures and the temperatures of the gasses that can be obtained in the

cylinders. However in these analyses maximum pressures and the temperature are applied for the most critical case (maximum extensions positions) of the blades to be in the safe side. The results of the turbine blade are more critical because of the high temperature and the pressure and the stress value is lower than the yield stress.

In the compressor & turbine valves analyses the maximum pressures and the temperatures are used with the centrifugal forces. The results of the analysis showed that deflections under the valves are much higher than the other sides and using another bearing for the lower part of the valves will be better to prevent any contact between the valves and the cylinders.

3.2 Combustion Chamber

Combustion takes place in the external combustion chamber of the novel engine which is designed using the geometric data calculated with the thermodynamic design code. By design the rolling piston compressor inlet volume is calculated as 450 cc. As the compression ratio is determined to be 4.5, the required combustion chamber volume, calculated by the code is 100 cc. As it is seen in the thermodynamic part the equivalence ratio of the engine is much smaller than the conventional spark ignition engines. In conventional spark-ignition engine the fuel and air are mixed together in the intake system, induced through the intake valve into the cylinder and then compressed. In this type of combustion min. equivalence ratio should be around 0.5. In the following table the flammability limits for various fuels can be seen. [23]

Table 3.3 Flammability Limits for Various Fuels

	Flammability Limits		
FUEL	Lean or Lower Limit Equivalence Ratio	Rich or Upper Limit Equivalence Ratio	Stoichiometric mass air-fuel ratio
Acetylene,	0.19	-	13.3
Carbon monoxide	0.34	6.76	2.46
n-Decane	0.36	3.92	15.0
Ethane	0.50	2.72	16.0
Ethylene	0.41	>6.1	14.8
Hydrogen	0.14	2.54	34.5
Methane	0.46	1.64	17.2
Methanol	0.48	4.08	6.46
n-Octane	0.51	4.25	15.1
Propane	0.51	2.83	15.1

So, for our engine which has very lean mixture, fuel should be directly injected to the combustion chamber. And the name of this type injection system in today's spark ignition engines is gasoline direct injection system. By this injection ultra lean mixtures are combusted, the air to fuel ratio could be as high as 65 to 1. These leaner mixtures (much leaner than any conventional engine) are desired because of reduced fuel consumption

In gasoline direct injection system the fuel is injected directly into the combustion chamber, as opposed to conventional multi point fuel injection that happens in the intake valve, or cylinder port injection in two-strokes.

This enables stratified charge (ultra lean burn) combustion for improved fuel efficiency and emission levels at low load. Further improving efficiency and high-load output-power, the engine power is governed by modulating fuel injection with unthrottled air intake, like a diesel engine; as opposed to restricting intake airflow, like a conventional gas internal combustion engine.

The volume of the chamber is defined by the thermodynamic code, also the inlet and exit port of the combustion chamber are known. Two parameters should be defined; length and diameter of the combustion chamber.

Before combustion for good mixing the flow velocity should be 7-12 m/s and the nominal velocity should be 9 m/s. [24] The angle β is chosen as 30^{o} for the same purpose.

The combustor chamber is a cylindrical combustor (for structural purposes) as it is seen in the following figure.

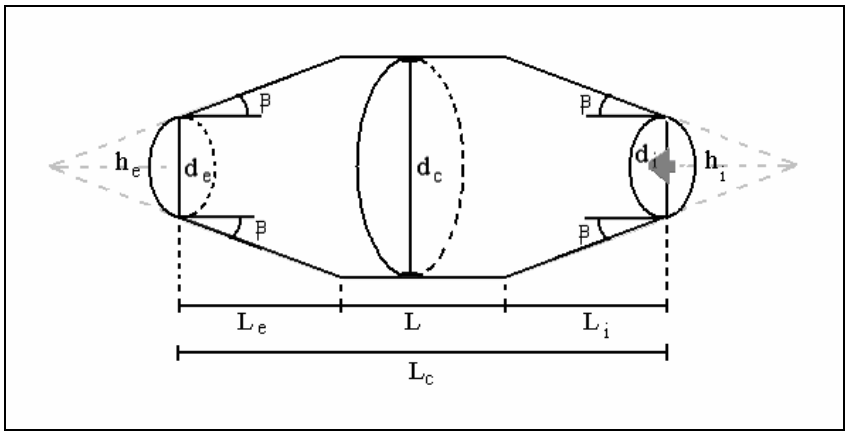

Figure 3.50 Combustion Chamber and Design Parameters

The inlet and exit port diameters d_i and d_e are known and:

$$d_e = d_i = 20cm \qquad \text{Eq.3.1}$$

And the angle β:

$$\beta = 30 \qquad \text{Eq.3.2}$$

And the intake air density is calculated by the thermodynamics code as:

$$\rho_c = 6.55kg/m^3 \qquad \text{Eq.3.3}$$

The area A_c in which velocity criteria should be satisfied is:

$$A_c = \pi.d_c^{\,2}/4 \qquad \text{Eq.3.4}$$

And the mass flow $\dot{m}_c$ rate at Ac where mixing of air and fuel will take place:

$$\dot{m}_c = \rho_c U_c A_c \qquad \text{Eq.3.5}$$

By using the formula above velocity of the air in the chamber is calculated by considering the mixing velocity criteria.

L_e and L_i lengths are found by geometric relations:

$$L_e = \frac{(d_c - d_e)}{\tan\beta} \qquad \text{Eq.3.6}$$

$$L_e = L_i \qquad \text{Eq.3.7}$$

And L_c combustor length is calculated from the volume of the combustion chamber.

$Vc = 100$ cc

$$Vc = 2\left(\frac{1}{3}\left[\left(\pi\frac{d_c{}^2}{4}\right)(h_i + L_i) - \left(\pi\frac{d_i{}^2}{4}\right)h_i\right]\right) + \pi\frac{dc^2}{4}L \qquad \text{Eq.3.8}$$

Where,

$$h_e = h_i = \frac{d_i L_i}{d_i + L_i \tan\beta - d_i} \qquad \text{Eq.3.9}$$

$$L_c = L_e + L_i + L \qquad \text{Eq.3.10}$$

All parameters are calculated for the velocities 7- 12 m/s and it is seen that there are no obligations to satisfy the nominal velocity requirement 9 m/s. Then sizing is done for the 9 m/s velocity condition.

Table 3.4 Results of the Combustion Chamber Sizing Calculations

Velocity	**Area**	**dc**	**Li**	**hi**	**L**	**Lc**
m/s	m^2	m	m	m	m	m
7	0,0014	0,042	0,022	0,020	0,133	0,178
8	0,0012	0,040	0,020	0,020	0,170	0,209
9	**0,0011**	**0,037**	**0,017**	**0,020**	**0,206**	**0,241**
10	0,0010	0,036	0,016	0,020	0,241	0,272
11	0,0009	0,034	0,014	0,020	0,275	0,303
12	0,0008	0,032	0,012	0,020	0,309	0,334

3.2.1 Combustion Chamber Parts

- Combustion chamber is composed of upper and lower parts bolted together.
- A spark is placed on top of lower part to ignite the fuel air mixture.
- An injector is placed on the top of the upper part to inject fuel on the compressed air.
- Two seal channels are placed at both sides of the chamber to avoid leakage from the contact surfaces of the parts.
- Four cooling passages are drilled on both parts in which cooling water is circulated.

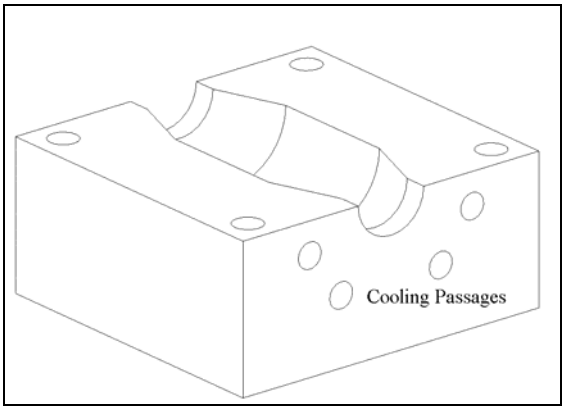

Figure 3.51 3-D Wire-Frames Drawing of Combustion Chamber

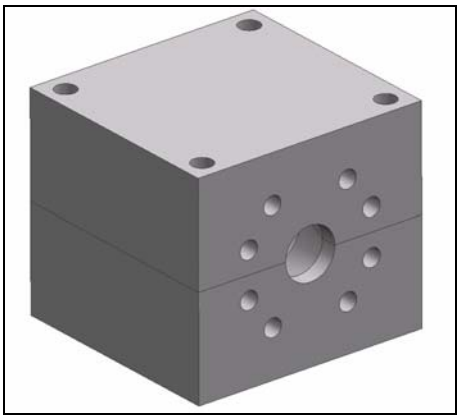

Figure 3.52 3-D CAD Model of the Combustion Chamber

3.2.2 Combustion Chamber Material

With respect to the structural analysis results, H13 Hot Work Tool Steel is selected as the material of the combustion chamber. The selection criteria of the material are given below;

- High thermal shock resistance.
- Good thermal conductivity and tolerate some water cooling in service.
- High temperature tensile strength.
- Good machinability.

Regarding these properties of the material, it is one of the best alternatives that can be used for the combustion chamber. Beside these properties, the structural analysis of the combustion chamber is done using this material and the analysis results showed that the selected material is suitable.

3.2.3 Thermal and Structural Analysis of the Combustion Chamber

Structural analysis of the combustion chamber of the novel engine is done in NX NASTRAN Environment (Finite Element Program). The aim of this work is to select the material of the chamber and to determine the required cooling. To do the structural analysis, firstly the critical parts are defined as follows;

For material selection;

- Stress distribution on the chamber due to pressure and temperature exerted by the combustion gases onto the inner surfaces.

For determining the required cooling;

- Stress distribution on the chamber due to pressure and temperature exerted by the combustion gases onto the inner surfaces while cooling the chamber with cooling water injected from the cooling passages.

To make the structural analysis of the combustion chamber, the necessary temperature and pressure data is taken from the thermodynamic design code. Maximum combustion temperature and pressure is applied to the inner surfaces of the chamber for safety considerations.

p_{max} =20 atm

T_{max} = 1200 K

B.C's:	Fixed all DOF on inlet and outlet surfaces
Loads:	Convection on divided surfaces
	Max. Pressure load on divided surfaces
Assumptions:	Convection Heat Transfer Coefficient for combustion gases is approximated as 50 W/m^2 .K
	Convection Heat Transfer Coefficient for cooling air is approximated as 100 W/m^2 .K
	Convection Heat Transfer Coefficient for cooling water is approximated as 150 W/m^2 .K

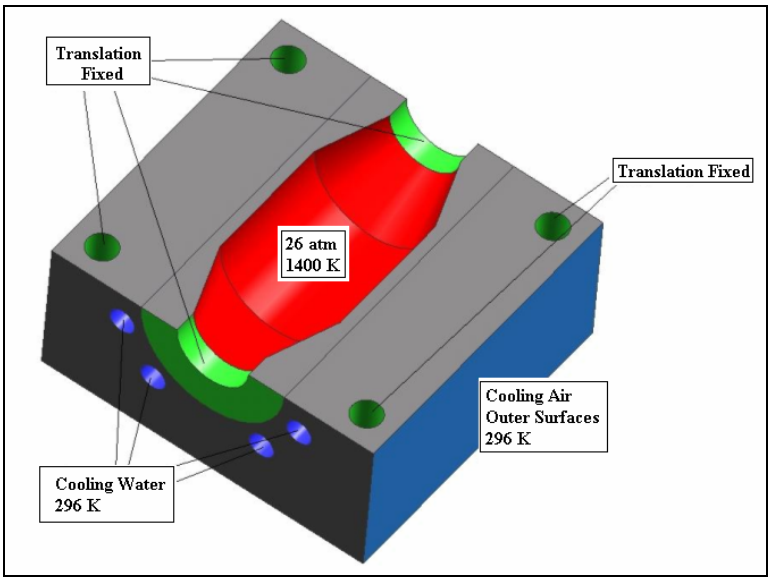

Figure 3.44 Structural Analysis Model of the Combustion Chamber

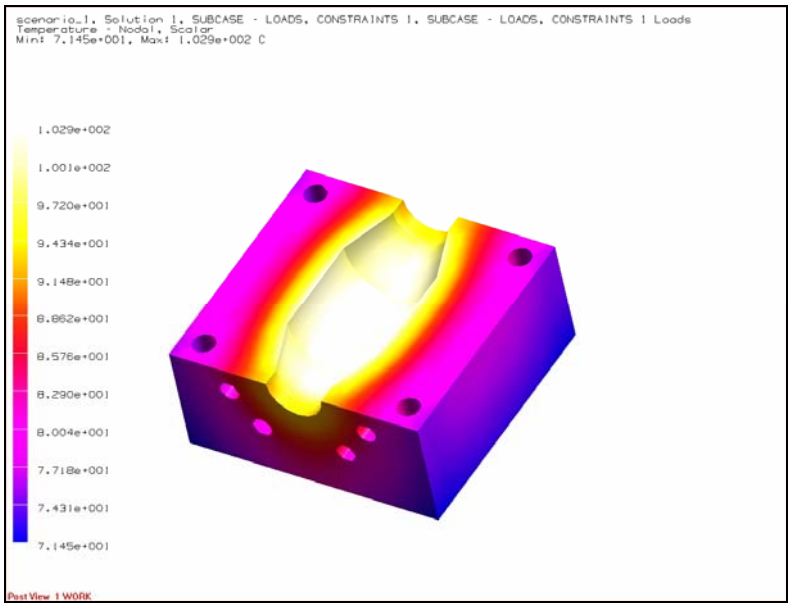

Figure 3.45 Temperature Distributions on the Combustion Chamber

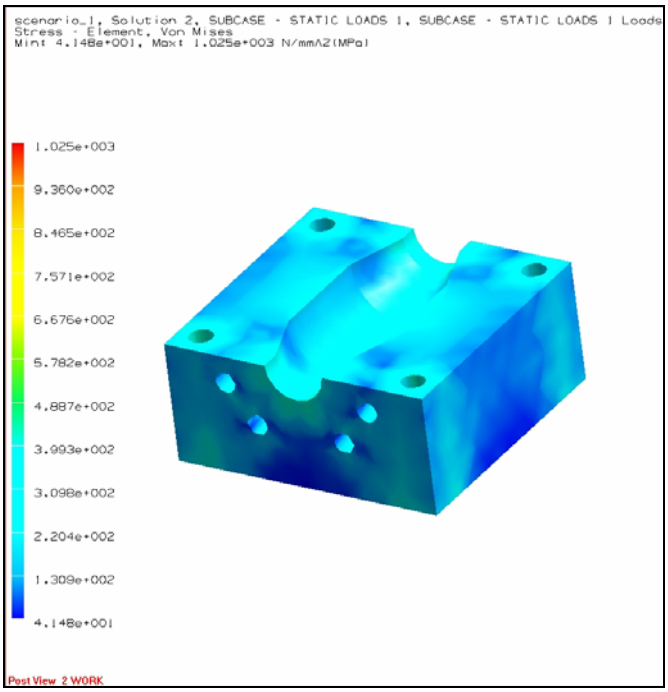

Figure 3.46 Stress Distributions on the Combustion Chamber

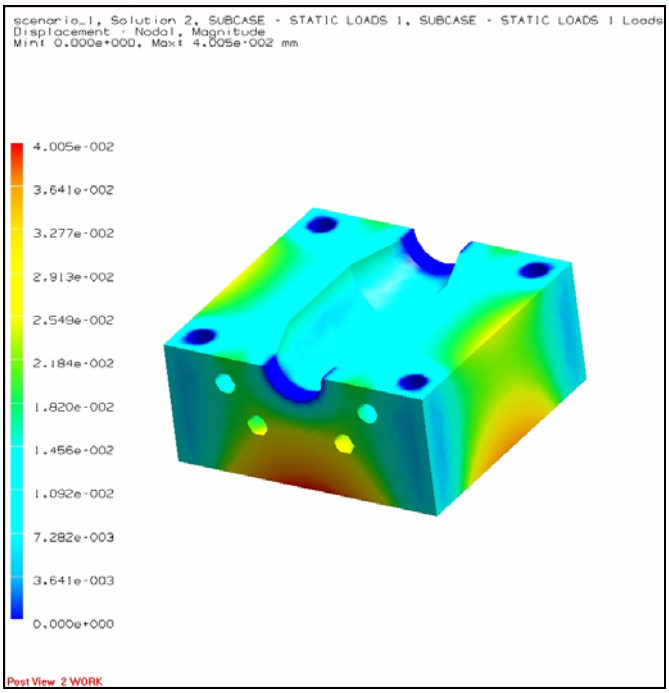

Figure 3.47 Displacements on the Combustion Chamber

3.2.4 Results & Discussions of the Thermal and Structural Analysis

Results of the combustion chamber structure analysis are shown on the following table.

Table 3.5 Results of the Combustion Chamber Structure Analysis

COMBUSTION CHAMBER	
Max. Temperature (^{o}C)	102.9
Max. Stress (MPa)	1025
Max. Deformation (mm)	4.05e-02

The structural analysis of the combustion chamber is done using H13 material.

In the analysis the convection between the hot combustion gasses and the chamber, convection between the cooling water and the chamber, convection between the cooling air and the chamber and the conduction through the material are calculated.

The analysis showed that necessary cooling by the air and the water could be achieved.

The stress values are much lower than the yield stress of the material and the deformations in the inner surface of the chamber are in the desirable range.

One of the most important results of the analysis is the stress concentrations, and the higher stress values are found on the bolt holes, this makes choosing proper bolts critical.

CHAPTER 4

ENGINE LOSSES

In this part engine losses are calculated. In the rotary engine there are two main loss sources. These are friction [25] and leakage [26]. Novel rotary engine has two moving parts, compressor and turbine. Compressor and turbine has the same geometric properties but they are different in size. So only compressor will be explained and formulas for the compressor will be derived because they have same relations these formulas will be used both for compressor and turbine.

Friction losses between rotating parts and non-rotating parts in compressor and turbine are calculated. Before calculating the friction losses velocities of the compressor and turbine components are calculated because they are necessary to calculate the friction losses. In the kinematics part all velocity calculations are seen. And also in this part geometric relations between the components of the compressor and turbine are defined and formulas are derived.To understand the components motions compressor (turbine) and its motion is briefly explained.

Compression process in rolling piston type compressors is accomplished by a piston and cylinder arrangement that employs circular or rotary motion instead of the usual reciprocating motion. In rolling piston compressors the rotor (or piston) “rolls” on the inside surface of the cylinder – hence forming the source of its name. Figure 4.1 shows a schematic sketch of compressor part of the engine. The roller (or the rolling piston) is mounted on a shaft having an eccentric. The shaft rotates about the center of the cylinder and the roller rolls over inside surface of the cylinder, thereby rotating about eccentric. If the tolerances are perfect, the roller would have a perfect rolling motion. However, in practice this does not

happen and the roller has a complicated motion consisting of rolling coupled with the slipping motion relative to the cylinder.

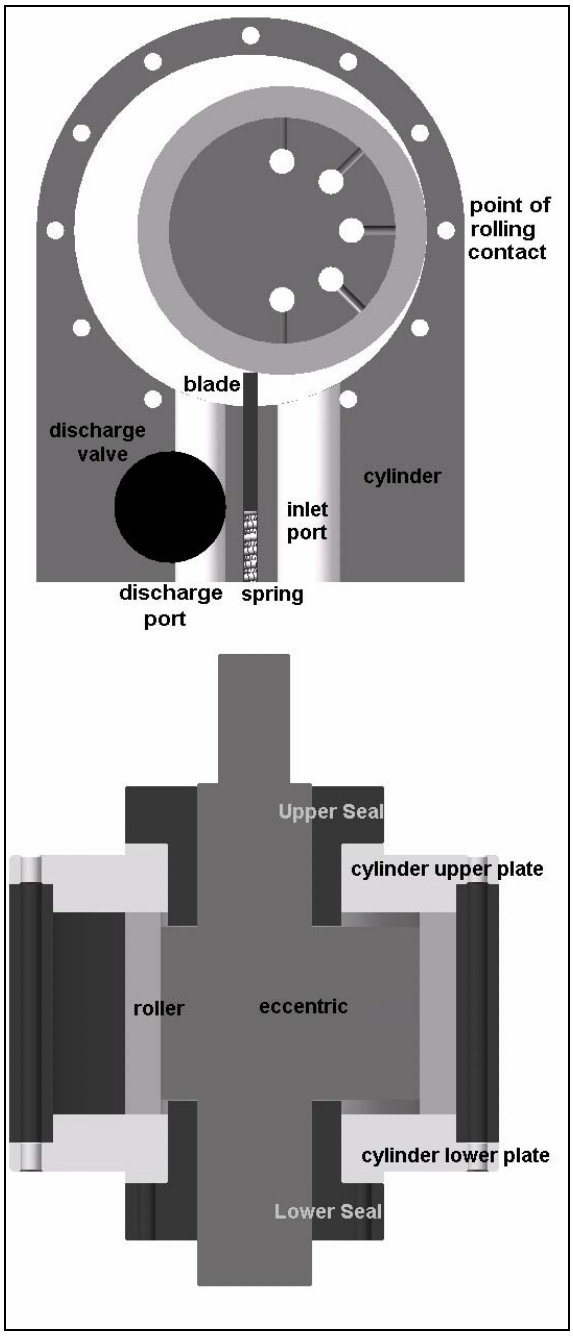

Figure 4.1 Cross Section of Compressor

4.1 KINEMATICS

4.1.1 Angular Speed of the Roller

Thus the motion of the roller can be considered as consisting of two different types of motions superimposed over each other. These are: Pure rolling motion and slipping motion. Referring to the Figure 4.2, if the motion is pure of rolling type, we would have following relationships:

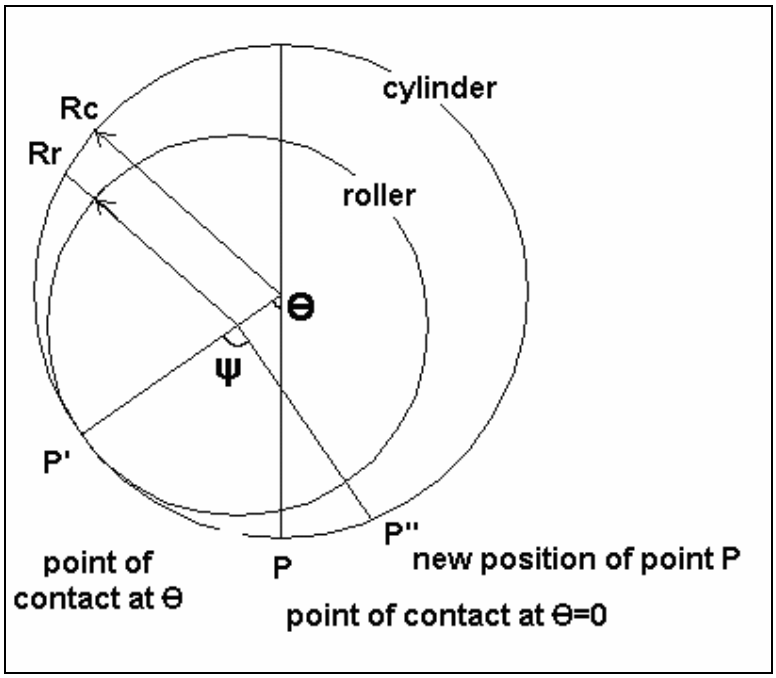

Figure 4.2 Rolling Motion of Roller

$$Rc\theta = Rr\psi \qquad \text{Eq.4.1}$$

$Rc\theta$ is the distance traveled by roller by rolling around its center

$Rr\psi$ is the distance traveled by roller by rolling around cylinder center

$$\psi = \frac{Rc}{Rr}\theta = \frac{1}{a}\theta \qquad \text{Eq.4.2}$$

Then, rotating of roller about its center because of pure rolling motion in the positive θ direction will be given by $\theta - \psi$,or

$$\theta - \psi = \theta\left(1 - \frac{1}{a}\right) \qquad \text{Eq.4.3}$$

where a is the radius ratio (Rr/R_c). ($a = \frac{R_r}{R_c} = \frac{R_r}{R_r + e}$, $a = \frac{1}{1 + \frac{e}{R_r}}$)

Therefore, roller speed due to rolling motion,

$$w_2 = (\dot{\theta} - \dot{\psi}) \qquad \text{Eq.4.4}$$

or

$$w_2 = \dot{\theta}(1 - \frac{1}{a}) = w_1(1 - \frac{1}{a}) \qquad \text{Eq.4.5}$$

Where w_1 is the engine speed (rad./sec.) Now suppose w_3 (rad/sec) is the angular speed of slipping only in the positive θ direction. Then the net angular speed w_4 of the roller is:

$$w_4 = w_2 + w_3 = w_1(1 - \frac{1}{a}) + w_3 \qquad \text{Eq.4.6}$$

This, then, is the absolute angular speed of the roller, However, the speed of the roller about is center or its speed relative to the eccentric w_r will be w_4-w_1 or,

$$w_r = w_4 - w_1 = w_3 - \frac{w_1}{a} \qquad \text{Eq.4.7}$$

Since w_1 is already known (engine speed) the only unknown in the equation is w_3 which is obtained as shown later from the free-body analysis of the roller once the friction forces have been analyzed.

4.1.2. Volume-Angle and Pressure-Angle, Temperature-Angle Relationships

By using Figure 4.3 following geometric relations can be established:

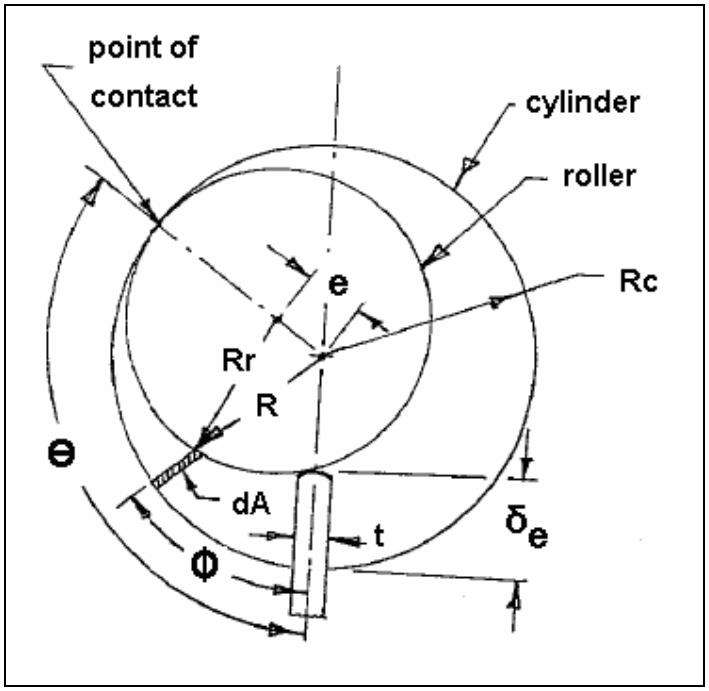

Figure 4.3 Rolling Motion of Roller

In the figure e is the eccentric which is Rc-Rr.

$$Rr^2 = e^2 + R^2 - 2eR\cos(\theta - \phi) \qquad \text{Eq.4.8}$$

Or

$$R = Rc(1-a)\cos(\theta - \phi) \pm \sqrt{Rc^2(1-a)^2\cos^2(\theta - \phi) + Rc^2(2a-1)} \qquad \text{Eq.4.9}$$

Since the radius ratio a is slightly less then 1 we can neglect the negative term so:

$$R = Rc\left[(1-a)\cos(\theta - \phi) + \sqrt{(1-a)^2\cos^2(\theta - \phi) + (2a-1)}\right] \qquad \text{Eq.4.10}$$

To find the total area trapped between the roller and the cylinder, we will integrate a differential annulus area dA as shown from ϕ=0 to $\phi=\theta$. Thus,

$$A(\theta)=\int_0^{\theta} dA=\int_0^{\theta}\frac{1}{2}(Rc^2-R^2)d\theta \qquad \text{Eq.4.11}$$

Substituting R from from Eq.4.1.9 into Eq.4.1.11 and integrating, we finally get the following relationship:

$$A(\theta)=\frac{Rc^2}{2}\begin{bmatrix}(1-a^2)\theta-\dfrac{(1-a)^2}{2}\sin 2\theta-a^2\sin^{-1}((\dfrac{1}{a}-1)\sin\theta)\\ -a(1-a)\sin\theta\sqrt{1-(\dfrac{1}{a}-1)^2\sin^2\theta}\end{bmatrix} \qquad \text{Eq.4.12}$$

or

$$A(\theta)=\frac{1}{2}Rc^2 f(\theta) \qquad \text{Eq.4.13}$$

where,

$$f(\theta)=\begin{bmatrix}(1-a^2)\theta-\dfrac{1}{2}(1-a)^2\sin 2\theta-a^2\sin^{-1}((\dfrac{1}{a}-1)\sin\theta)\\ -a(1-a)\sin\theta\sqrt{1-(\dfrac{1}{a}-1)^2\sin^2\theta}\end{bmatrix} \qquad \text{Eq.4.14}$$

The volume $V(\theta)$ will then be given as follows:

$$V(\theta)=hA(\theta)=\frac{1}{2}hRc^2 f(\theta) \qquad \text{Eq.4.15}$$

So far we neglected the blade thickness, but for accurate results blade effect can be considered as:

True value of $V(\theta)$

$$= \text{apparent value of } V(\theta)-\frac{1}{2}th\delta_e \qquad \text{Eq.4.16}$$

where δ_e is the blade extension and t is the blade thickness. But

$$\delta_e=\left\lfloor Rc-(R)_{\phi=0}\right\rfloor \qquad \text{Eq.4.17}$$

or

$$\delta_e=Rc\left\lfloor 1-(1-a)\cos\theta-\sqrt{(1-a)^2\cos^2\theta+2a-1}\right\rfloor \qquad \text{Eq.4.18}$$

Then,

$$V'(\theta) = V(\theta) - \frac{1}{2} th\delta_e \qquad \text{Eq.4.19}$$

Where $V(\theta)$ is given by Eq.4.1.15 and δ_e by Eq.4.1.18

So we have found the volume-angle relationship of the compressor.

To find the pressure-angle relationship we use the following formula,

PV^n = constant where n is the coefficient of polytrophic compression process so we can express pressure corresponding to any angle θ as follows:

$$P(\theta) = P_s \left[\frac{V'(2\pi)}{V'(\theta)} \right]^n \qquad \text{Eq.4.20}$$

After finding all these relations temperature-angle relation is found easily by using the following formula,

$$T(\theta) = T_s \left[\frac{V'(2\pi)}{T'(\theta)} \right]^{n-1} \qquad \text{Eq.4.21}$$

4.1.3. Torque-Angle Relationships

Calculation of pressure distribution on the roller made possible to calculate the torque distribution on the roller of the compressor. Here torques caused by compressed air – angle relationships is found. Figure 4.4 shows the relationship between torque and angle.

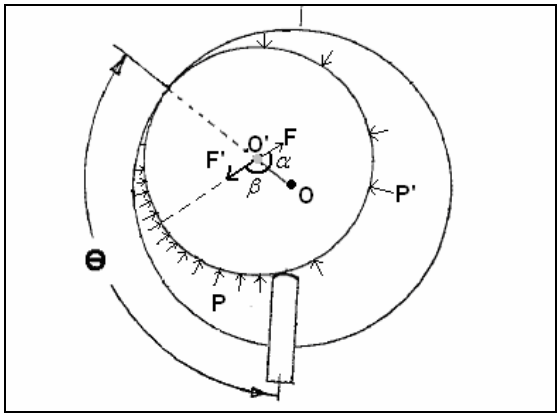

Figure 4.4 Torque-Angle Relations

In the figure above it is seen that in the compressor we have two different pressures on each side of the compressor, and the angle θ is known for this angle P and P' can be calculated as described previously. After calculating the pressures, force due to these pressures F and F' is calculated by multiplying the areas of each sides of the compressor. F is the force due to pressure P, F' is the force due to pressure P' and the angles α and β are the angles between the forces and the moment arm. O is the center of cylinder and O' is the center of rotor the distance between them is e eccentric which is constant and the moment arm. So T is the torque due to F, T' is the torque due to F'and the formulas derived for torque calculations are:

$$\alpha = \theta / 2 \qquad \text{Eq.4.22}$$

$$\beta = 180 - \theta / 2 \qquad \text{Eq.4.23}$$

$$F(\theta) = P(\theta).A(\theta) \qquad \text{Eq.4.24}$$

$$F'(\theta) = P'(\theta).A'(\theta) \qquad \text{Eq.4.25}$$

$$T(\theta) = F(\theta).e.\sin(\alpha) \qquad \text{Eq.4.26}$$

$$T'(\theta) = F'(\theta).e.\sin(\beta) \qquad \text{Eq.4.27}$$

4.1.4. Results

4.1.4.1 Compressor

Compressor volume is found by using the thermodynamic design code which is explained in the previous chapter. According to the compressor volume compressor geometry is specified. Rc compressor cylinder radius, Rr compressor rotor radius, h compressor height, t blade thickness are calculated. The dimensions are seen in the following table.

Table 4.1 Compressor Dimensions

Compressor	
Rc (m)	0,07
Rr (m)	0,0575
h (m)	0,09
t (m)	0,006
ac	0,821429

After calculating the dimensions angular speeds are calculated as explained before. Angular speed calculation results are seen in the Table.4.2.

Table 4.2 Compressor Angular Velocities

Angular Velocities *(rad/sec)*				
W1	**W2**	**W3**	**W4**	**Wr**
628,300	-136,587	13,551	-123,035	-751,335

The important part of the compressor design is to derive the volume-angle relationship which is also necessary to calculate the pressure and temperature distributions on the compressor; they are used in both thermodynamic analysis and structural analysis. So the volume-angle and the pressure-angle relations are very critical through out the design process. The following Figures show the volume, blade extension and pressure, temperature variation due to angle.

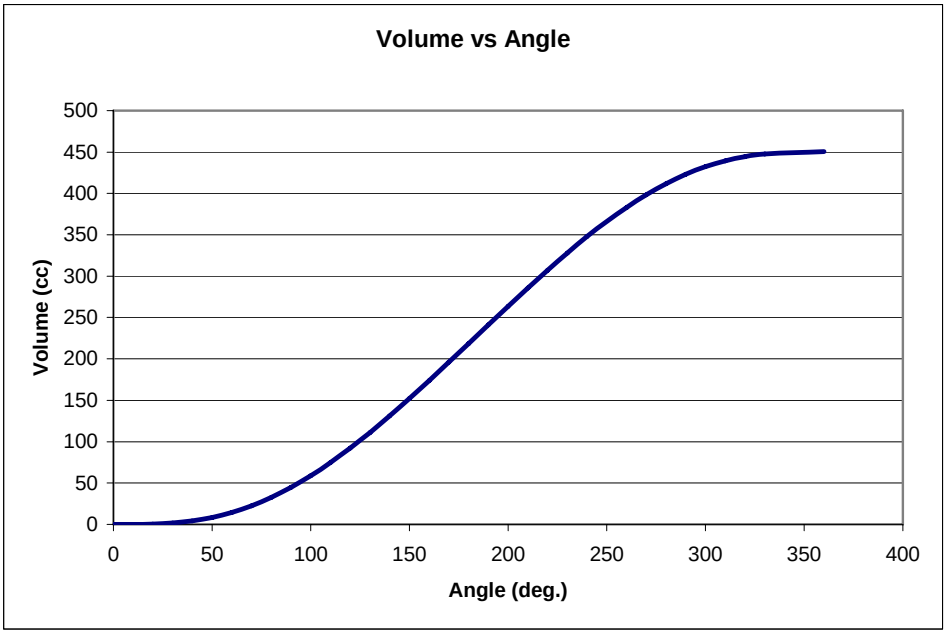

Figure 4.5 Compressor Volume vs. Angle

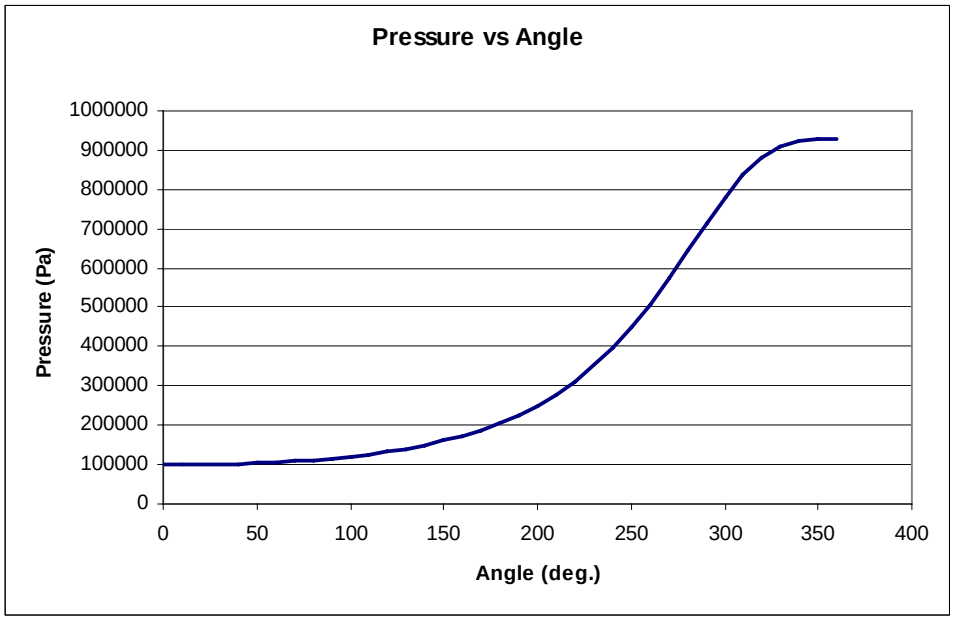

Figure 4.6 Pressure Distributions in the Compressor

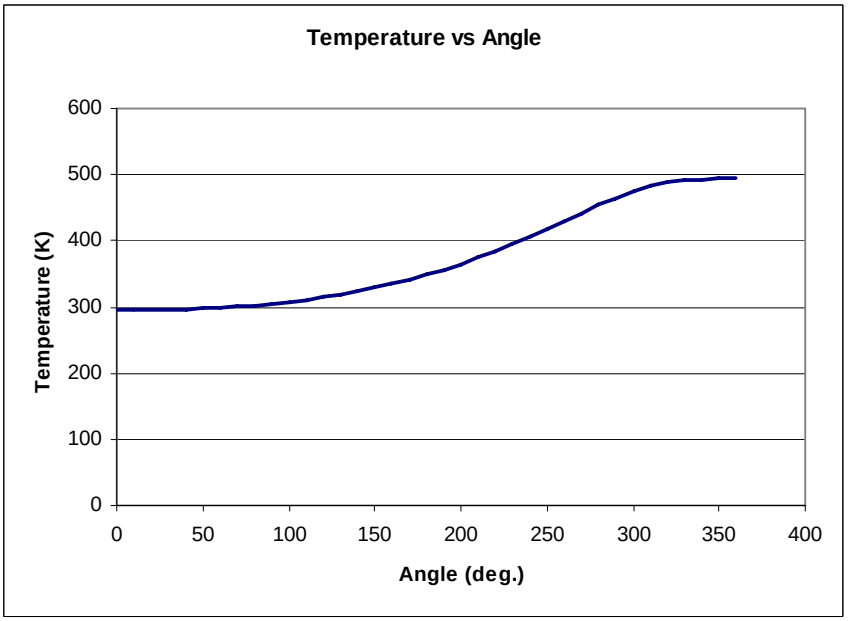

Figure 4.7 Temperature Distributions in the Compressor

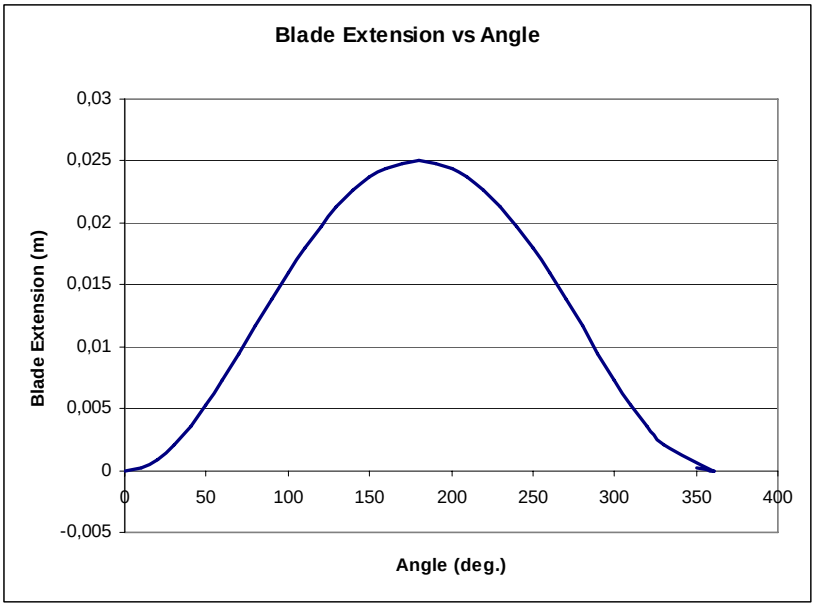

Figure 4.8 Blade Extension in the Compressor

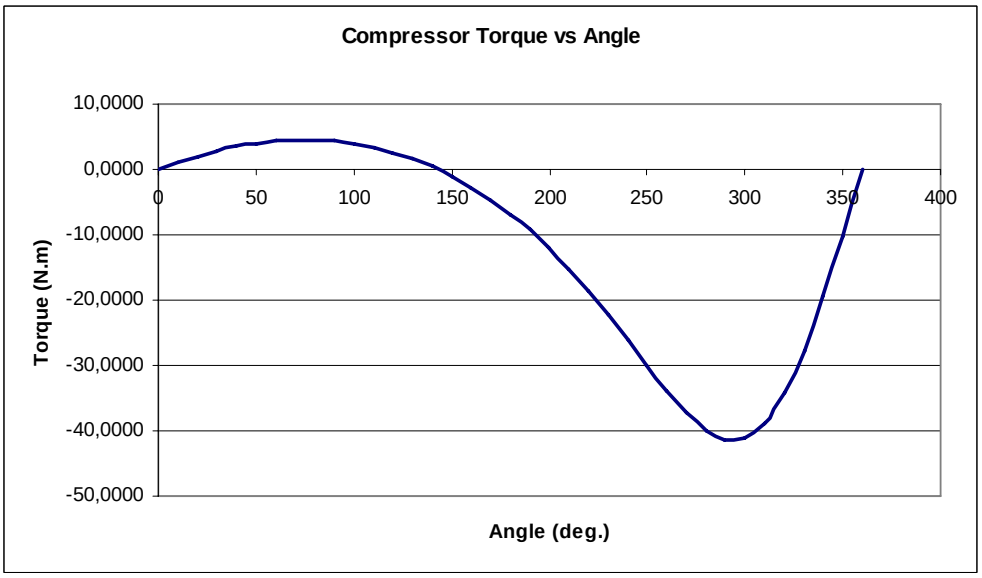

Figure 4.9 Torque Distributions in the Compressor

4.1.4.2 Turbine

Turbine volume is found by using the thermodynamic design code which is explaned in the previous chapter. According to the turbine volume turbine geometry is specified. Rc turbine cylinder radius, Rr turbine rotor radius, h turbine height, t blade thickness are calculated. The dimensions are seen in the following table.

Table 4.3 Turbine Dimensions

Turbine		
Rc	(m)	0,95
Rr	(m)	0,070
h	(m)	0,110
t	(m)	0,006
ac		0,823

After calculating the dimensions angular speeds are calculated as explained before. Angular speed calculation results are seen in the Table.4.4.

Table 4.4 Turbine Angular Velocities

Angular Velocities			*(rad/sec)*	
W1	**W2**	**W3**	**W4**	**Wr**
628,3	-7898,63	8080,159	181,53	-446,769

The following figures show the volume, blade extension and pressure, temperature variation due to angle. These results are both used in thermodynamics calculations and structural analysis.

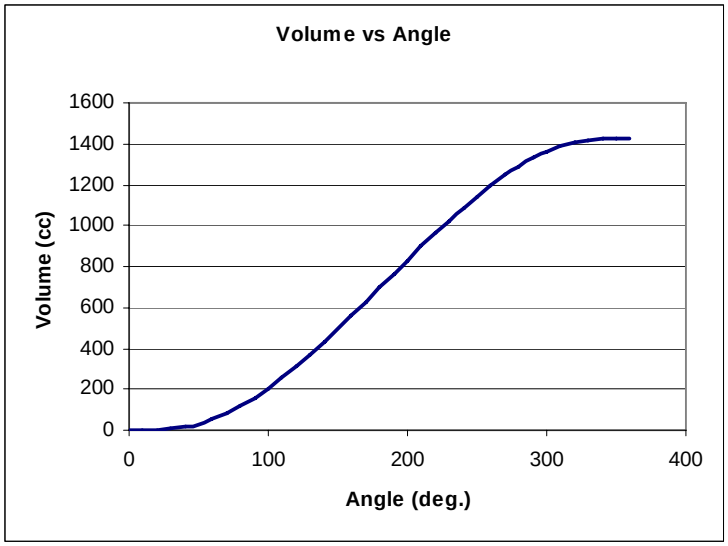

Figure 4.10 Turbine Volume vs. Angle

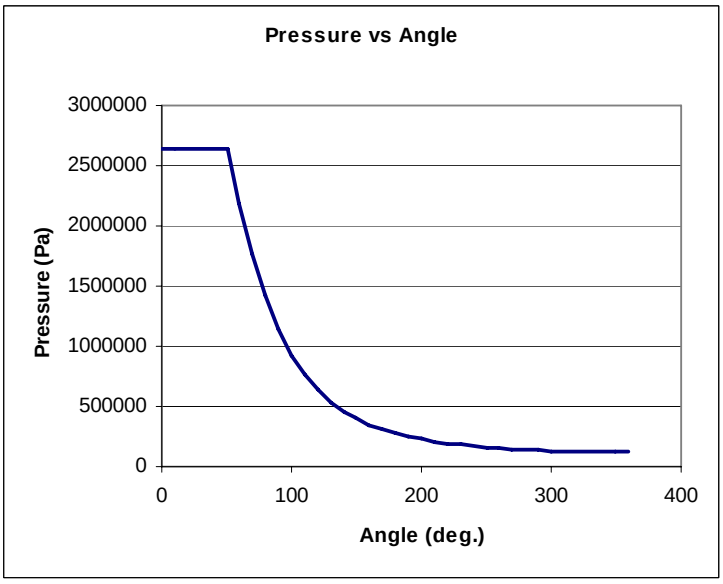

Figure 4.11 Pressure Distributions in the Turbine

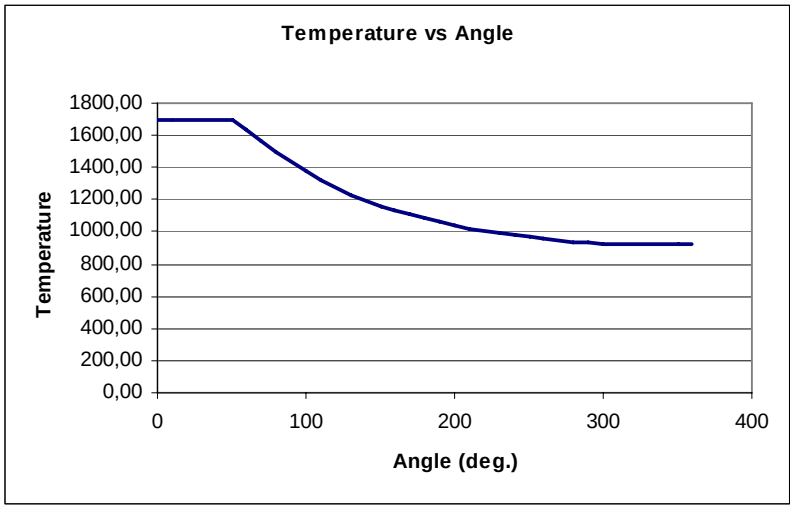

Figure 4.12 Temperature Distributions in the Turbine

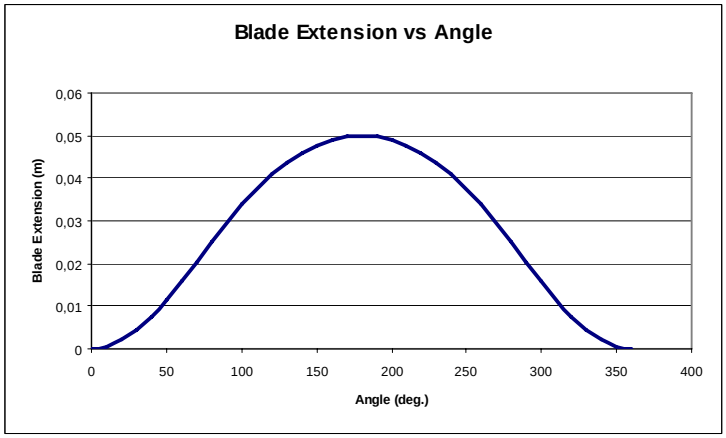

Figure 4.13 Blade Extensions in the Turbine

After calculating the pressure distribution turbine torque due to the pressure is calculated.

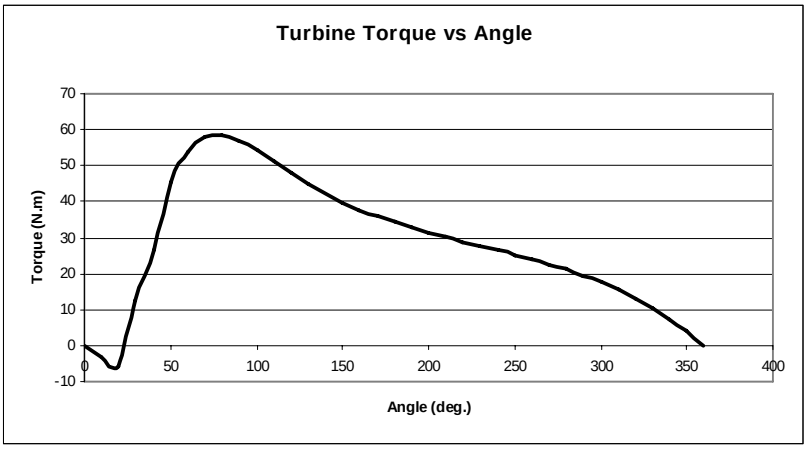

Figure 4.14 Torque Distributions in the Turbine

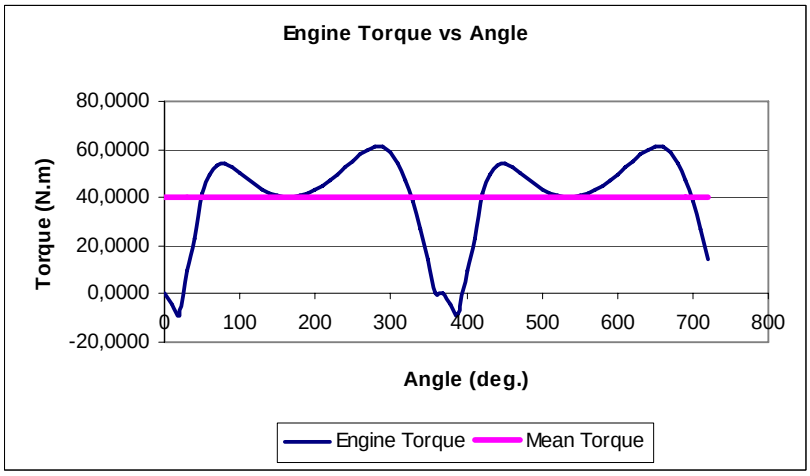

Figure 4.15 Engine Torque Distributions

4.2. FRICTION LOSSES

Referring again to Figure3 it can be seen that the possible friction loss mechanisms in the cylinder are: (1) friction between the blade tip and the roller, (2) friction between the cylinder plates and the two faces of the roller, (3)) friction between the cylinder plates and the two faces of the eccentricity, (4) friction at the point of contact between the roller and the cylinder, (5) friction between the roller and the eccentric, and (6) blade-slot friction.

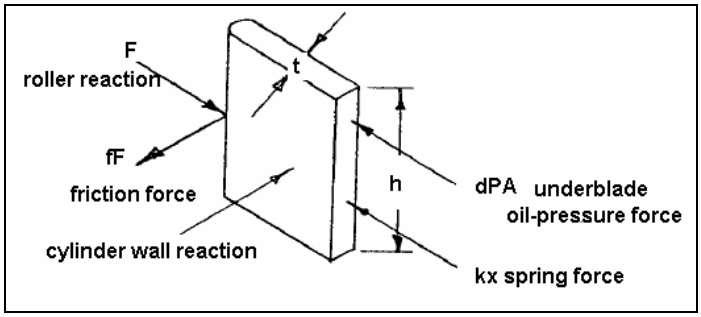

Figure 4.16 Blade Tip Friction

The last one can be conveniently disregarded since there will not be any appreciable side pressure between the blade and the slot, thereby rendering the friction force between the blade and the slot negligible. Also, since relative motion between the cylinder and the roller is rolling plus sliding without any appreciable contact force (the only force is due to centrifugal effect of the roller mass which can be neglected) it is assumed that energy loss due to friction between the roller and the cylinder at the contact point will be negligible. The remaining four losses can be treated as follows.

4.2.1 Blade Tip Friction

The relative motion between the blade tip and the roller is of pure sliding nature, with the speed of rotation of the roller given by Eq. 4.1.6. and lying somewhere between zero and eccentric velocity w_1. Moreover, the spring force together with the under-blade oil pressure acting behind the blade (Figure4.2.1) give rise to considerably high unit pressure between the blade tip and the rotor. These considerations suggest that the lubrication between the blade-tip and the roller surface possibly of mixed nature and is somewhere between the boundary lubrication with a very thin film of lubrication between the two surfaces and the hydrodynamic lubrication with full fluid film between the two surfaces. Therefore, the friction loss can be calculated by assuming a suitable coefficient of friction (f). For this type application f can be taken from 0.008 to 0.2. [27] An average value of 0.015 seems to be reasonable for most cases. From the free body diagram of the blade (Figure 4.17) we notice that the blade will exert a force on the roller that will vary continuously from a maximum of $dPth+kx_{max}$ when the spring is in fully compressed position to a possible minimum of dPth when the spring is in its free position, where x is the spring compression.

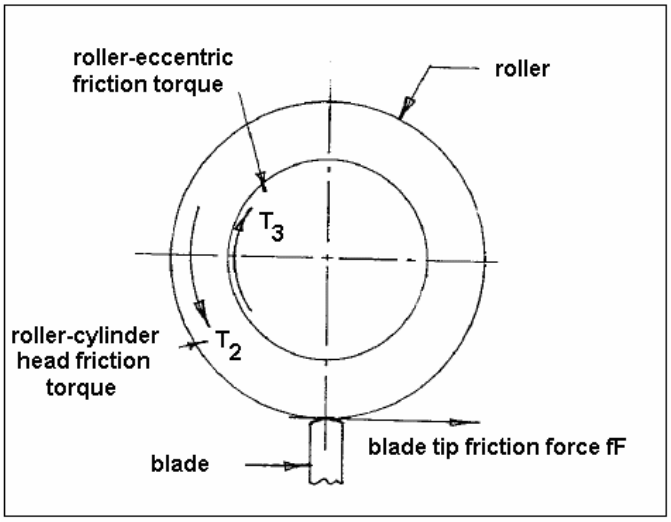

Figure 4.17 Free-Body Diagram of Roller

The analysis will, therefore, be approximated by taking the average value for both dP and x. Thus:

Average Friction Force F:

$$F = f\left[(dp)_{av}\, th + kx_{av}\right] \qquad \text{Eq.4.28}$$

Where,

$$(dp)_{av} = \frac{1}{2}\left[p_s + \frac{1}{2}(p_s + p_d) \right]$$

$$= \frac{3p_s + p_d}{4}$$

$$x_{av} = \frac{1}{2} x_{\max} \qquad \text{Eq.4.29}$$

Then the power loss due to blade tip friction is given by:

$$E_{FL1} = R_r w_4 f\left[\frac{1}{4}(3p_s + p_d)th + \frac{1}{2} kx_{\max} \right] \qquad \text{Eq.4.30}$$

4.2.2. Roller-to-Cylinder Plate Friction

The clearance space between the roller faces and the cylinder plate is assumed to be filled with lubricant which gives rise to viscous drag acting upon the roller as it rotates. The radial velocity of the fluid in this clearance space will be assumed negligible as compared to the tangential velocity. Then using viscous drag formula between two rotating discs [28] we can write:

Friction torque on the roller:

$$= \frac{\pi \mu w_4}{\varepsilon_1}\left[R_r^{\,4} - R_e^{\,4} \right] \qquad \text{Eq.4.31}$$

Corresponding friction loss E_{FL2}:

$$= \frac{\pi \mu w_4^{\,2}}{\varepsilon_1}\left[R_r^{\,4} - R_e^{\,4} \right] \qquad \text{Eq.4.32}$$

4.2.3. Eccentric-to-Seal Friction

This case is exactly similar to the previous case. The only difference here is that the angular speed of the eccentric is different from that of roller and in some cases it is possible that the clearance between the eccentric and the seal may also be different from the clearance between the roller and the cylinder plate.

Friction torque on eccentric:

$$= \frac{\pi \mu w_1}{2\varepsilon_2}\left[2R_{seal}{}^4 - R_s{}^4\right] \qquad \text{Eq.4.33}$$

Corresponding friction loss E_{FL3}:

$$= \frac{\pi \mu w_1{}^2}{2\varepsilon_2}\left[2R_{seal}{}^4 - R_s{}^4\right] \qquad \text{Eq.4.34}$$

4.2.4. Friction between the Roller and the Eccentric

There is a relative motion between the roller and the eccentric due to the fact that both rotate with different absolute angular velocities, which are w_1 and w_4 for the eccentric and the roller respectively. The relative angular velocity between is given by Eq. 4.7 as w_3-w_1/a. Thus, the eccentric and the roller will behave somewhat similar to a journal and a bearing and a similar analysis is done. However, since the only bearing loss acting in this case is the centrifugal force of the roller due to eccentric mounting, which is insignificant, we can approximate our analysis by assuming that the hydrodynamic film of lubricant is not created and instead the friction loss is only as a result of viscous drag between the two concentric cylinders. (roller and eccentric) with a concentric film of lubricant being developed between the two.

Friction torque on the roller:

$$= \frac{\mu(2\pi R_e h)R_e(-w_r)R_e}{\delta} \qquad \text{Eq.4.35}$$

$$= -\frac{2\pi \mu R_e{}^3 h w_r}{\delta} \qquad \text{Eq.4.36}$$

Loss of power due to friction E_{FL4}:

$$= -\frac{2\pi\mu R_e^{\,3} h w_r^{\,2}}{\delta} \qquad \text{Eq.4.37}$$

4.2.5. Total Friction Loss

In the friction loss expressions there is one unknown term w_3, angular speed of slipping of the roller relative to the cylinder. From the free-body diagram of the roller Figure4.2.2 following relation can be written for the steady condition:

$$T_1 + T_2 = T_3 \qquad \text{Eq.4.38}$$

or

$$R_r f\left[\frac{1}{4}(3p_s + p_d)th + \frac{1}{2}kx_{\max}\right] + \frac{\pi\mu}{\varepsilon_1}\left[w_1(1-\frac{1}{a}) + w_3\right](R_r^{\,4} - R_e^{\,4}) = \frac{2\pi\mu R_e^{\,3} h}{\delta}\left[\frac{w_1}{a} - w_3\right] \qquad \text{Eq.4.39}$$

Solving for w_3:

$$w_3 = \frac{\frac{\pi\mu w_1}{a}\left[\frac{2R_e^{\,3}h}{\delta} - \frac{(a-1)}{\varepsilon_1}R_r^{\,4}\right] - R_r f\left[\frac{(3p_s + p_d)}{4}th + \frac{kx_{\max}}{2}\right]}{\pi\mu\left[\frac{2R_e^{\,3}h}{\delta} + \frac{R_r^{\,4} - R_e^{\,4}}{\varepsilon_1}\right]} \qquad \text{Eq.4.40}$$

So substituting w_3 to the related loss equations all power losses caused by friction is found.

4.2.6. Results

In compressor/turbine design after calculating the geometric and thermodynamic variables of the compressor/turbine, the most important part of the analysis of the compressor/turbine in practice, friction analyses are done. The results of the analysis are seen in the following tables and it also shows the energy loss due to the frictions in the compressor/turbine.

Table 4.5 Friction Calculation Inputs

Rr	Roller radius
Rc	Cylinder radius
Re	Radius of eccentric
Rs	Radius of shaft
h	Height of blade
δ	Radial clearance between roller and eccentric
δ_c	Min. clearance between roller and cylinder
ε_1	Clearance between roller and cylinder plate faces, clearance between blade and cylinder plate
ε_2	Clearance between eccentric and cylinder plate faces
t	Blade thickness
RPM	RPM of the motor
Ru	Seal Radius
xmax	Max. spring compression
k	Spring constant
ρ_s	Suction density
Ps	Suction pressure
Ts	Suction temperature
Pd	Discharge pressure
Td	Discharge temperature
f	Coefficient of friction
μ	Viscosity coefficient

Table 4.6 Friction Calculation Results for Compressor

Friction			ENGINE POWER %
Blade-tip Friction Loss	18,99	W	3,31E-02
Eccentric-to-seal friction loss	3,24	W	5,65E-03
Roller faces-to-cylinder plate	2,79	W	4,87E-03
Roller to eccentric friction loss	104,14	W	1,82E-01
Total Friction Loss	129,16	W	2,25E-01

Table 4.7 Friction Calculation Results for Turbine

Friction			ENGINE POWER %
Blade-tip Friction Loss	209,57	W	3,66E-01
Eccentric-to-seal friction loss	11,01	W	1,92E-02
Roller faces-to-cylinder plate	15,50	W	2,70E-02
Roller to eccentric friction loss	93,89	W	1,64E-01
Total Friction Loss	329,97	W	5,76E-01

4.3. LEAKAGE LOSSES

In the figure below there are various leakage paths occurring in a rolling piston compressor and turbine. These are:

i. Leakage past the contact point between the roller and the cylinder.

ii. Leakage past the blade edges

iii. Leakage across the roller faces

iv. Leakage past the blade tips

Between these leakage losses the most important ones are the first two ones. The others are negligible if we compare them with the first two ones.

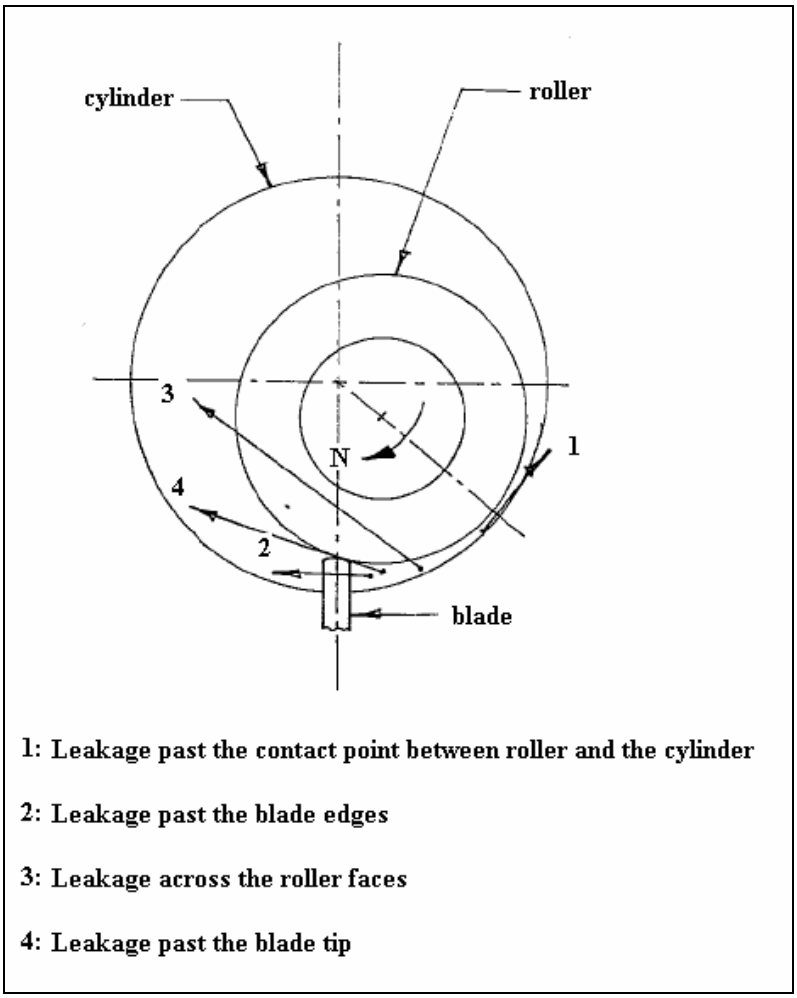

Figure 4.18 Leakage Flow-paths in a Rolling Piston Compressor & Turbine

4.3.1. Leakage Past the Contact Point

Assuming that the leakage is only due to the pressure differential we can model the leakage past the contact point as flow through convergent-divergent nozzle. So the amount of leakage loss can be calculated by the max. mass flow through the converging-diverging nozzle formula,

$$\dot{m}_{LL1} = \rho_u U A \qquad \text{Eq.4.41}$$

$$\dot{m}_{LL1} = \frac{\rho_u}{RT_{Tu}} aMh\delta_c \qquad \text{Eq.4.42}$$

Where: M = 1

$$p_{Tu} = p_u(1+\frac{\gamma-1}{\gamma}M^2)^{\frac{\gamma}{\gamma-1}} \qquad \text{Eq.4.43}$$

$$T_{Tu} = T_u(1+\frac{\gamma-1}{\gamma}M^2) \qquad \text{Eq.4.44}$$

So:

$$\dot{m}_{LL1} = \delta_c h p_u \sqrt{\frac{\gamma}{RT_u}\left(\frac{2}{\gamma+1}\right)^{(\gamma+1)/(\gamma-1)}} \qquad \text{Eq.4.45}$$

Where:
Pu: Upstream Pressure
Tu: Upstream Temperature

Pu and Tu are changing continuously throughout the cycle.

4.3.2. Leakage Past the Blade Edges

Leakage through the clearance between the blade edges and the cylinder plate can be modeled as a max. flow rate through the converging-diverging nozzle. So:

$$\dot{m}_{LL2} = 2\delta_e \varepsilon_1 p_u \sqrt{\frac{\gamma}{RT_u}\left(\frac{2}{\gamma+1}\right)^{(\gamma+1)/(\gamma-1)}} \qquad \text{Eq.4.46}$$

Where:

δ_e : Blade extension

ε_1 : Clearance between blade and the cylinder plate.

4.3.3 Results

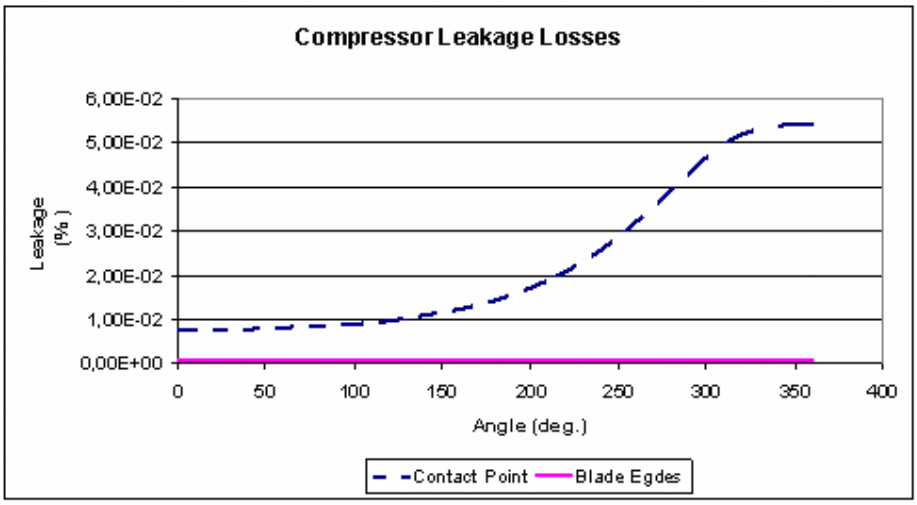

Figure 4.19 Compressor Leakage Ratios to the Engine Mass Flow Rate

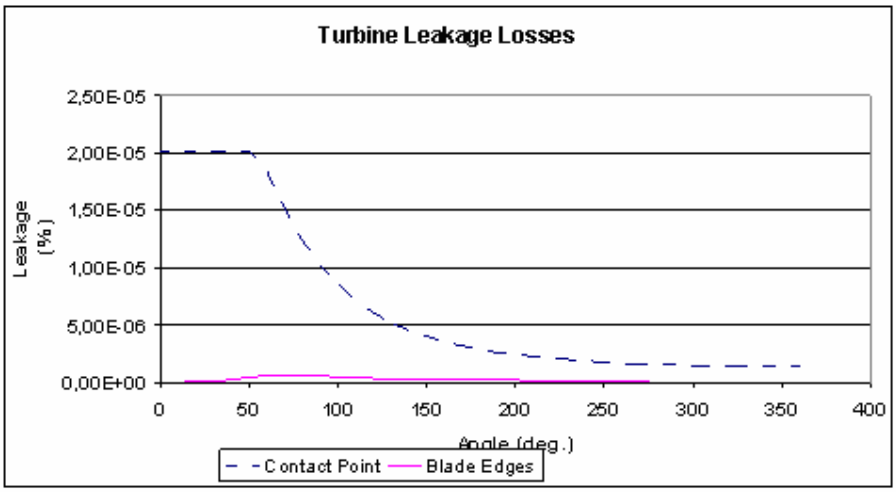

Figure 4.20 Turbine Leakage Ratios to the Engine Mass Flow Rate

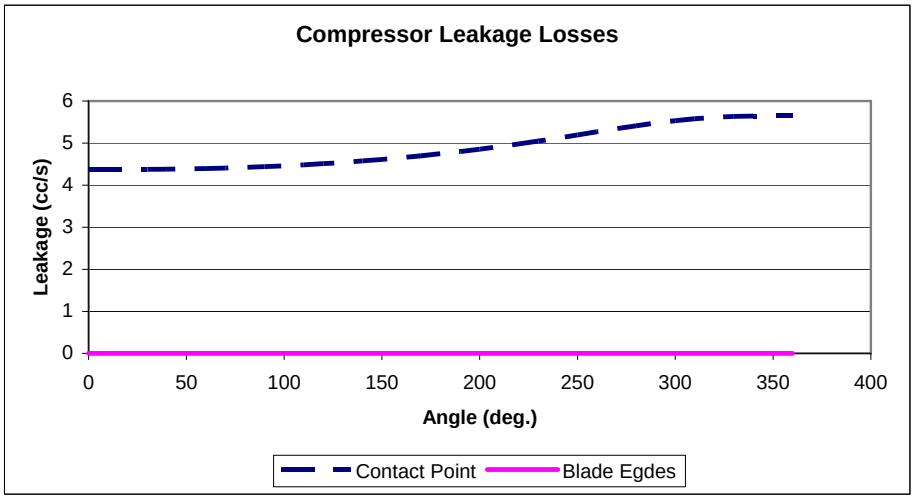

Figure 4.21 Compressor Volumetric Leakage Losses

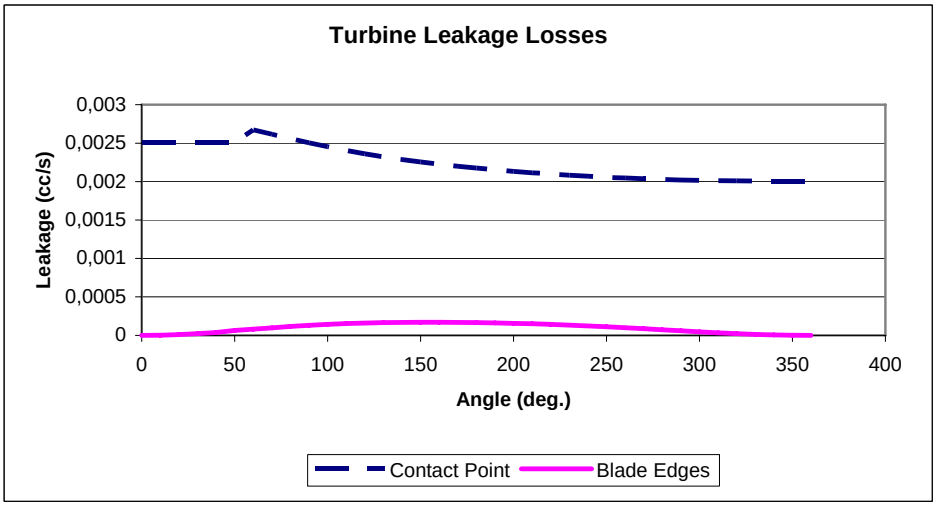

Figure 4.22 Turbine Volumetric Leakage Losses

CHAPTER 5

CONCLUSION

5.1 Summary of Work

During the thesis the works which has been done is summarized as follows;

- Thermodynamic analysis of the novel rotary engine working on a novel thermodynamic cycle has been done. A thermodynamic design code has been written to determine the geometrical dimension of the novel rotary engine. The rotary compressor and the rotary turbine of the engine have also been matched along with the geometric dimensions of the engine components (rotary compressor, rotary turbine, external combustion chamber)

- Structural and mechanical design of the components of the novel rotary engine has been done according to the geometric data taken from the thermodynamic design code. All the components of the novel rotary engine have been modeled and assembled in CAD environment Structural analyses of the critical components have been done using finite element software.

- Engine geometric and kinematics characters were determined and the critical problem for rotary engines, friction and leakage were analyzed.

5.2 Recommendations for Future Work

The thermodynamic design code should be improved after making experiments about the compression and the expansion, by doing so more realistic compression and expansion coefficients can be found and also heat losses during the compression and the expansion can be determined.

Material selection of the rotary compressor, turbine and the combustion chamber should be revised. The selected rotary compressor material seemed well but care should be taken when selecting the turbine material taking into account the high temperature load on the components and also the weight of the engine should be taken into the account.

Structural analysis of the critical components of the novel rotary engine should be revised using the real temperature and pressure data taken through out the experiments.

In the engine induction process when the air goes through the air inlet ports there can be analyzed by considering the things such as flow separation, inlet pressure loss or any other problem restricts air to go into the compressor should be determined by CFD analysis or experimental methods.

REFERENCES

1. **V. Ganesan.:** "Internal Combustion Engines", McGraw-Hill Inc., 1996.

2. **Kromer, Herbert, Kittel, Charles:**" Thermal Physics", W.H. Freeman Company, 1980.

3. **Smith D.G.** and **Rudge, P.G.,** "Pressure-Volume Diagrams for Sliding Vane Rotary Compressors", *Proc. Instn. Mech. Engineers, Vol.184 Pt3R, Paper 17,* (1970), 159-166).

4. **Chou, Y.,** "Rotary Vane Engine", *USPTO 5,352,295,* (October 4th 1994).

5. **Vading, K.,** "Rotary-Piston Machine", *PCT WO 02/31318,* (April 18th 2002).

6. **Umeda, S.,** "Rotary Internal Combustion Engine", *USPTO 4,414,938,* (November 15th 1983).

7. **LAI, J.H.,** "Stage Combustion Rotary Engine", *USPTO 5,596,963,* (January 28th 1997).

8. **Jirnov, A., and Jirnov, O.,** "Sliding-Blade Heat Engine with Vortex Combustion Chamber", *USPTO5, 511,525,* (April 30th 1996).

9. **Ssketa, Masami: "**A cat-and mouse type rotary engine: engine design & performance evaluation, Proceedings of the Institution of Mechanical Engineers, Part D, Journal of Automobile Engineering, 220 (D8):1139-1151 AUG,2006

10. **Wankel, F.:** Rotary Piston Machines, Iliffe Books, London, 1965.

11. **Yamamoto, K**.: Rotary Engine, Toyo Kogyo Co. Ltd., Hiroshima, 1969.

12. **Rory R, Davis:** "The Ball Piston Engine: A New Concept in High Efficient Power Machines", Convergence Eng. Corporation.

13. **REGI. Us. Inc.:** Rand-Cam Engine, US Patent No:0746071, January 10th 2001

14. **Dyna-Cam Engine Corporation:** "Two-cycle swash plate internal combustion engine"**,** USA Patent No:7137366, November 21st 2006

15. **Renegar, David, C.:** "The Quasiturbine", USA Patent No:6629065 September 12th 2003

16. **Koushi Akasaka:** Japanese Patent No:38617, February 7th 1997

17. **Akmandor, İ.S., Ersöz, N.:** Novel Thermodynamic Cycle, PTC / WO / 2004 / 022919 AI. (March 18th 2004)

18. **Taylan Ercan**:"Thermodynamic and Structural Design and Analysis of a Novel Turbo Rotary Engine", September 2005.

19. **Heywood, J. B.:** "Internal Combustion Engine Fundamentals", MIT Press1988.

20. Keenan, J, H.: "Thermodynamics", MIT Press, 1970.

21. Haywood, R, W.:"A Critical Review of Theorems of Thermodynamics Availability" J. Mech. Eng. Sci. vol.16 MIT Press, 1970.

22. Clarke, J. M.: "Thermodynamic Cycle Requirements for Very High Rotational Efficiencies" J. Mech. Eng. Sci. 1974

23. Stephen R. Turns: "An Introduction to Combustion" McGraw-Hill Series in Mech. Eng. 1996.

24. A.M. Mellor: "Design of Gas Turbine Combustors", Academic Press,1990.

25. Chlumsky. V.: "Reciprocating and Rotary Compressors", E&PN Ltd., London, 1965.

26. Beck, W. D., Stein R. A. and Eibling, J. A.: "Design for Minimum Friction in Rotary-Vane Refrigeration Compressors" ASHRAE Transactions, vol.72, Part 1, 1966.

27. Baumeister T.: "Mark's Standard Handbook for M. Engineer" McGraw-Hill Inc., New York, 1966.

28. Fuller. D. D.: "Theory and Practice of Lubrication for Engineers." John Wiley & Sons Inc., New York, 1966

APPENDIX

ROLLING PISTON ENGINE MATERIAL

Properties of H13 Hot Work Tool Steel

Table A.1 Chemical Composition of H13

Chemical Composition (Weight %)					
C	Cr	Fe	Mo	Si	V
0.32 – 0.4	5.13 -	Min 90.95	1.33 – 1.4	1	1

Physical Properties

Density 7.8 g/cc

Mechanical Properties

Hardness	52-54 Rockwell
Ultimate Tensile Strength	1990 MPA
Yield Tensile Strength	1650 MPa
Elongation at Break	9 %
Modulus of Elasticity	210 GPa
Bulk Modulus	140 GPa
Poisson's Ratio	0.3
Machinability	50 %
Shear Modulus	81 GPa

Thermal Properties

CTE, Linear 20^{o}C	11 μm / m-^{o}C
CTE, Linear 250^{o}C	11.5 μm / m-^{o}C
CTE, Linear 500^{o}C	12.4 μm / m-^{o}C
Heat Capacity	0.46 J / g-^{o}C
Thermal Conductivity	24.3 W / m-K